technische universität dortmund

Towards the design and construction of self-replicating RNA nanostructures

Dissertation

Submitted for the degree of
Doctor of Natural Science
(Dr. rer. nat.)

by
David Rubert

TU Dortmund University
Department of Chemistry and Chemical Biology

1st Examiner: Prof. Dr. Hannes Mutschler
2nd Examiner: Prof. Dr. Daniel Summerer

"L'universo è un gran libro

che non si può intendere finché prima

non s'impara a intender la lingua

e conoscere i caratteri

ne'quali è scritto."

G. Galilei

Summary

The transition from an RNA-based world to DNA as the genetic storage of information is one of the most intriguing areas of origin of life research. Recreating such a primordial entity in a controlled laboratory setting could provide valuable insights and information on this transition. Additionally, this could have potential biotechnological applications. This work aims to design and prototype a technology for creating a hybrid genome system based on DNA and RNA that can be transferred via replication and evolved, first in *in vitro* and later *in vivo*. In detail, the design and test of a synthetic self-replication system based on the phage Qβ replicase in order to build segmented RNA genomes has been carried out. The system is coupled with the self-assembly capability provided by the pRNA, a structural RNA present packaging machinery of Phi29 phage that allows the self-assembly into compact nanorings of increasing dimension. This structural motif has been introduced as cargo into the sequence of the RQ135 and MDV-1 replicons, two templates of the Qβ replicase. The assembly and replicability of these replicons was also tested first separately and later in a coupled assembly and replication reaction. Qβ is an ideal system for the development of such a synthetic self-replication system due to its high amplification efficiency and template flexibility. This is the initial checkpoint for constructing RNA genomes that could potentially be transplanted into *Escherichia coli* at a later stage. Previous research has identified potential challenges in building such synthetic self-replicating systems, such parasite formation. The phenomenon is caused by the formation of shorter RNA strands that replicate more rapidly. This leads to a faster consumption of the components necessary for RNA synthesis, resulting in the termination of the reaction. To prevent parasite formation, a water-emulsion system has been adopted and validated as a potential solution.

A milestone in this work was the modular assembly of the newly designed replicons, carrying the pRNA motif, into nanorings, drawing on the technology established by the Guo group, with emphasis on system reproducibility and the influence of Mg^{2+} concentrations on nanoring size and stability.

As a final focus, this work aims to merge the self-replication and self-assembly of the replicons. Assembly-coupled replication of the replicons will be designed and tested, which represents a crucial step in testing the generation of a segmented and modular RNA genome capable of storing genetic information in vitro. In conclusion, this work presents an extensive review of the challenges, solutions, and advancements towards the development of a synthetic self-replication system based on replicating nanorings for potential genomic transplantation in *E. coli*.

Zusammenfassung

Der Übergang von einer RNA-basierten Welt zur DNA als genetischer Informationsspeicher ist eines der faszinierendsten Gebiete der Forschung über den Ursprung des Lebens. Die Nachbildung einer solchen ursprünglichen Einheit im Labor könnte wertvolle Erkenntnisse und Informationen über diesen Übergang liefern. Außerdem könnte dies potenzielle biotechnologische Anwendungen nach sich ziehen. Ziel dieser Arbeit ist es, eine Technologie zur Schaffung eines hybriden Genomsystems auf der Grundlage von DNA und RNA zu entwerfen und zu prototypisieren, das durch Replikation übertragen und entwickelt werden kann, zunächst in vitro und später in vivo. Im Einzelnen wird ein synthetisches Selbstreplikationssystem auf der Grundlage der Phagen-Qβ-Replikase entworfen und getestet, um segmentierte RNA-Genome zu erzeugen. Das System ist mit der Fähigkeit zur Selbstorganisation gekoppelt, die von der pRNA bereitgestellt wird, einer strukturellen RNA-Verpackungsmaschinerie des Phi29-Phagen, die die Selbstorganisation zu kompakten Nanoringen mit zunehmender Größe ermöglicht. Dieses strukturelle Motiv wurde in die replizierende Gerüstsequenz der RQ135- und MDV-1-Replikons eingebettet, zwei hocheffiziente RNA-Substrate für die Qβ-Replikase. Die Assemblierung und Replizierbarkeit der daraus resultierenden RNA-Konstrukte durch Qβ wurde getestet, zunächst separat und später in einer gekoppelten Assemblierungs- und Replikationsreaktion. Qβ ist aufgrund seiner hohen Amplifikationseffizienz und Vorlagenflexibilität ein ideales System für die Entwicklung eines solchen synthetischen Selbstreplikationssystems. Dies ist der anfängliche Kontrollpunkt für die Konstruktion von RNA-Genomen, die zu einem späteren Zeitpunkt möglicherweise in *Escherichia coli* transplantiert werden könnten. Frühere Forschungsarbeiten haben mögliche Herausforderungen beim Aufbau solcher synthetischen selbstreplizierenden Systeme aufgezeigt, z. B. die Bildung von sogenannten „RNA-Parasiten“. Dies ist auf die Bildung kurzer, hocheffizient replizierter RNA zurückzuführen, die zu einem raschen Verbrauch der für die RNA-Synthese benötigten Komponenten durch die Replikase führen kann, was schließlich zum Ende der Reaktion führt. Um dem entgegenzuwirken, wurde ein Wasser-Emulsionssystem als potenzielle Lösung zur Eindämmung von Parasiten eingesetzt, das erfolgreich validiert wurde.

Ein entscheidender Aspekt dieser Arbeit war die Bestätigung des Zusammenbaus des neu entworfenen Replikons zu Nanoringen unter Einbeziehung des pRNA-Motivs, das zum Zusammenbau führt. Der modulare Zusammenbau aus einzelnen pRNA-Monomeren wurde untersucht, wobei eine vom Arbeitskreis Guo entwickelter Ansatz genutzt wurde. Besonderes Augenmerk wurde auf die Reproduzierbarkeit des Systems und den Einfluss der Mg^{2+}-Konzentration auf die Größe der Nanoringe gelegt.

Ein letzter Schwerpunkt dieser Arbeit ist die Zusammenführung der Selbstreplikation und der Selbstassemblierung der Replikons. Eine mit der Selbstassemblierung gekoppelte Replikation der RNA-Konstrukte wurde entworfen und getestet, was einen entscheidenden Schritt bei der Erprobung der Erzeugung eines segmentierten und modularen RNA-Genoms darstellt, das in der

Lage ist, genetische Informationen in vitro zu speichern. Zusammenfassend lässt sich sagen, dass diese Arbeit einen umfassenden Überblick über die Herausforderungen, Lösungen und Fortschritte bei der Entwicklung eines synthetischen Selbstreplikationssystems auf der Grundlage replizierender Nanoringe für eine potenzielle Genomtransplantation in *E. coli* bietet.

Table of Contents

Abbreviations

3WJ = 3-Way junction

bp = base pair

C-terminus = carboxy terminus

CDS = coding sequence

CRISPR = Clustered Regularly Interspaced Short Palindromic Repeats

CV = column volume

Cy3 = Cyanine3

Cy5 = Cyanine5

DHFR = dihydrofolate reductase

DNA = deoxyribonucleic acid

dsRNA = double strand RNA

EDTA = ethylenediamine tetraacetic acid

EF-Ts = elongation factor Ts

EF-Tu = elongation factor Tu

FAM = fluorescein amidites

HF1 = host factor 1

His6 = hexahistidine-tag

IVT = *in vitro* translation

IVTxT system = *in vitro* translation system

kb = kilobase

LB = lysogeny broth

LUCA = Last Universal Common Ancestor

MDV-1 = midivariant

miRNA = microRNA

mRNA = messenger RNA

N-terminus = amino terminus

nt = nucleotide

oligo = oligonucleotide

PAGE = polyacrylamide gel electrophoresis

PCR = polymerase chain reaction

pRNAs = prohead RNA

PURE = protein synthesis using recombinant elements

Qβ PB1 = Qβ Purification Batch 1

Qβ PB2 = Qβ Purification Batch 2

RBS = ribosome biding site

RdRp = RNA-dependent RNA polymerase

RNA = ribonucleic acid

rNTPs = ribonucleotide triphosphates

rRNA = ribosomal RNA

S1 = S1 Ribosomal protein S1

SDS-PAGE = polyacrylamide gel-electrophoresis with sodium dodecyl sulfate

SELEX = systematic evolution of ligands by exponential enrichment

sfGFP = Super Fold Green Fluorescent Protein

siRNA = small interfering RNA

ssDNA = single strand DNA

ssRNA = single strand RNA

tRNA = transfer RNA

UTR = untranslated region

1. Introduction

1.1. Deciphering life's blueprint: synthetic biology and evolution

In a 1955 interview with LIFE magazine, Einstein once stated: “The important thing is not to stop questioning. Curiosity has its own reason for existence. One cannot help but be in awe when he contemplates the mysteries of eternity, of life, of the marvellous structure of reality. It is enough if one tries merely to comprehend a little of this mystery each day.” This powerful idea not only embraces the concept that science progresses incrementally, but also maintains a positive outlook toward discovering possible explanations for the most complex and controversial questions that philosophers, scientists, and theologians have sought to answer for centuries.

One of the topics that is mentioned by Einstein and still debated is how life works and when, where, and how it originated. Recent efforts to answer these questions from a biological perspective have led to the emergence of the field of synthetic biology, a novel and interdisciplinary approach to the study and engineering of life based on the principles of design and modularity, which allows the rational design and creation of synthetic systems that can mimic existing organisms, thereby shedding light on the mechanisms of life and embracing Feynman's affirmation: "What I cannot make, I do not understand”. As in engineering, also in synthetic biology, there is a tendency toward simplification or abstraction by identifying the minimum number of components necessary to achieve a desired function within the complexity of cells and bacteria, and life on Earth might have evolved from nonbiological components to simple entities in an increasing complexity towards more mechanistic sophistication and energetic efficiency (De Lorenzo, 2018; Moger-Reischer *et al.*, 2023). To achieve that, synthetic biologists scour the natural world to find suitable molecular tools to achieve their goals and tackle this challenge through two distinct approaches. One, the "top-down" approach involves using an existing cell as the starting point, reducing its genome to its minimal components, and introducing foreign elements to give it a new function not previously present (Ivanov *et al.*, 2021). The other, the “bottom-up” approach involves the creation of new modules and systems from scratch, based on biological principles, rather than starting from existing cells (Guindani *et al.*, 2022). When considering this approach, various challenges arise. These include providing the synthetic cells with their own energy production system and recycling capabilities, compartmentalising reactions to increase efficiency, metabolising detrimental products, and synthesising essential products necessary for basic functions. Additionally, an efficient

system must be provided for the synthetic cell to store, replicate, and evolve its genetic information. Nature has already provided examples of how to solve these basic challenges through 3.8 billion years of evolution. Therefore, synthetic biologists are taking inspiration from nature in a biomimetic fashion. They apply biological methods and systems found in nature without further engineering, as evolution has already led to the most efficient form of it. Thanks to modern genetic engineering and bioinformatic techniques, synthetic biologists can optimize natural tools in a biomimetic fashion. This will enable the redesign of existing biological systems and the construction of new biological parts, devices, and systems, converging towards the creation of tuneable synthetic organisms. In addition, this approach might enable the creation of biomolecular systems similar to those that existed in the past during early evolution but have now disappeared (Schwille and Diez, 2009; Green, 2019). Researchers can use this method to observe and explain the evolutionary stages of life, from the formation of the first primitive cells to the complexity of multicellularity we see today.

Examining the diversity of nature today, it is evident that certain systems and entities have persisted for millions of years, leaving an evolutionary footprint that could aid the scientific community in reconstructing the simplest and most archaic 'living' forms (Oliver, 2013). Additionally, this could serve as a valuable tool in building more complex synthetic organisms. Viruses are one such entity. Although most people outside the scientific community view them as pathogens, they can also be seen as one of the simplest examples of efficient energy production, genetic information storage, propagation, and compartmentalization (Durzyńska and Goździcka-Józefiak, 2015; Koonin, 2016). Viruses are a proper reservoir of basic tools and simple structural motifs for the bottom-up assembly of complex systems that have already evolved and been optimized. This reservoir can be used for the bottom-up assembly of complex systems in the creation of synthetic organisms, shedding light on the mechanisms and origins of life.

1.2. Viruses

A virus is a microscopic agent that is ubiquitous and causes devastating disease in humans, animals, plants and other living things. In agriculture, viral diseases threaten not only the nutrition of the world's population but also the production of fibres, ornamental plants and medicines that are essential to humanity, as they can lead to significant losses in crop yield or drastic reductions in product quality (Jones and Janssen, 2021). In the medical field,

viruses such as those that cause smallpox, influenza, AIDS and COVID-19 have had a major impact on the history of mankind. Therefore, it is not surprising that viruses are often seen in a negative light and considered to be our “enemies” (Varanda *et al.*, 2021). Therefore, there is general scepticism towards the potential uses of viruses for clinical and biotechnological applications.

Despite this negative general view, in the complex world of molecular biology and genetic engineering, viruses possess positive roles. They could easily be defined as nature's “molecular engineers”. They possess distinctive structural elements and replication mechanisms that inspire scientists to explore new horizons in synthetic biology. Viruses have been used for research purposes for several decades. They have contributed to the study of infectious diseases, the development of vaccines, the exploitation of their architecture for nanotechnological purposes, and as vectors for gene therapy (Varanda *et al.*, 2021). Additionally, they have been used in the fight against antibiotic resistance (Principi, Silvestri and Esposito, 2019). This class has unique structural elements and replication mechanisms that inspire scientists to explore new frontiers in synthetic biology.

In the vast world of viruses, bacteriophage have a special niche. Their impact on synthetic biology is massive since they are as a significant source of molecular machines for the development of genetic engineering tools. These viruses, also known as phages, have the ability to infect bacteria and archaea. The discovery and characterization of phages should be attributed to Frederick W. Twort, who first isolated them from Staphylococcus (Twort, 1915), and to Felix d’Herelle, who isolated them from Shigella (D’Hérelle F., 2007). They are the most abundant biological entities on the planet, despite their simple viral structures that consist of nucleic acids and coat proteins (Whitman, Coleman and Wiebe, 1998; Wommack and Colwell, 2000; Suttle, 2007). Phages rapidly invade and multiply using two modes of replication, lytic cycle and the lysogenic cycle (Campbell, 2003). Phages can be genetically manipulated due to their small genome size, which ranges from 5 kb to 500 kb (Hatfull, 2008). Recognised as essential models for molecular biology, phage has laid the foundation for modern virology and biology, giving an huge contribute to the comprehension of DNA self-replication (Hatfull, 2008), the elucidation of the complex structure of microorganisms (Sun, Overman and Thomas, 2007), the molecular mechanism of mutations (Poteete and Hardy, 1994), and the study of gene regulation (Scanlan *et al.*, 2011). The study of phage biology has resulted in the creation of significant molecular tools that are extensively utilised in biology and genetic engineering. Phage-derived RNA

polymerases, transcriptional regulators, and integrases are universally used gene regulation tools in synthetic biology that stem from phage biology research. Furthermore, the interactions between prokaryotes and phages have led to the discovery and development of the revolutionary clustered regularly interspaced short palindromic repeats (CRISPR) system (Szczepankowska, 2012). Additionally, phage-based applications are widely used in various fields, including bacterial detection (Meile *et al.*, 2020) , drug delivery (Karimi *et al.*, 2016), novel vaccine design (de Vries *et al.*, 2021), and nanomaterials (Paczesny and Bielec, 2020). Due to the vast diversity of phage species, phage research has not yet uncovered all their secrets. Phage research has significant potential for technological development and breakthroughs.

The viral structural elements and replication mechanisms provide a toolkit for constructing complex synthetic systems (Oliver, 2013; Varanda *et al.*, 2021). To promote their own growth and proliferation, phages divert the ribosomes, various factors required for protein synthesis, amino acids, nucleic acids, and energy production systems of bacterial cells; moreover, they have evolved various strategies to amplify their genetic material and have evolved sophisticated capsid structures and several essential components to exploit host cell resources (Zhang and Wu, 2020; Ioannou, Baliou and Samonis, 2023). These characteristics provide a solid foundation for the RNA-based field of synthetic biology to build intricate synthetic systems and explore the potential for creating artificial cells. In recent years, phage technologies have become a major focus of synthetic biology. New insights into biological evolution have been discovered through the study of the phage lifecycle and its interactions with host cells, leading to the development of more functional synthetic modules. Additionally, the phage lifecycle provides synthetic biologists with another tool for building novel artificial systems. As the last point of investigation, phage-bacterial interactions are another aspect that allows for the discovery and application of technologies widely used in different hosts (Zhang and Wu, 2020) **(fig. 1)**.

These characteristics offer a valuable foundation for the RNA-based field of synthetic biology to build intricate synthetic systems and explore the potential for creating artificial cells. These synthetic entities are built using components derived from bacteriophages and could allow the recreation of synthetic cells that resemble the primitive entities produced on the primordial Earth, shedding light on how life evolved and having major implications for the study of the origins of life.

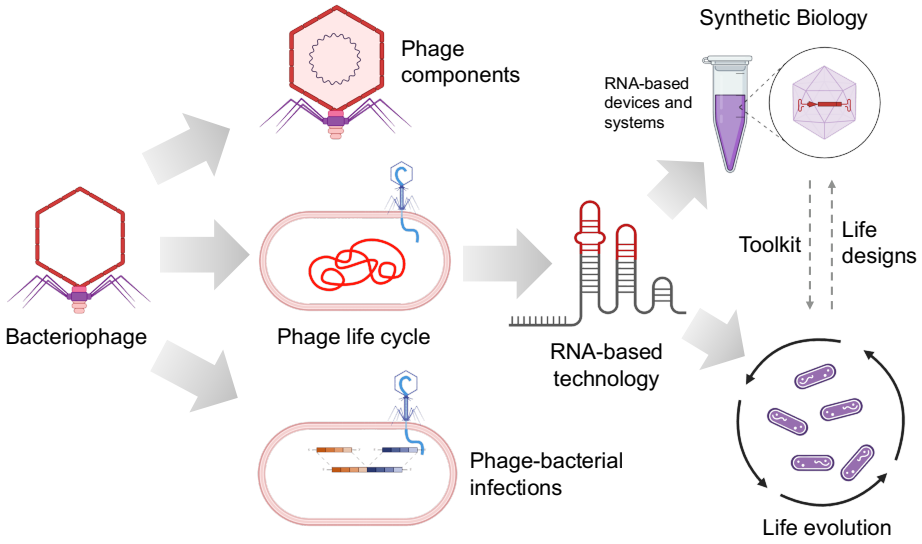

Figure 1: Phage as tool for synthetic biology. *When considering phages, three specific characteristics are taken into consideration that have practical impacts on the development of new technologies and devices and the understanding of how life evolved on the planet: the components of the phages, their life cycle, and the interactions between phages and bacteria.*

1.3 Viruses as natural engineers: self-replicating systems

Replication enables living organisms to reproduce, inherit mutations, and undergo natural selection, which drives evolution and therefore is a fundamental mechanism of living and non-living systems (Ichihashi, 2019). The ability to replicate is often considered an absolute requirement in most proposed definitions of life as it drives evolution (Luisi, 1998; Dix, 2002; Zhuravlev and Avetisov, 2006). For instance, NASA working definition states that life is a self-sustaining system capable of Darwinian evolution, making replication and evolution central characteristics of life (Deamer and Fleischaker, 1994). In biology, self-replication refers to the process or mechanism by which organisms can produce functional and independent copies of themselves. Advances in in vitro technologies have made it possible to construct systems capable of replication or other biological functions from chemical compounds or biological molecules, such as RNA, DNA and proteins (Ichihashi, 2019).

Many templated self-replicating systems **(fig. 2)** are classified as translation-independent systems, in which replication is based on physicochemical properties in the absence of translation. These systems include both nontemplate and template replication. Biologically relevant nontemplated autocatalytic reactions were reported in the 1980s and 1990s using

peptides (Lee *et al.*, 1996, 1997; Vagt *et al.*, 2006), nucleotides and nucleotide analogues (Zielinski and Orgel, 1987; Tjivikua, Ballester and Rebek, 1990; Li and Nicolaou, 1994; Sievers and Von Kiedrowski, 1994), molecules that replicate themselves by autocatalysis.

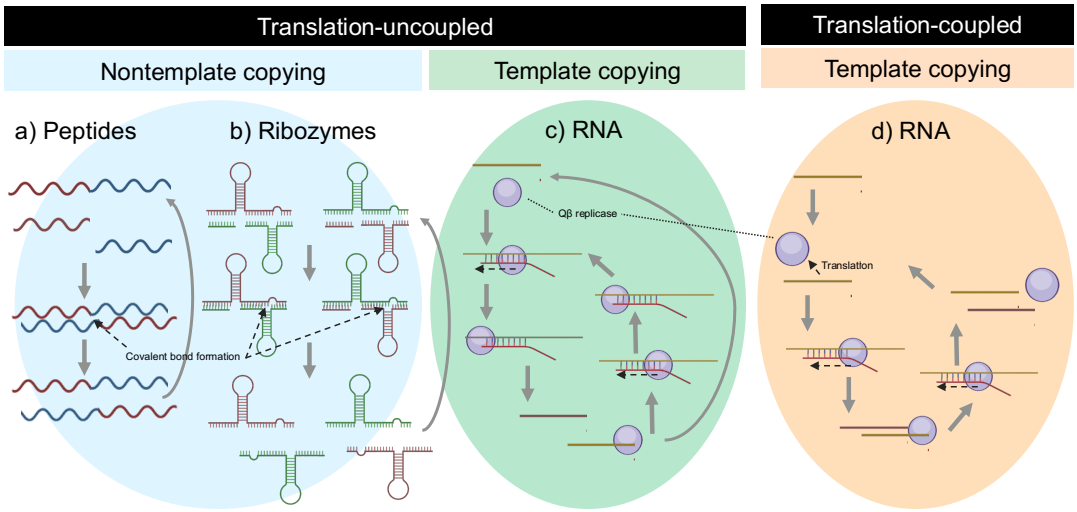

Figure 2: Most common self-replication systems. *Most famous type of self-replication systems.* ***a)*** *Peptide replication (Lee et al., 1996)* ***b)*** *Ribozyme replication scheme (Lincoln and Joyce, 2009).* ***c)*** *RNA replication scheme (Mills et al., 1967). Qβ replicase is provided from the outside and produces the complementary strand (yellow) starting from the template RNA (red). In a cycle, the newly produced complementary strand can also produce the template RNA.* ***d)*** *Translation-coupled RNA replication (Kita et al., 2008). The translation of Qβ begins with the template RNA, as the ribosomes recognize and translate the mRNA sequence of the replicase. Following translation, the process is identical to that of c). (Ichihashi, 2019).*

Another example of an autocatalytic reaction is ribozyme replication developed by Joyce's group, who directly evolved self-ligating ribozymes to construct a ribozyme system by interdependent ligation of precursor RNA fragments (Kim and Joyce, 2004; Lam and Joyce, 2009; Lincoln and Joyce, 2009). A replication system composed of fragmented recombinant ribozymes was reported by Lehman's group (Vaidya et al., 2012). In addition, ribozyme combinations were shown to emerge spontaneously, replicating as a single unit from partially random ribozyme fragments (Hayden, Von Kiedrowski and Lehman, 2008). Spiegelman's group first reported replication systems with template copying mechanisms (Mills et al., 1967). They used Qβ genomic RNA and purified Qβ replicase, a RNA-dependent RNA polymerase. Qβ is capable of synthesising a complementary strand of RNA from a single-stranded RNA template without primers, provided that this template meets specific sequence and structure requirements (Blumenthal and Carmichael, 1979; Biebricher, Diekmann and Luce, 1982; Chetverin, Chetverina and Munishkin, 1991; Usui,

Ichihashi and Yomo, 2015). Qβ replicase first synthesises the complementary strand of the template RNA genome and then synthesises the original strand using the complementary strand as a template in the presence of all nucleotide triphosphates. Through the serial dilution cycle, the replication reaction was repeated for many generations. The template RNA replicates itself using this process. This could also be seen as first cell-free in vitro Darwinian evolution.

Many researchers have developed other replication systems that use combinations of RNA, DNA and proteins using the template-copying mechanism since the seminal work done by Spiegelman's and his group (Guatelli *et al.*, 1990; Terrance Walker *et al.*, 1992; Walker *et al.*, 1992; Breaker and Joyce, 1994; Ellinger, Ehricht and McCaskill, 1998; Notomi *et al.*, 2000; Vincent, Xu and Kong, 2004; Kurn *et al.*, 2005; Jeong, Park and Kim, 2009). A famous example of these replication systems is the polymerase chain reaction (PCR). It is important to note that while PCR requires artificial thermal cycling, the other systems described above do not require it. The polymerase chain reaction (PCR), which, unlike the other systems described above, requires artificial thermal cycling, is a well-known example of such a replication system (Saiki *et al.*, 1985).

In the above systems, the replication of the molecules depends solely on their physico-chemical properties, specifically their catalytic and hybridisation activities (Hayden *et al.,* 2008; Lincoln & Joyce, 2009; Vaidya *et al.*, 2012), whereas in the Spiegelman RNA-replicating system, RNA is replicated by a replicase (Mills *et al*., 1967). The RNA that replicates may encode genes, but they are non-functional due to the lack of translation machinery in the reaction mixtures, which prevents protein translation. The Qβ phage template RNA encodes the sequence of a replicase, capsid protein and lysis protein in the system, but these genes have not been used for replication (Mills *et al*., 1967).
In terms of their physicochemical properties, all molecules have distinct unique capabilities and constraints. RNA, for instance, have the extraordinary ability to act as biocatalysts and replication templates, but the efficiency of RNA-catalysis is much lower than that of protein-based enzymes (Narlikar and Herschlag, 1997). In addition, the correct fold is essential for an RNA to act as a catalyst, and this may affect its ability to serve as a template (Szostak, Bartel and Luisi, 2001). As a result, pure RNA replicators may have restricted replication capacity due to these constraints.

Translating the RNA sequence into a protein, is one possible strategy to bypass these limitations, and acquiring the ability of RNA to serve as a translation template is considered to be one of the major transitions during molecular evolution (Szathmáry and Smith, 1995; Ruiz-Mirazo, Umerez and Moreno, 2008; Witzany, 2016). Looking at the Spiegelman RNA replication system and studying the natural functioning of the Qβ phage provides a clear example of how coupling RNA replication to a protein can overcome the limitations of RNA-based catalysis.

1.3.1 The Qβ replicase

The Qβ phage is a non-segmented positive-sense single strand RNA (ssRNA) phage belonging to the family *Leviviridae* (genra *Allolevivirus*) (Kuhn, 2021) whose genome consists of roughly 4200 nucleotides. It encodes for four proteins, specifically the A2 protein, A1 protein, coat protein, and replicase, called Qβ replicase (Priano *et al*., 1995).
The replicase is a heterotetrametric complex consisting of a phage-encoded catalytic subunit (β-subunit) and three host-encoded proteins, including the ribosomal protein S1 and two protein synthesis elongation factors, EF-Tu and EF-Ts. RNA-dependent RNA polymerase (RdRp), present in all positive-stranded RNA viruses, is encoded by the phage and uses the viral RNA as a template to make new strands of RNA. (Kamen, 1970; Kondo, Gallerani and Weissmann, 1970; Blumenthal, Landers and Weber, 1972; Fedoroff and Zinder, 1973; Blumenthal and Carmichael, 1979). The core-complex, consisting of the β-subunit (65 kDa), EF-Tu and EF-Ts, can polymerize RNA in vitro. The assembly of the β-subunit with EF-Tu (45 kDa) and EF-Ts (35 kDa) is required to synthesise the (-) RNA strand from the (+) template and is also thought to play an important role in assembling and stabilizing the entire core-complex. S1 (70 kDa) is a protein that is part of the 30S ribosomal subunit **(fig. 3)**. This subunit is responsible for translating mRNA within the cell by helping mRNA bind to the 30S ribosomal subunit. S1 is the final protein required for efficient in vivo replication of the Qβ phage genome in *E. coli*. The β subunit "hijacks" these three bacterial subunits to form the replicase holoenzyme when the phage infects *E. coli* (Kidmose *et al.*, 2010; Kashiwagi and Yomo, 2011). It is worth noting that S1 is not necessary for (+) strand RNA synthesis from (-) strand RNA. The presence of host factor 1 (HF1) in *E. coli* bacteria is required for replication initiation (Kajitani *et al.*, 1994). Mechanistic insights into Qβ replicase-mediated RNA polymerisation remain unclear, as

do their effects on phage RNA replication and transcription (Singleton *et al.*, 2018).

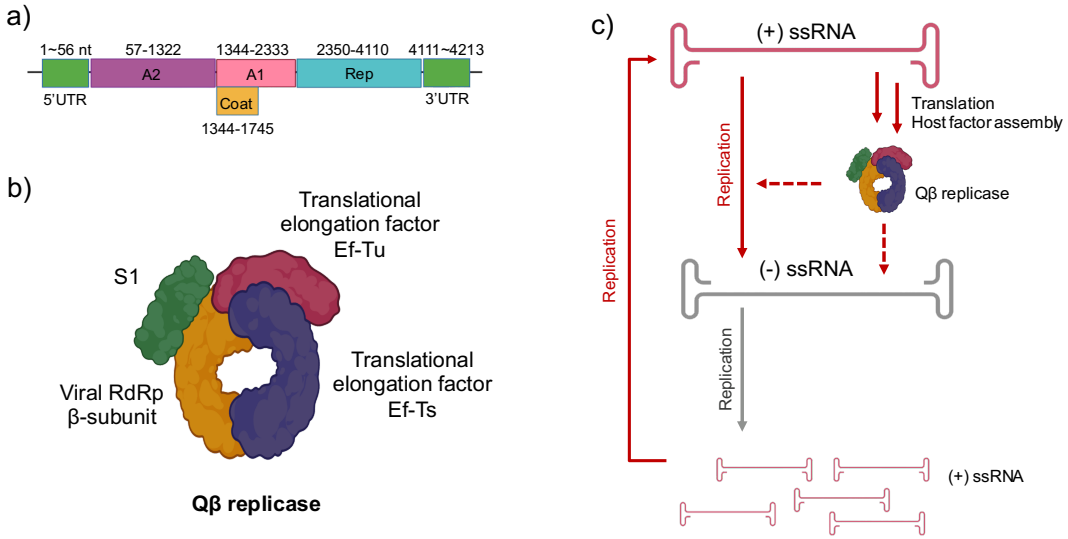

Figure 3: The Qβ phage. *Panel with details of the RNA genome, the RdRp Qβ replicase, and the mechanism of replication of the RNA of the phage Qβ.* ***a)*** *The genome of the Qβ phage is composed of the 5'UTR and 3'UTR replication regions, which are recognized by the Qβ replicase to synthesize the complementary strand, protein A2, protein A1, coat protein, and the Qβ replicase gene.* ***b)*** *The fully functional Qβ replicase holoenzyme is composed of the virus RdRp Beta-subunit, the translation elongation factor Ef-Tu, the translational elongation factor Ef-Ts, and the ribosomal protein S1.* ***c)*** *The mechanism of replication of the Qβ replicase is described here. It enables the production of more (+) strands, starting a cycle of amplification. The (+) strand ssRNA genome is translated to produce the Qβ protein, which binds to other host factors and then binds again to the (+) strand to produce the (-) strand (Zhang and Wu, 2020).*

Replication of Qβ's (+) ssRNA genome occur when the assembled holoenzyme, S1 protein, and EF-Tu and EF-Ts are present and a complementary (-) ssRNA is first synthesized to serve as a template for the synthesis of more (+) ssRNA. Both the (+) and (-) strands can serve as templates for replication, but it is important to note that the (+) strand can also serve as mRNA for the synthesis of the resulting protein. The Qβ replicase has unique features that distinguish it from other replicases. It uses a unique structural base recognition system based on specific folding of hairpin-like loops at the 5'-UTR and 3'-UTR to amplify its genome more than 10^4-fold in less than an hour. Furthermore, for replication to occur, the CCC motif must be present at the 3′ end and there must be an internal C/U-rich domain (Kueppers and Sumper, 1975; Biebricher and Luce, 1993; Brown and Gold, 1995; Ugarov and Chetverin, 2008). It can also distinguish between its own RNA and a large amount of host RNA, and only replicates its own RNA (Singleton *et al.*, 2018).

Endogenous primers are not required. In addition, the highly structured 5' and 3' UTR secondary structure of Qβ RNA protects it from digestion by host exonucleases (Singleton *et al.*, 2018). The mechanism of Qβ replicase recognition is highly specific: in fact, SELEX experiments aimed at selecting new potential replicons resulted in only a few replicable RNA species from a population of 10^{12} random sequences of 50-70 nucleotides in length flanked by 5′-GGG and 3′-CCC (Brown and Gold, 1995b).

The recognition of the stencil is mediated by the S1 protein (Blumenthal and Carmichael, 1979) and the EF-Tu. The CCCA sequence located at the 3'-end of the template RNA is needed for Ef-Tu:EF-Ts to recognize the strand (Brown and Gold, 1996a). Both the positive and negative strands contain CCA-3' and 5'-GG sequences (Dahlberg, 1968; Weissmann *et al.*, 1973). Polymerization takes place when the 3′ end of the template enters the replicase initiation site. The first template nucleoside used in RNA polymerization by Qβ replicase is the 3'-penultimate C, not the 3'-terminal A. The process of non-primed RNA polymerization by Qβ replicase begins with GTP (*de novo* initiation) (Silverman, 1973; Blumenthal and Carmichael, 1979; Blumenthal, 1980). After copying the positive strand, the replicase stops and anneals to the negative strands. This can be done by template switching or by annealing to a free-floating negative strand. Qβ replicase adds the 3'-A during the last step of RNA replication through its intrinsic terminal nucleotidyltransferase activity (Weber and Weissmann, 1970; Blumenthal and Carmichael, 1979; Bausch *et al.*, 1983) **(fig. 4)**.

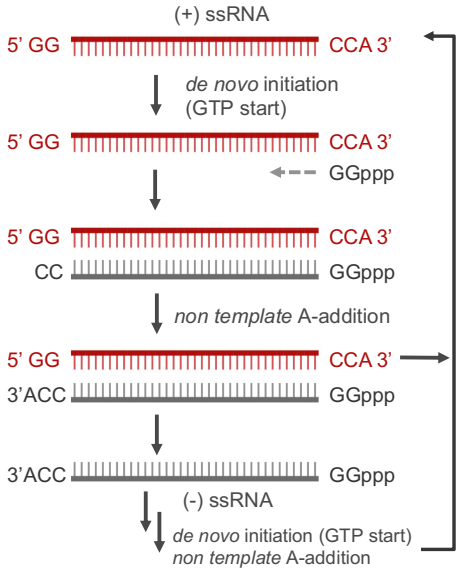

Figure 4: Detailed replication cycle of Qβ RNA. *The Qβ phage genome is a single-stranded RNA. Both the (+) and (-) strands contain 5'-GG and CCA-3' sequences. The de novo initiation that leads to the synthesis of the (-) strand requires GTP to start. During the last step of the (-) strand synthesis, a non-template A-addition is performed, adding A-3' to the new strand. This addition is not a template nucleoside (Tomita, 2014).*

Back to Spiegelmann's first Qβ "world's first extracellular Darwinian evolution" experiment, the evolution of replicable short non-coding RNAs in this in vitro system was later demonstrated by experiments based on serial transfer experiments of the first reaction, in which Qβ was incubated with its RNA genome and rNTPs. The results show

that reducing the incubation time to 5 minutes for 75 rounds, instead of 20 minutes, caused the Qβ RNA genome to shrink to 83% of its original dimensions, losing the genes responsible for infectivity and reducing it to the essential sequences that make it capable of being recognized and replicated by the replicase (Mills *et al*., 1967). In evolutionary experiments, shorter naturally occurring RNAs known as "Spiegelman's monsters" or "minimonsters" took over the population as templates that can be replicated by Qβ more efficiently than genomic DNA because they replicate more efficiently than genomic DNA. (Mills *et al*., 1967).

That said, apart from the genomic RNA, several natural occurring templates recognized and replicate by the Qβ replicase have been discovered and characterized during the years. These templates are also called being "satellite" RNAs, which are shorter than the genomic Qβ RNA but often replicate more efficiently (Chetverin, 2018).

One of the best known naturally occurring RNA templates is the "Midivariant RNA", MDV-1, (218 nt) which can be recognized and replicated by Qβ replicase even when it lacks nucleotides at either the 5' or 3' end. The 3' end of the template is required to initiate RNA synthesis. The 3' end sequences and central binding region of the (+) strand of the MDV-1 RNA are very similar to the 3' end sequences and an internal region of Qβ (-) strand RNA. Another RNA Qβ template is RQ135, named for its length of 135 nucleotides that is not related to the sequence of Qβ bacteriophage genomic RNA and comprises only segments homologous to ribosomal 23S RNA and the phage lambda origin of replication (Morozov *et al.*, 1993; Ugarov *et al.*, 1994). A recently developed and tested replicon scaffold consists of the Qβ RdRP gene inserted into the 5′ and 3′ UTRs of Qβ bacteriophage genome (Yao *et al.*, 2019).

The ability of Qβ replicase to recognize specific templates can be utilized to create artificial *in vitro* replication systems for exponential amplification by Qβ replicase based on in-silico designed recombinant RNAs. In order to make any recombinant RNA amplifiable by the Qβ replicase using the strategy proposed by Kramer's group (Miele, Mills and Kramer, 1983), these sequences must be added between the 5' and 3' ends of the replicon to be recognized by the replicase. Both RQ135 and MDV-1 replicons can be used to incorporate a additional gene "cargo" on their (+) strand, as successfully proved by several groups in the past (Kramer *et al.*, 1974; Kita *et al.*, 2008) **(fig. 5)**.

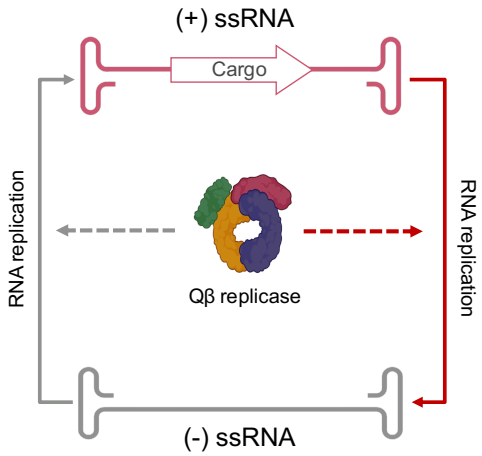

Figure 5: Qβ replication cycle. *Heterologous (+) strand replicators carrying the RQ135 or the MDV-1, or other variant scaffolds, are recognized by the Qβ replicase, and the (-) strand is produced as it would be for the genomic RNA. The replication happens efficiently and it's possible to add a desired cargo in between the replicating regions 5' and 3' UTR in order to have it replicated.*

Similar to the Qβ sequences observed in nature, several features must be taken into account in order to design proper RNA replicons that can be efficiently recognized and replicated by the Qβ replicase: a 5′-triphosphorylated end with GGG-triplet in the end, a 3′ CCC-triplet with a free 3′-OH, as observed in the natural Qβ genome replication event and that are necessary for the de novo initiation of the newly designed heterologous RNA (Kueppers & Sumper, 1975; van Dijk *et al*., 2004). ssRNAs with highly folded and strong secondary structures, such as partial internal double-strand areas, can also be processed and amplified by Qβ replicase. According to in silico folding prediction software, highly folded secondary structures, e.g. stems loops, of about 2 to 60 nucleotides can already be found in the sequence of Qβ genome and MDV-1 and RQ135.

Since Qβ replicase is incapable of using dsRNA as a template (Biebricher, Diekmann and Luce, 1982; Nishihara, Mills and Kramer, 1983) and dsRNA formation leads to the termination of the RNA replication, one of the potential problems in designing Qβ in vitro exponential self-amplification reactions is the design of heterologous RNAs that do not form dsRNA. Longer constructs have been shown to be more susceptible to dsRNA formation besides the accumulation of deleterious mutations due to the low fidelity of the Qβ replicase, which could ultimately lead to the cessation of replication (Usui *et al.*, 2013). This poses a challenge for the development of longer and more sustainable self-replicating systems (Kun *et al.*, 2015; Tomita, Ichihashi and Yomo, 2015; Iranzo *et al.*, 2016). These studies highlight the importance of evaluating the folding of the newly designed RNA replicon in-silico to optimize its structure based on the aforementioned criteria. This process can be time-consuming, as multiple designs are typically created and tested to determine the most efficiently recognized and replicated by the replicase (Mizuuchi & Ichihashi, 2018; Ueda *et al*., 2019; Usui *et al*., 2015).

The first example of a self-replicating MDV-1-based replicon was reported by Kita *et al*., 2008. In this study, the group inserted a ribosome-binding site and the 586-amino-acid-long Qβ RdRP catalytic subunit gene sequence into the (+) strand of the replicon and verified replication. Additionally, the group also designed a replicon with a slightly modified sequence carrying a lacZ gene on its (-) strand, which was tested in an IVTxT system and found to be efficiently replicating. The RQ135 replicating scaffold was utilized by Morozov *et al*., 1993 and Ugarov *et al*., 1994. The dihydrofolate reductase (DHFR) mRNA sequence was inserted into a RQ135 slightly modified scaffold, called RQ135(-1), and the replication and translation of the DHFR protein were assayed and verified in a cell-free *E. coli* translation system with the addition of Qβ replicase from the outside. (Kopsidas *et al.*, 2007) used another modified RQ135 scaffold to manufacture complex mRNA libraries by incorporating mRNA with a large mutational spectrum using a novel RNA-based random mutagenesis strategy, thanks to the high mutational rate of the Qβ replicase. The long-term performance of these artificial self-replicating systems remains a major goal, since the formation of small "selfish" replicators, also known as parasites, leads to a competition for resources between the parasite and the designed replicon, and thus brings the reaction to an end, as it will be described in the following chapter.

1.3.2 Molecular parasites

One of the main challenges of protein-catalysed in vitro RNA replication and evolution in cell-free systems is the fast appearance of small "selfish" RNA sequences, also known as parasites, which can take over the system and often ultimately inhibit the reaction since they replicate faster than the genomic or heterologous in-silico designed RNAs (Lehman, 2012). As mentioned before, the formation of these small replicators was first observed in the 1960s during extracellular Darwinian experiments using RNA from the Qβ phage, conducted by Sol Spiegelman, and called by him “minimonsters” (Mills *et al*., 1967). These parasites often do not contain the replicase since their sequence shrinks after several generations. If no new resources are added externally to the reaction, they can dominate through a functional loss of self-replicating molecules and drive the whole system to the end (Bansho *et al*., 2012; Koonin *et al*., 2017). Several groups have observed that parasitic molecules can compete with and even take over the main replicator, even in serial dilution experiments. Recent evidence suggests that the presence and formation of parasites is inevitable, and that parasites have likely exerted strong pressure on the evolution of more

complex life systems since prebiotic times and the presence of the very earliest molecular replicators, the latter of which must have been "infested" by molecular parasites (Eigen, 1971; Smith, 1979; Koonin and Martin, 2005; Koonin, Wolf and Katsnelson, 2017).

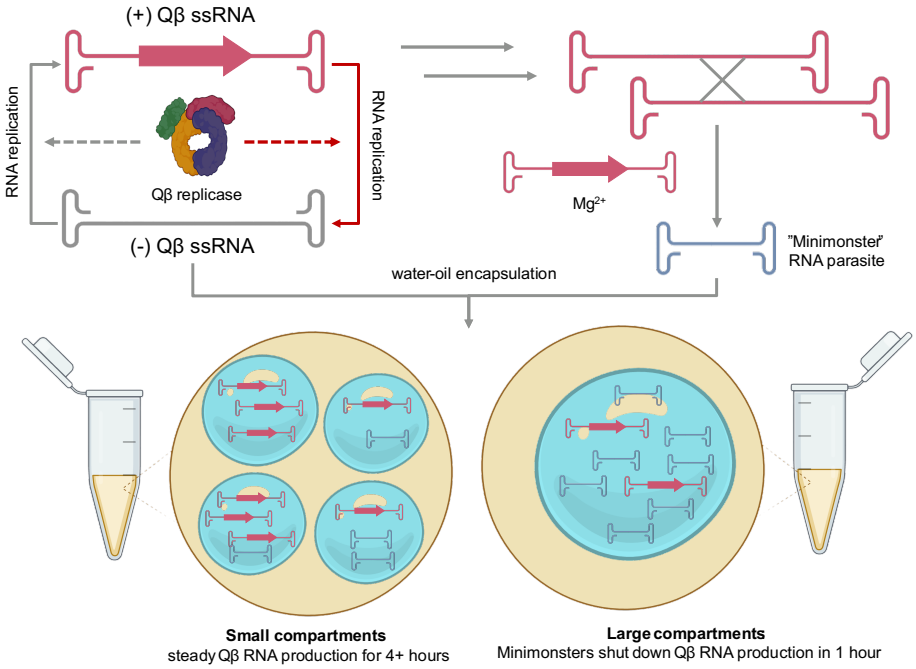

Figure 6: Mechanism of formation and containment of molecular parasites. *The Qβ replicase is a highly processive enzyme that allows for the production of the (-) strand from the (+) strand of its own genome or a heterologous template. Several other species, known as parasites, can arise from replication errors or non-homologous recombination mechanisms driven by the presence of* Mg^{2+} *and hot-spot regions internally present in the specific replicon. The formation of parasites has a negative impact on the yields. Compartmentalizing the reaction in small compartments can increase the reaction's suitability and prevent the formation of parasitic RNA, resulting in a longer-lasting reaction. Larger compartments are less efficient than smaller ones (Lehman, 2012).*

As shown by the Ichihashi group, in long-term evolution experiments where Qβ is incubated with a heterologous replicator carrying the Qβ replicase gene, the error-prone replicase introduces mutations randomly into both the host and parasitic RNAs and two types of parasites are produced. One is short, replicates very fast, its formation is rare, but when occur, drives the reaction to the end completely, and it is the result from deletion of the internal replicase gene from the original template RNA by heterologous recombination, and cannot produce a functional replicase. The other is long, replicated with a similar kinetics of the template RNA and results from mutations that lead to the formation of a non-functional replicase. Both short and long parasites depend on the Qβ replicase from the host template RNA for replication (Bansho *et al.*, 2012; Ichihashi *et al.*, 2013). Therefore, the major causes of parasite production, as also observed by other groups, can

be attributed to non-homologous recombination (Bansho *et al*., 2012; Chetverin *et al*., 1997), spontaneous Mg^{2+}-ion-catalysed strand exchange in specific sequences, trans-esterification reactions involving the 3′ end of RNA (Lutay, Zenkova and Vlassov, 2007), or the sloppy replication activity of Qβ replicase in the presence of Mg^{2+} that can lead to the production of parasitic products with some recombinase activity (Lehman, 2008) **(fig. 6)**. To ensure long-term replication of a selected replicon, it is necessary to contain or ideally repress completely the formation of parasites.

In nature, primitive cells, as well as procaryotic and eukaryotic cells, have developed various methods to deal with parasite formation and to protect themselves from entities that do not contribute to the maintenance and survival of the cell, including hypercycles, spatial heterogeneity, DNA, and, maybe the most important, compartmentalization (Lehman, 2012). The latter can be seen as the development of organelles to separate reactions.
In the laboratory setting, the most relevant and efficient evidence that compartmentalization is an effective tool for parasite formation were provided by the Yomo group and later by the Griffith group. The Yomo group showed that a heterologous RNA replicon based on the MDV-1 scaffold carrying the Qβ replicase gene produced fewer parasite species of 220 nt via Mg^{2+}-catalyzed non-homologous RNA-RNA recombination starting from specific sequences present in the (+) strand and leading to the generation of sequences similar to the Spiegelman's "Monster", as previously called MDV-1. The system was able to operate for a longer time in water-in-oil droplets of about 2 μm diameter and produced more parasites in droplets larger than 10 μm. The larger droplets produced a higher number of parasites, which led to the completion of template replicon production due to resource depletion within the droplet. One of the most interesting observations that come out of this study is that small compartments are more efficient in preventing parasite formation than large ones. This can also be observed from an evolutionary perspective, where many small cells are more efficient than larger ones (Lehman, 2012). Four years later, the Griffith group demonstrated, using a sophisticated droplet-based microfluidic setup, that compartmentalization of an MDV-1-based replicon carrying a ribozyme in its (-) strand in water-in-oil emulsion, combined with cycles of transient compartmentalization and mixing, can effectively suppress the spontaneous production of parasitic RNAs and maintain the proper function of the replicon RNA under continue selection pressure. The ribozyme digested a non-fluorescent RNA substrate, which allowed both the replication and the retention of the replicator activity to be observed and verified **(fig. 7)**. This selection process

enabled the identification of droplets that retained the replicator with replication activity, thereby eliminating those containing a high number of parasites (Matsumura *et al.*, 2016). The results presented by the Griffith group provide extensive evidence that compartmentalization is a crucial factor in constructing self-replicating systems in a laboratory setting. From an origin of life perspective, these results could shed light on the emergence of the first replicators and their evolution towards periodic compartmentalized systems. These systems could take advantage of pre-existing abiological compartments such as aerosols (Dobson *et al.*, 2000), hydrothermal vents (Koonin and Martin, 2005b), eutectic ice (Kanavarioti, Monnard and Deamer, 2001), minerals (Szabó *et al.*, 2002), or lipids (Luisi, Walde and Oberholzer, 1999). It is important to note that this is an objective evaluation and not a subjective one. Therefore, while parasites may be viewed negatively in the context of building self-replicating systems in synthetic biology, and their containment is an important step towards increasing efficiency and duration of the system, they can also be viewed as drivers of evolution towards more complex systems during the evolution of primitive life.

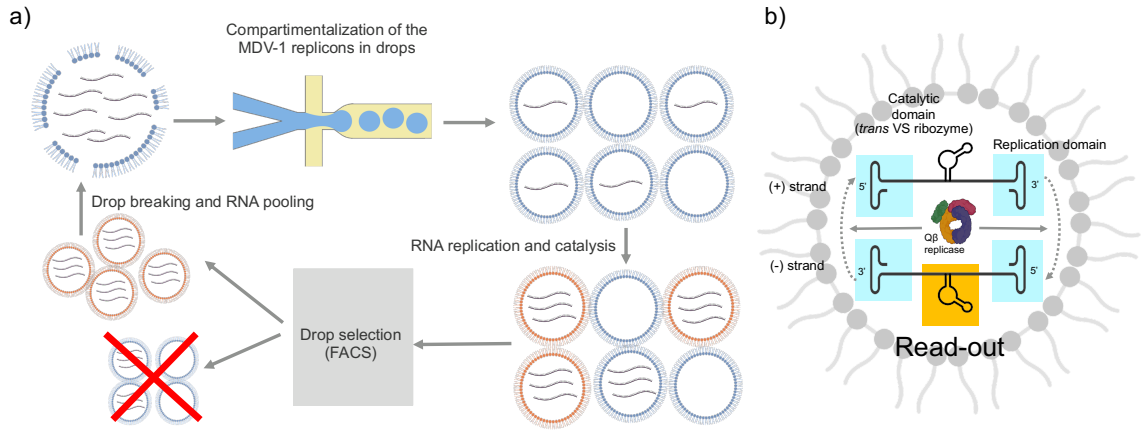

Figure 7: Transient compartmentalization contains the emergence of parasite in Qβ templated reactions. a) *Microfluidic encapsulation and selection protocol by the Griffiths group in order to contain the formation of parasite and enhance the specific replication of the targeted replicon. The RNA replicons are first encapsulated in droplets with the Qβ replicase. Then, the RNA replication is carried out by the replicase, resulting in the formation of a pool of droplets containing the replicator emitting the fluorescent signal, the parasite, and empty droplets. The droplets that give a positive fluorescent read-out are selected via fluorescent-activated sorting, and the non-fluorescent ones are discarded. The positively selected droplets then take part in another cycle of encapsulation and selection.* ***b)*** *Structure of the replicon designed by the Griffiths group. The structure includes the MDV-1 replication domain and the catalytic domain, followed by the trans VS ribozyme. In the presence of the substrate, the ribozyme cleaves it, allowing the Alexa 594 fluorescent product to emit. This confirms the successful production of the (-) strand by the Qβ replicase (Matsumura et al., 2016).*

1.4. Virus as natural architects: RNA nanotechnology and pRNAs

Viruses can be viewed as complex replicating machines and natural architects. The intricate and complex structural components of viruses have been exploited in materials science, nanotechnology, and synthetic biology, contributing significantly to the emerging field of RNA nanotechnology, which is focused on the characterization, manipulation, modification, and assembly of the RNA molecules at the nanoscale (Schmidt and Eberl, 2001; Baneyx, Baugh and Vogel, 2002; Niemeyer, 2002; Goldberger *et al*., 2003). RNA, in this case, can be seen as simple building block via modular and sophisticated assembly principles for the bottom-up construction of more complex structures (Cruz and Westhof, 2009). Compared to DNA, RNA is thermodynamically more stable and a versatile molecule with different structures, folds, and functions that can be designed similarly to DNA and, similarly to proteins, can fold in complex ways, such as forming single-stranded loops for cis- and trans-molecular interactions (Guo, 2005; Haque *et al*., 2018). This approach has enabled the construction of nanostructures by assembling multiple RNA molecules with different folding patterns and origins, including nanoparticles, bundles, membranes, and

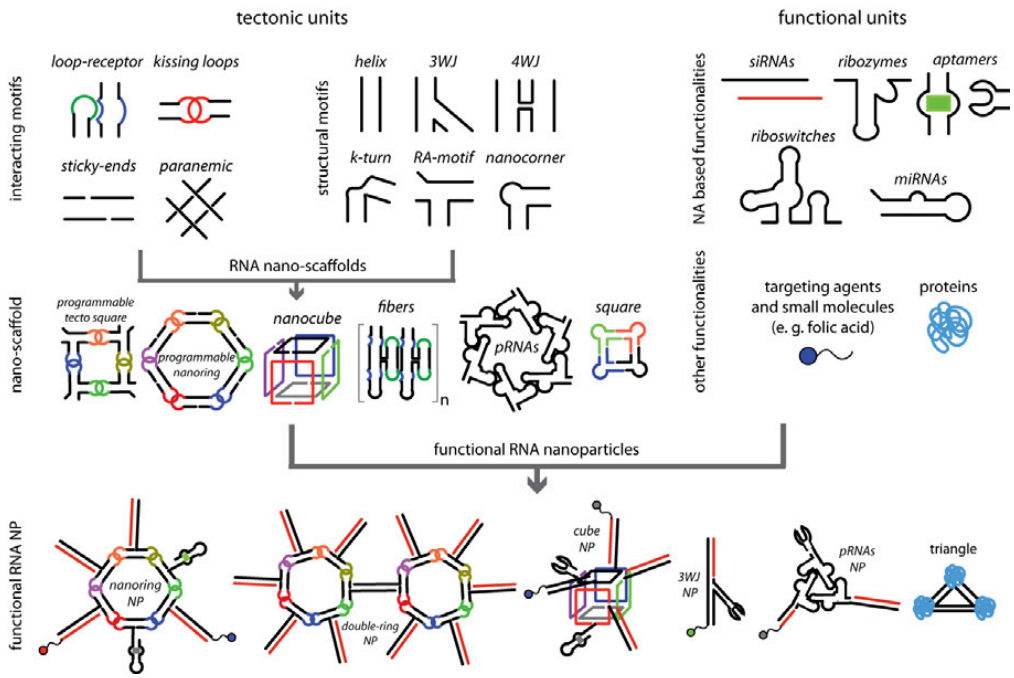

Figure 8: Overview of the modules used in RNA nanotechnology*. Complex and modular structures can be assembled from simple parts, including tectonic units that give the nanostructure its shape and functional units that give it its function. This makes RNA nanotechnology a potential application in biosensors and nanomedicine (Afonin, Lindsay and Shapiro, 2013). Figure reproduced with permission from the publisher De Gruyter.*

polygons (Cruz and Westhof, 2009). To date, several types of structured RNA molecules that can be used as starting scaffold units have been discovered in natural contexts or designed in-silico, characterized, and subsequently used to assemble an incredibly huge variety of complex and robust RNA nanostructures. Among the most commonly used and relevant structural motifs are the 3-Way junction (3WJ) (Lescoute and Westhof, 2006; D. Shu *et al*., 2011), 4-Way junction (4WJ) (Laing and Schlick, 2009), kink-turn (Schroeder *et al.*, 2010), hairpin (Leontis, Lescoute and Westhof, 2006), pseudo-knot (Bindewald *et al.*, 2011), C-loops (Leontis, Lescoute and Westhof, 2006), rectangular motif (Severcan *et al.*, 2009), tetraloop receptor (Afonin *et al.*, 2012), paranemic motif (Afonin, Cieply and Leontis, 2008), and kissing loop (Bindewald *et al*., 2008; Shu, Haque, *et al*., 2013) **(fig. 8)**.

Among the most important and best-characterized structural examples of structural elements that provide stable and specific multivalent RNA:RNA interactions and that can be used as structural building blocks for the construction of larger nanostructures is prohead RNA (pRNA), included in the category of the 3WJs structures (Peixuan, Erickson and Anderson, 1987)

The discovery of this unique 174-nt pRNA molecule dates back to 1987, when it was discovered during the study of the packaging machinery of phi29 **(fig. 9)**, a DNA bacteriophage, which allows the DNA of the virus to be packed into a protein shell called the procapsid, fuelled by ATP (Peixuan, Erickson and Anderson, 1987). In this unique case, the viral packaging motor differs from other dsDNA phages in that it consists of a combination of proteins and a hexametric pRNA ring formed by hand-in-hand or loop-loop interactions, which is typically replaced by proteins in the same class of viruses (Rao and Feiss, 2008).

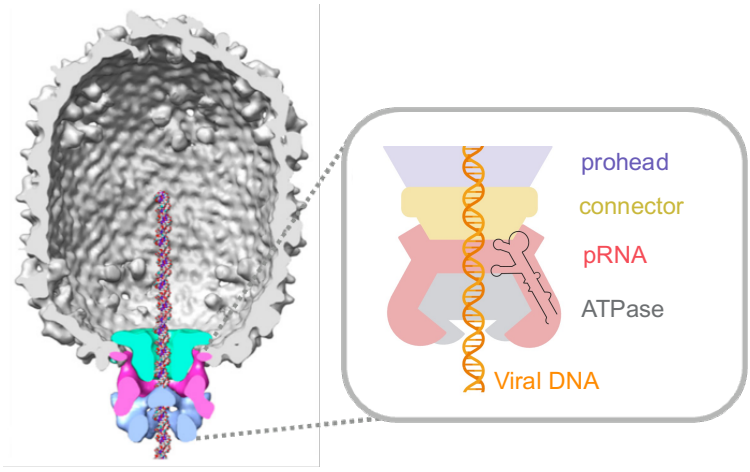

Figure 9: The phi29 DNA packaging motor. *The molecular motor comprises the viral capsid, connector, pRNA, and ATPase. The viral DNA is displayed in the centre. Cryo-EM reconstruction from S. Grimes et al., 2011. Cryo-EM image reproduced with permission from Elsevier.*

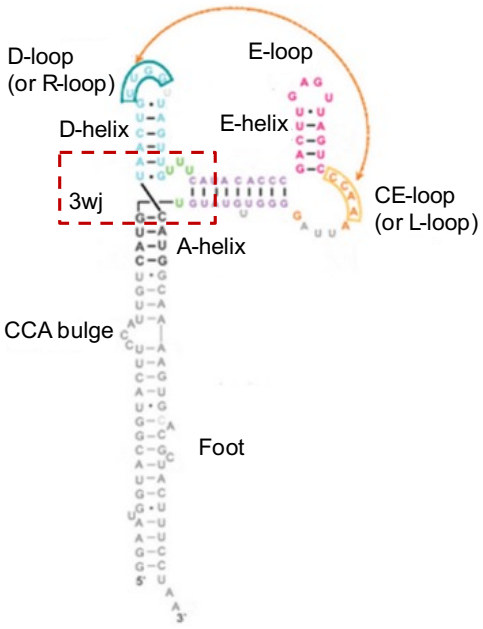

Figure 10: pRNAs. *Structural representation of the pRNA, which presents the 3WJ core (in red), the foot, and the essential loops required for binding and interaction formation the CE-loop (also called L-loop) and the D-loop (also called R-loop). Moreover, it's possible to see the name of the other helix structures and the CCA bulge present at the foot of the structure.*

Structurally, the pRNA molecule **(fig. 10)** is Y-shaped, mostly double-stranded, consisting of an A-helix domain consisting of paired 5′ or 3′ ends, called the foot, and a central domain formed by the 3WJ junction the core that confers flexibility and stability. The central domain branches into right (also called R-loop or D-loop) and left (also called L-loop or CE-loop) loops for intermolecular interaction with other pRNA monomers having complementary loop sequence (Y. Shu, Haque, *et al*., 2013).

The stability and function of pRNA assemblies are strongly influenced by the presence of divalent metal ions, particularly Mg^{2+} (or Mn^{2+}) (Zhang *et al.*, 2013). Different concentrations of these ions in solution can have a dramatic effect on folding, either exposing or hiding the binding sites that allow multiple monomers to assemble into a nanostructure (Draper, 2004; Kazantsev, Krivenko and Pace, 2009).

Within the D and CE loop sequences of each monomer, a sequence of 4-nt is responsible for the binding of two or more different pRNA molecules. These sequences can be engineered to design larger nanostructures formed by self-assembly of an increasing number of monomers in a bottom-up fashion. However, as shown, these structures are not stable in vivo, so increasing the complementary loop sequences to 7-nt leads **(fig. 11 and 12)** to higher thermodynamic stability of the assembled nanostructure due to increased binding stability between the two loop-loop interactions, in this case generating via modular design synthetic pRNAs that can be programmed in silico (Y. Shu, Haque, *et al*., 2013; Y. Shu, Shu, *et al*., 2013). Moreover, the synthetic pRNA has just 117-nt (Y. Shu *et al.*, 2011). Starting from single synthetic pRNA molecules, it is possible to design more stable ring-shaped assemblies of different valences. These assemblies offer greater control over size

and shape, as well as tuneable thermodynamic, chemical, and mechanical properties compared to their natural counterparts (Haque *et al*., 2018). Each pRNA is described with a specific annotation. The annotation consists of 'Ex' followed by a capital letter indicating the sequence of the CE-loop and a lowercase letter indicating the sequence of the D-loop, for example ExAb.

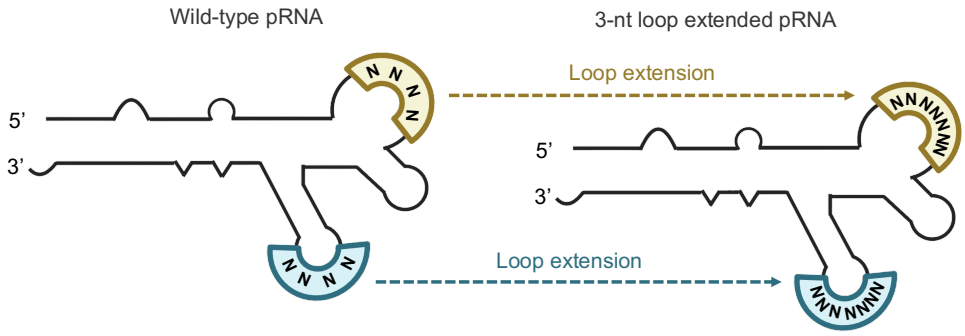

Figure 11: pRNA loop extension. *Compared to the wild type pRNA, the synthetic version modified by the Guo group has seven nucleotides that are essential for complementary binding with those present on the other pRNA molecule, enabling assembly into nanostructures. Adapted from Shu, Haque, et al., 2013.*

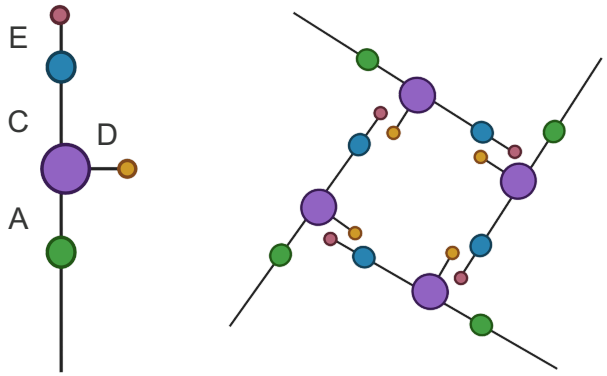

Figure 12: Ball (loops) and stick (helices) model of pRNA structure. *The self-assembly of multiple pRNA into nanorings is driven by the CE- and D-loops. The assembly follows a minimal pattern of interaction, allowing for the formation of complex and large nanorings from simple monomers.*

The pRNA nanorings have potential applications as delivery systems for targeting molecules with therapeutic potential in immunotherapy and chemotherapy (Pi *et al.*, 2017), such as siRNA (Afonin *et al.*, 2014), miRNA (Obad *et al.*, 2011), ribozyme (D. Shu *et al.*, 2011b) and aptamers (Pi *et al.*, 2017), to specific sites in the human body. These nanorings can be easily functionalized by incorporating them into the RNA nanoparticle scaffold

through sequence fusion. In addition, these assemblies are highly stable at high temperature and in 8M urea, making them a very good delivery technology (Shu, *et al.*, 2013).

1.5. RNA nanotechnology as tool for building multipartite RNA genomes

Having described viruses as marvellous engineers when it comes to their ability to store, replicate and transfer their genetic information, and as architects when it comes to building sophisticated structures based on proteins and RNA to assemble complex machines such as the viral packaging motor and envelopes such as capsids, these molecular technologies, brought to us by evolution, could be an exciting starting point for building bottom-up and top-down synthetic systems. These may hold the potential for a variety of biotechnological application or serve as a platform to recreate, in a controlled and artificial set-up, mode systems for primitive life forms, thus shedding light on the processes that led to the emergence and development of life on Earth. Recreating primitive living systems by taking parts from viruses could be a good place to start, as there is evidence that life in its earliest days relied solely on using RNA as genetic material in an age called the "RNA World" (Gilbert, 1986), before evolving into more complex organisms such as the Last Universal Common Ancestor (LUCA) (Theobald, 2010), probably a hybrid entity carrying both RNA and DNA (Siegel *et al.*, 1999; Di Giulio, 2006) that cannot be reconducted to any present living organism. As we know, today's cellular organisms encode genetic information exclusively on DNA, so recreating a potential hybrid synthetic cell could serve as models to study cellular systems that preceded LUCA.

In line with these concepts and objectives, this experimental work aims to integrate current advances in RNA nanotechnology with RNA self-replicating systems to generate multipartite and transferable RNA genomes, first in vitro and then in vivo, to recreate a potential RNA:DNA hybrid living and evolving cell that can recreate a potential precursor of LUCA, shading a light on primitive lifeforms. In addition, if seen in the context of nanotechnology, this could be the first time in the field that a replication capability has been given to static nanostructures, in this case RNA based. This breakthrough could lead to the engineering of nanostructures capable of replication for potential use in medicine and biotechnology.

More in the detail, the objective of this work is to explore the potential of combining the Qβ self-replicating system with the self-assembly capability of the pRNA to create

synthetic replicons and enable their replication. These replicons can be assembled into nanorings of various dimensions to construct small multipartite RNA genomes. Constructing with RNA and encoding information presents several challenges, including RNA's chemical instability and the error-proneness of viral replicases. This work will discuss one potential solution to these challenges: segmentation. Segmentation is a mechanism that increases resistance to mutations that can damage genetic information. This resistance can be further increased through segment reassortment, which selects only functional segments through division. This approach to genome construction is modular, achieved by segmenting coding regions as cargo in separate replicons, allowing increased modularity and coding capacity. This mechanism is also found in nature in some RNA viruses, may have been used by primordial RNA-based life forms, and may represent an essential requirement for the construction of RNA-based genomes. The non-covalent coupling of RNA segments (Takeda *et al.*, 2006) enables their replication and stable inheritance after cell serial transfers in an *in vitro* context or cell division if *in vivo* **(fig. 13)**. In addition to understanding the ideal conditions for self-assembly, it will be investigated whether it is possible to increase the size of the synthetic replicons by adding elements in the "cargo" region such as aptamers and genes to increase the coding capacity and functionality of the genome, while retaining the pRNA sequence that drives assembly into nanorings of different valences by the programmable intermolecular interaction of two RNA loops (Shu, Haque, *et al.*, 2013). The theoretical limit for the size of an RNA genome

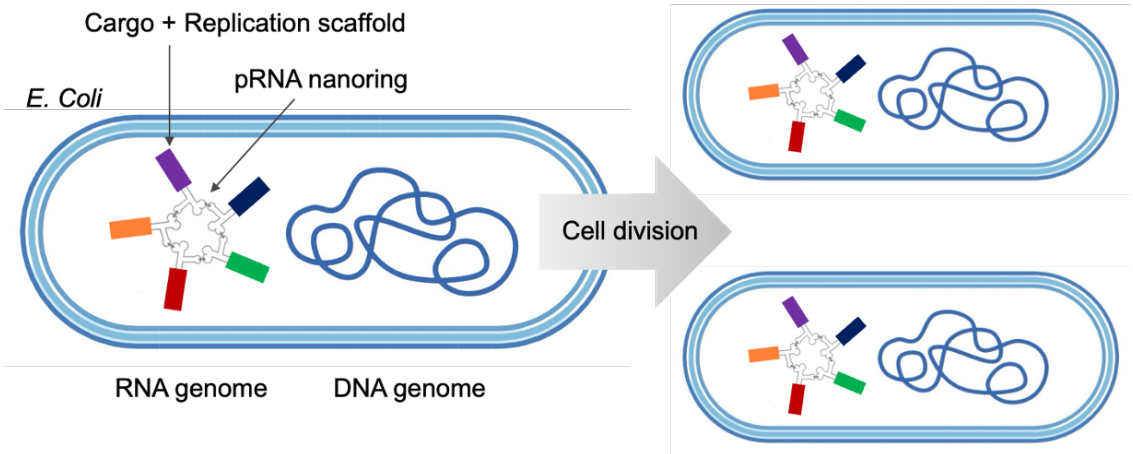

Figure 13: Mechanism of replication of an DNA:RNA genome. *The RNA genome is formed through assembly driven by pRNA sequences inserted in a Qβ replication scaffold and can be replicated by replicase. It can be transferred, along with the DNA genome, to new cells during cell division. Each module can be retained due to the efficient assembly of each segment in the nanoring structure.*

is estimated to be 20-30 kb, which is the basis for the coding of essential cellular functions (Holmes, 2003; Moya, Holmes and González-Candelas, 2004).

To maintain the RNA genome in a cell, a proper method for passing the segmented RNA genome is necessary. Viruses can efficiently fold their genome in their new capsids due to a system provided by evolution. However, in cells with a hybrid DNA:RNA genome, a potential segregation mechanism for the RNA part is necessary to avoid loss during division. Therefore, a methodology to transplant core cellular functions from DNA to RNA genomes is needed. In other words, achieving a stable genotype-phenotype coupling is crucial. One possible solution to this challenge could be to encode essential housekeeping genes and multiple selection markers on the RNA genome, while simultaneously knocking them out and selecting for cells that can survive and pass on the RNA segments to their progeny. This could be achieved through an evolutionary process, by adding survival pressure during several cycles of continuous evolution and selecting for cells that can retain the RNA genome due to a better fitness.

2. Aims and Objectives

The goal of this work is to evaluate the feasibility of transforming RNA nanostructures into multivalent and organized self-replicating systems capable of storing genetic information and able to assemble starting from physically linked and modular RNAs. As mentioned previously, RNA nanostructures can be designed to have specific sizes, shapes, and stoichiometries through RNA motifs, but they lack the ability to replicate. By combining the assembly of multiple pRNA molecules with the replication capability of the Qβ replicase, this capability could be achieved. The next step will be to evaluate the possibility of transplanting this system in vivo. This will allow the coexistence of DNA and RNA hybrid genomes in a way that allows the RNA genome to store housekeeping genes and facilitate its inheritance and maintenance during cell replication.

This work is divided into three sections and focus establishing and testing *in vitro* a basic technology for the construction of the RNA genome starting from simple replication modules that can be assembled in core units. The first section investigates the possibility of designing and testing various replicons based on the two replicating motifs, RQ135 and MDV-1 as platform, that can be recognized and replicated by the Qβ replicase. This section focuses on testing whether replicons carrying a structural domain, pRNA, and a light-up aptamer domain can be replicated by the replicase, and whether compartmentalization could be a valuable tool for containing parasite formation. It could be confirmed that compartmentalization is a necessary to contain the formation of parasites and enhance the specific replication of the input RNA replicons. Additionally, the co-replication of two replicons carrying two compatible pRNA motifs and two different aptamer domains was evaluated in one-pot reactions.

The second section of this work focuses on the evaluation of the assembly of the designed replicons for the two replicative scaffolds RQ135 and MDV-1. Higher hierarchy nanorings were successfully assembled starting from monomers and their stability analysed under different buffer conditions. In addition, a gel visualization of the assembly was obtained by RNA labelling of each replication with fluorescent UTP. This technique allowed us to accurately visualize each of the RNA monomers in the assembly.

The third and final section of this work investigates the possibility of coupling the previously achieved replication and assembly abilities of the replicons to build a self-replicating nanoring. In this phase, both RQ135 and MDV-1 replicons carrying pRNAs

were tested in bulk and in droplets. Unfortunately, this section's results did not confirm the replicability of our nanorings, which opens the door for potential system improvements.

3. Results and Discussion

3.1. Engineering and replication assays of Qβ-derived RNA replicons

3.1.1. Background and concept

The initial section of this work is focused on building a synthetic self-replication system based on the Qβ replicase system. As a result, various scaffolds will be tested to determine the optimal conditions for efficient replication of the replicons carrying a cargo, such as a structural motif, pRNA, a gene, sfGFP, and a light-up aptamer domains, F30-Broccoli and F30-Mango. In the case of the aptamers, these will be found to be very efficient to be used as a readout system to monitor the development of the replication reaction (Weise *et al*., 2019). The Qβ replicase possesses unique and desirable features that make it suitable for developing an artificial self-replication system. The high amplification efficiency of this genome allows for significant amplification, with the potential for a 10,000-fold increase within one hour (Brown and Gold, 1996). Additionally, potential heterogenic templates present specific characteristics that enable rapid and efficient replication (Singleton *et al*., 2018). Furthermore, the replicase has an ideal template flexibility, allowing it to use both (+) and (-) RNA strands as templates. This enables exponential amplification and differentiation between its own RNA and host RNA. Additionally, Qβ replicase offers advantages in terms of purification efficiency and activity preservation in cell-free extracts, resulting in high purification efficiency (Zhang and Wu, 2020). In this section, two templates are exploited in order to design synthetic replicons, RQ135 and MDV-1, both recognised and replicated by the Qβ replicase. Although both templates are efficient for the Qβ replicase and are efficiently replicated by it, they have different origins and sequences. RQ135 RNA is 135 nucleotides long and its sequence consists entirely of segments that are homologous to ribosomal 23S RNA and the phage lambda origin of replication (Morozov *et al.*, 1993; Ugarov *et al.*, 1994). The sequence segments are not related to the sequence of Qβ bacteriophage genomic RNA. Despite its sequence consisting entirely of segments that are homologous to ribosomal 23 RQ135 RNA is replicated in vitro at a rate equal to the most efficient of the known Qβ RNA variants (Munishkin *et al.*, 1991). The other RNA replicon template, MDV-1, serves as a natural template for the Qβ replicase. It contains tRNA-like structures at its terminal end, similar to those found at the ends of most phage RNAs. These structures enhance the stability of embedded mRNA sequences (Mizuuchi,

Usui and Ichihashi, 2020a). The nucleotide sequences of both the 3' terminus and the central binding region of MDV-1 (+) RNA are nearly identical to sequences at the 3' terminus and an internal region of Qβ (-) RNA (Weise *et al.*, 2019). The Qβ replicase initiates replication on RQ135 RNA through its 3'-terminal CCC cluster, which matches the 5'-terminal GGG cluster of the replicase. This recognition is not based on sequence-specific primers or promoters, but rather on the structural features of the RNA template (Chetverin, 2004; Ugarov and Chetverin, 2008).

During the replication reaction, a common challenge is the spontaneous formation of parasites, which are smaller replicators that can cause the extinction of the main replication reaction. These small replicators are also recognized by the Qβ replicase and replicate at a faster rate (Koonin, Wolf and Katsnelson, 2017; Furubayashi *et al.*, 2020). Also, in this work it will be noticed that parasites will form and therefore solutions for their containment will be investigated. Encapsulation of the self-replication reaction in a water-oil emulsion system has previously been shown to be an effective method of limiting parasite formation (Matsumura *et al.*, 2016) and will therefore be one of the options considered.

The final section of the chapter will evaluate whether two similar MDV-1 replicons can be co-replicated in the same reaction using the Qβ replicase.

3.1.2. Results

The development of a self-replicating system requires two critical components: a replicase, in this case Qβ, and a suitably designed and structured RNA template, also called replicon, that possesses all the features necessary for efficient recognition and replication by its replicase.

Purification of the Qβ replicase. The Qβ replicase was not available on the market and had to be the subject of recombinant in-house expression and purification. In the first section of the project, where the RQ135 based replicons were tested, a first Qβ batch (Qβ PB1) with a lower level of purity was used, as described in the Materials and Methods section. For all the following sections, starting from the test of the MDV-1 replicons in a water-oil emulsion, a second Qβ batch (Qβ PB2) was used. This second batch was obtained after several crucial purification steps, resulting, in an extremely polished Qβ available for experimental use, without potential residual nucleic acid contaminations.

As a first step of this project, Qβ PB1 was expressed and purified with a protocol adapted from Kita *et al*., 2006, and present in material and methods. In order to construct self-replicating systems based on the Qβ replicase in vivo, it was necessary to purify the Qβ in the presence of its essential host factors S1, EF-Tu and EF-Ts, which are already present *in vivo* in *E. coli*, where are involved in protein synthesis, but not in vitro, and are crucial for the formation and functional of the fully functional Q-replicase holoenzyme (Takeshita and Tomita, 2010; Urabe *et al*., 2010; Tomita, 2014). Therefore, they must also be expressed in *E. coli* concomitantly with the replicase. The S1 protein plays a crucial role in preventing the formation of RNA duplexes during the production of the (-) strand by the replicase from the (+) strand. This is essential for ensuring the exponential amplification of heterologous RNA without the formation of dsRNA that could prematurely terminate the reaction (Vasilyev *et al.*, 2013).

A plasmid containing Qβ with all subunits (pBAD33utsfusion) and cofactors EF-Tu and EF-Ts was already available in-house and was used for overexpression and purification. Since S1 has been shown in the literature to co-purify with Qβ when expressed in *E. coli*, expression of the S1 factor was omitted. This phenomenon has been proven to occur since Qβ has a strong affinity for S1, and for the other cofactors EF-Tu and EF-Ts (Vasiliev *et al.*, 2010; Vasilyev *et al.*, 2013) and it facilitate the expression. A potential problem present in literature is that the Qβ replicase core complex can separate into monomeric and dimeric fractions during purification and therefore compromise the *in vivo* activity of the enzyme (Gytz *et al.*, 2015). The purification was performed as described in the general section of material and methods. Following the purification, Qβ PB1 replicase activity was assayed in combination with a control template.

Self-replication assays of RQ135-based replicons in bulk. After the purification the Qβ PB1 replicase, a suitable scaffold was required to facilitate the functional replication of our structural cargo sequence, the pRNAs. As first choice, the RQ135 replicating scaffold was selected for the purpose since it was already cloned on a plasmid in-house (pGEMT_RQ135 NotI + EcoRV) and, moreover, it was shown to be one of the most efficient Qβ replicase RNA templates to date (Munishkin *et al.*, 1991; Ugarov *et al.*, 1994). To preserve its folding, the pRNA sequence was inserted at position 54 of the RQ135 replicon sequence **(fig. 14)**.

After inserted the novel sequence, the preservation of both the pRNA and RQ135 folds were subsequently verified in silico using RNAfold Vienna **(fig. 15)**. When adding new cargos, it is highly recommended to perform an in-silico structure preservation check of the 5' and 3' UTR. This is because the recognition mechanism of the Qβ replicase relies heavily on structure, as previously described. Disrupting the folding of the 5' and 3' UTR sections leads to non-recognition by the replicase.

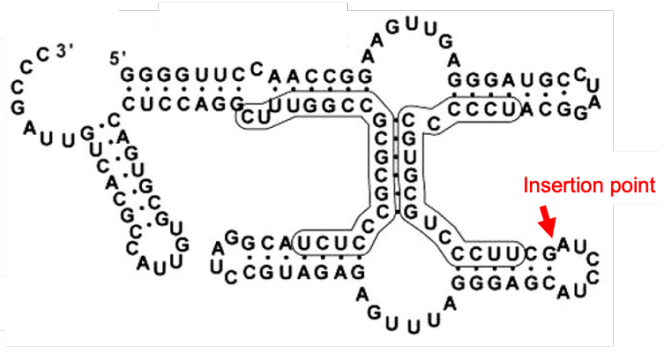

Figure 14: RQ135 scaffold. *In red is indicated the insertion point where the cargos were inserted in order to maintain the proper folding of the RQ135 sequence. Adapted from Ugarov, Demidenko and Chetverin, 2003.*

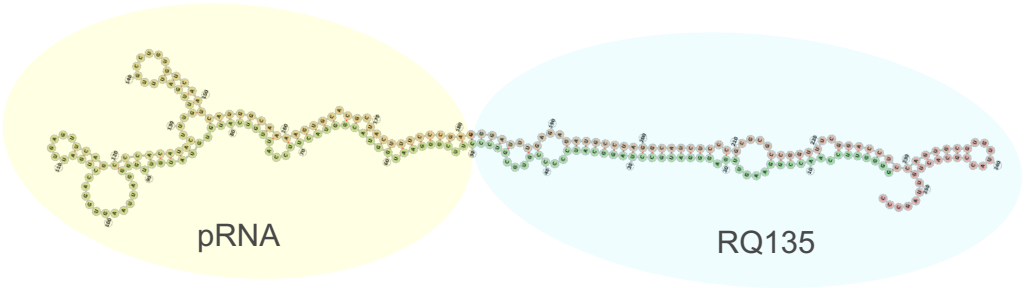

Figure 15: RQ135_pRNA structure. *The folding of the newly designed replicon RQ135, which carries a pRNA as cargo, was predicted by RNAfold Vienna. As can be seen, the structural pRNA module and the RQ135 replicating scaffold maintain their correct fold after the insertion.*

Two replicons were designed and tested. Since a plasmid carrying the sfGFP as cargo located in between the RQ135 5' and 3' UTR was already assembled before in our group, two new plasmids were assembled by Gibson assembly as describe in material and methods, leading to the final construct *1.3_Assembled_pgemt_rq135notiecorv+pRNA*, and *1.6_Assembled pgemt_rq135notiecorv + pRNA + sfGFP*, carrying, respectively, a single pRNA sequence and a pRNA sequence and the sfGFP gene.

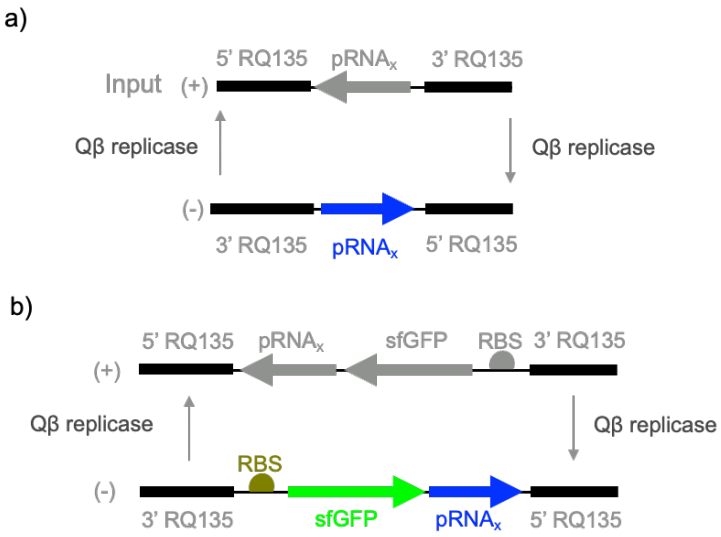

Figure 16: Replication mechanism of the RQ135_pRNA and RQ135_sfGFP_pRNA. a) *The (+) strand of the RQ135_pRNA template is added to the reaction and the (-) strand is synthetised by the Qβ replicase. The pRNA sequence is functional when the (-) strand is produced, making it a suitable read-out to test the success of the replication reaction by Qβ.* ***b)*** *Same mechanism for the RQ135_sfGFP_pRNA. RBS: ribosome binding site.*

Afterwards, the two new replicons were amplified from the plasmid via PCR from the two previously assembled plasmids *1.3_Assembled_pgemt_rq135notiecorv+pRNA* and *1.6_Assembled_pgemt_rq135notiecorv+pRNA+sfGFP* and then the 2 separate IVTs were carried out in order to obtain the RNA replicons RQ135_pRNA (261 nt) and RQ135_pRNA_sfGFP (1017 nt). **Fig. 16** show the details of the composition of the RQ135 based replicons here designed and the orientation of each component on the (+) and (-) strand, a crucial factor that impacts actively they functionality. In both cases, the pRNA sequences in the RQ135_pRNA replicon and the RBS, sfGFP, and pRNA sequences in the RQ135_pRNA_sfGFP replicon become functional only when the (-) strand is produced by the Qβ replicase since they will be on the right orientation **(fig. 16)**. In the case of the replicon carrying the sfGFP, if it were added to a PURE system, lysate, or *E. coli*, where a translation system is present, ribosomes can bind to the (-) strand and synthesize the resulting protein.

To determine whether Qβ was able to recognize and replicate the two replicons, replication assays were set-up as followed. All these preliminary experiments with the RQ135 scaffold were performed in bulk. For these assay, 8 nM of template RNA and 5 nM of template RNA for the RQ135_pRNA_sfGFP were added to the replication reactions. For each of the

two replicons different concentration of Qβ replicase PB1 where tested, respectively 0 nM, 10 nM and 100 nM, and samples were taken at time 0 hours (0h), 1 hours (1h), 2 hours (2h), 3 hours (3h). The reaction buffer (RQ135 buffer) was composed of 0.25 mM each rNTP (1 mM in total), 1 mM Tris-Cl (pH 7.5), 100 mM $MgCl_2$, 5 mM EDTA and 1% Triton X-100. Replication was characterized by 1% denaturing agarose gel electrophoresis.

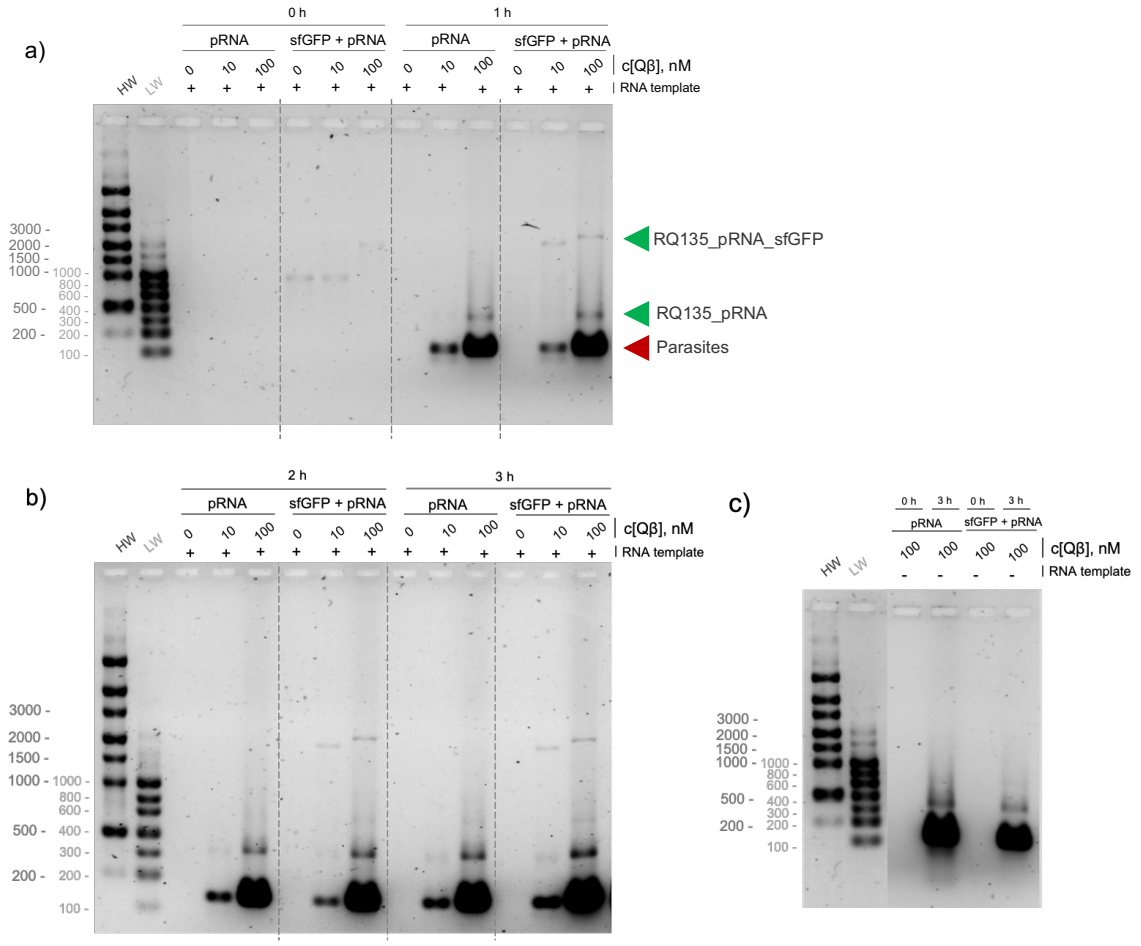

Figure 17: Replication assay of RQ135_pRNA and RQ135_pRNA_sfGFP replicons. *1% Agarose gel of the self-replication reaction of RQ135_pRNA (261 nt) and RQ135_pRNA_sfGFP (1017 nt) replicons. Each template was incubated with 0, 10, 100 nM of Qβ replicase at 37 °C and samples were taken at 0, 1* ***(a)****, 2, 3 hours* ***(b)****. Controls without the RNA template were also run* ***(c)****. The red arrow indicates the presence of parasites at lower sizes. HW: RiboRuler High Range ssRNA Ladder (nt). LW: RiboRuler Low Range ssRNA Ladder (nt) (Thermo).*

From the gels, it was observed that the replicon RQ135_pRNA **(fig. 17)** was effectively replicated as evidenced by the band at around 261 nt and an increase in yields over time. In addition, the formation of other non-specific products in higher amount was also observed. This was attributed to the formation of parasites by de novo synthesis and amplification of short RNAs by the replicase from simple rNTPs in the solution or from

the surrounding environment, as previously observed by (Chetverin, Chetverina and Munishkin, 1991), or templated, presumably based on nucleic acid contamination present in the Qβ stock. This spontaneous formation was also observed by other groups (Moody *et al.*, 1994), and represent a serious limitation to the development for the sustainability of the self-replicating system in this work.

The replication of the RQ135_pRNA_sfGFP replicon by Qβ replicase **(fig. 17)** exhibited similar results. Specifically, replication of our targeted replicon was observed (band about 1017 nt) at 1 hour, but there was no increase in intensity at t = 4 hours, indicating that the reaction stopped and there was no more product formation after that time. Furthermore, it was noticeable that the band has shifted towards higher sizes. This suggests that the Qβ replicase may still be attached to the replicon, which could explain the observed shift. The termination of the reaction after four hours could be explained by the parasite taking over the resources, competing with the desired replicon and thus stopping its replication. These findings highlight the issue of parasite formation, which negatively affects the yield of our replicon due to faster replication. It was important to find solutions to contain this issue.

Self-replication assays of MDV-1-based replicons in water-oil emulsion. To achieve higher yields of our desired replicon and prevent parasite formation, the reaction was encapsulated into water-in-oil droplets. Numerous research groups have previously used this solution to contain parasite formation during the Qβ replication reaction (Bansho *et al.*, 2012). To design the new water-oil emulsion system, inspiration was drawn from research carried out by the Griffiths group in which a replicon containing a VS ribozyme as a cargo between the 5'-UTR and 3'-UTR of MDV-1 (Nishihara, Mills and Kramer, 1983) was

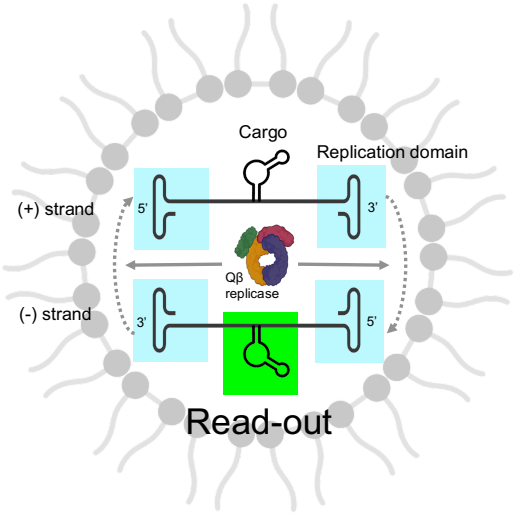

Figure 18: Water-oil emulsion self-replicating system based on the MDV-1 scaffold. *The MDV-1 scaffold, carrying a payload of interest, is encapsulated within the Qβ replicase reaction in droplets formed by the water-oil emulsion. Replication occurs when the (-) strand is synthesized. In the case of a fluorescent read-out, the sequence of the payload is now in the correct orientation and provides the detection of the signal. This system makes it possible to contain the parasite formation.*

encapsulated and replicated in a microfluidic system in a cyclic manner. This work allowed, beside a control of the droplet size, for an estimation of the parasite formation rate and containment through encapsulation (Matsumura *et al.*, 2016).

Having the system designed by the Griffiths group in mind, the design of a new MDV-1 replicon tailored the purposed was carried on **(fig. 18)**. Both for the aim to have a visible read-out and test if the increasing of the length of the cargo sequence could impact the recognition and the replicability of our MDV-1 replicon, a fluorescent aptamer, F30-Broccoli (F30Bro), was added in between the 5' and 3'UTR of the replicon leading to the creating of MDV-1_F30Bro of a final length of 353 nt. The F30-Broccoli aptamer was selected for their short sequence and strong fluorescence enhancement upon ligand binding (Filonov *et al.*, 2015). The inverted and non-functional sequence of the F30-Broccoli aptamer has been inserted into the (+) strand. The functional sequence of the aptamer is only present in the (-) strand; thus the read-out can only be detected if the Qβ replicase recognizes our starting (+) strand and synthesizes the (-) strand accordingly **(fig. 19)**. This allowed us to verify that the replicase recognizes and replicates our designed replicon. The The RNAFold Vienna software was used to simulate the prospective structural integrity of each section of the newly designed replicon containing the fluorescent aptamer F30-Bro and the MDV-1 replication sequences. **(fig. 20)**.

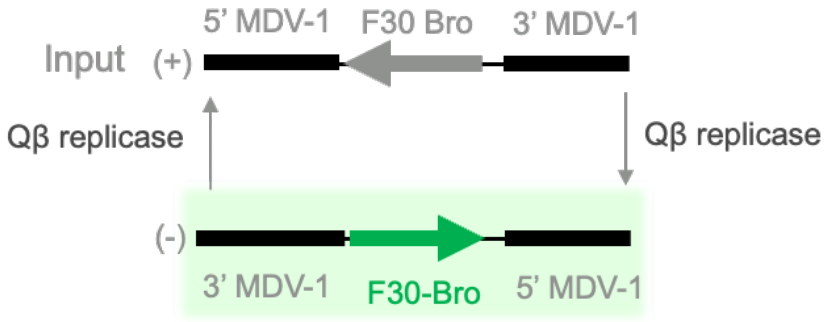

Figure 19: Replication mechanism of the MDV-1 _F30Broccoli replicon. *The (+) strand of the MDV-1 _Bro template is added to the reaction and the (-) strand is synthetised by the Qβ replicase. The F30-Broccoli aptamer is functional when the (-) strand is produced, making it a suitable read-out to test the success of the replication reaction by Qβ.*

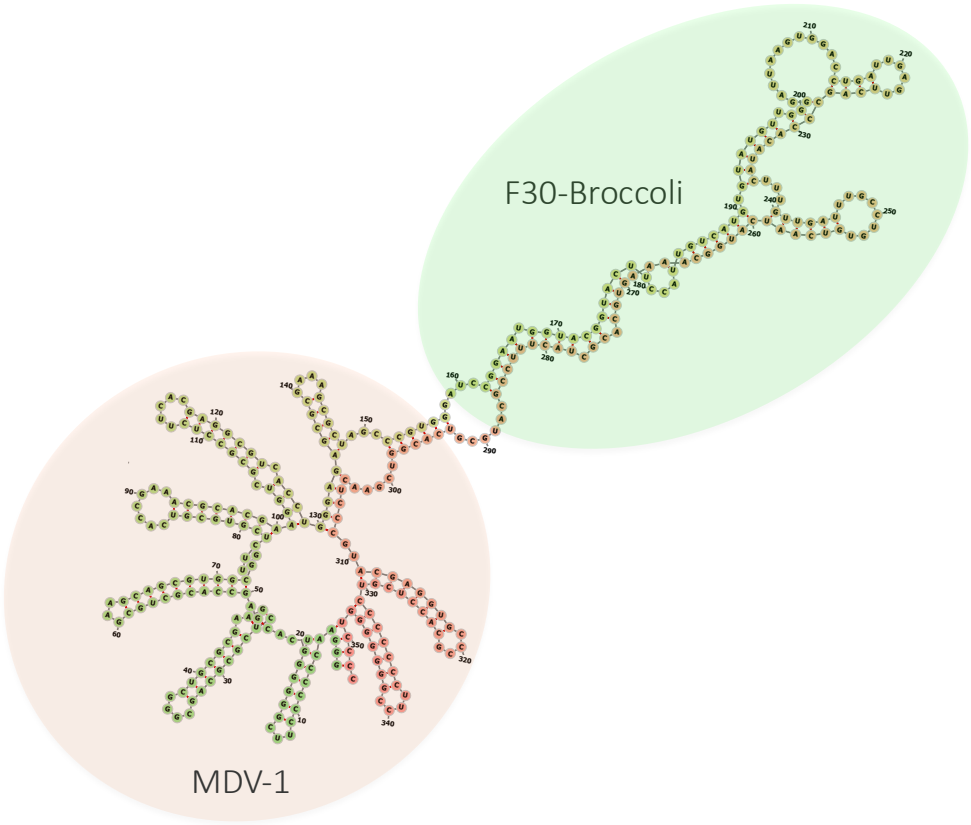

Figure 20: (-) MDV-1 _F30Bro_pRNA*. RNAfold Vienna in-silico folding prediction of the (-) strand of the MDV-1 _F30Bro replicon. F30-Broccoli: fluorescent unit. MDV-1: replication unit.*

To avoid the risk of nucleic acid contamination during enzyme purification, which could also explain the proliferation of parasite species during the previous self-replication assays with the RQ135 replicons, a new batch of Qβ (Qβ PB2) was obtained in collaboration with the Max Plank Institute of Biochemistry protein purification facility in Martinsried, as described in the general section of the Materials and Methods . This batch achieved a high level of purity, and, therefore, was used in all future assays.

In order to test if our new replicon MDV-1_F30Bro was able to be recognized and replicated by the Qβ in emulsion conditions, a new replication assay protocol was set-up. Three different concentrations of Qβ PB2 were tested (0 mM, 100 mM and 321 mM) and reactions aliquots were taken at 0 hours and 3 hours. The reaction buffer used was the MDV-1 buffer, also used by Matsumura *et al*., 2016. The aliquots there were run on an 8% urea-PAGE gel and stained accordingly in a specific buffer containing the Broccoli aptamer ligand DFHBI to selectively detect the MDV-1_F30Bro replicon if replicated **(fig. 21)**.

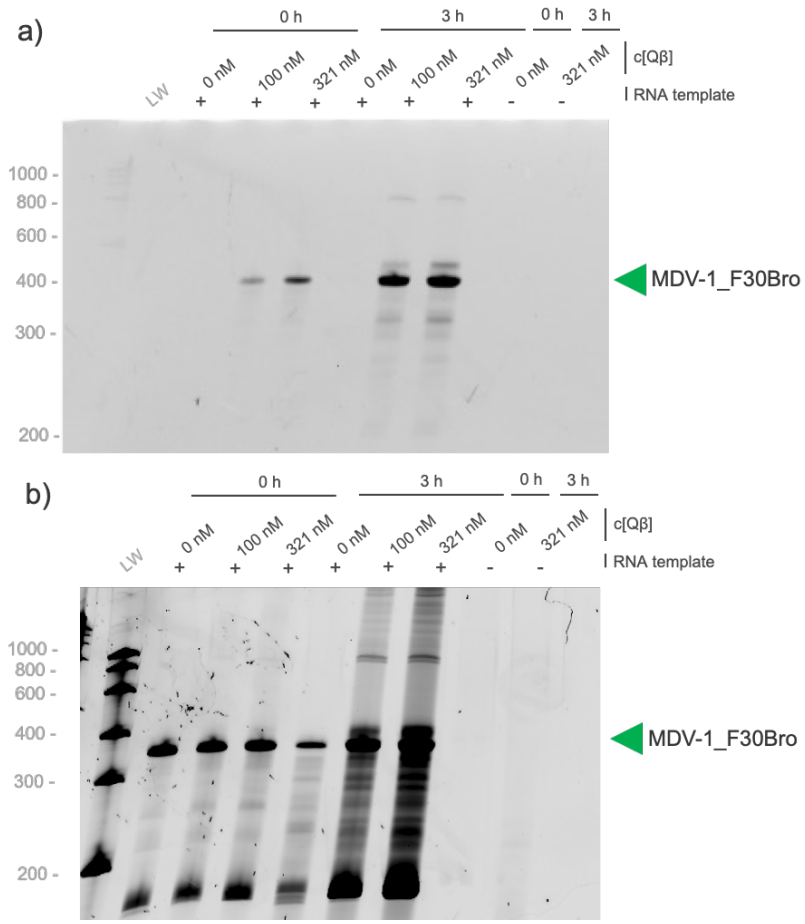

Figure 21: Replication assay of MDV-1 _F30Broccoli replicon in water-oil emulsion. *8% urea-PAGE of the replication assay for the MDV-1 _F30Broccoli template (353 nt).* ***The RNA template*** *was incubated with 0, 10, or 321 nM of Qβ replicase at 37°C in a water-oil emulsion system, as described in the Materials and Methods section. Controls without the RNA template were also run. Samples were taken at 0 and 3 hours.* ***a)*** *DFHBI stain,* ***b)*** *SYBR Gold stain. LW: RiboRuler Low Range ssRNA Ladder (nt) (Thermo).*

The use of the new scaffold and the emulsion systems resulted in improved yields, allowing the replicon to be selectively replicated by the Qβ replicase. With the new set-up, parasitic species emerged, as shown in Figure 23 of the SYBR Gold-stained gel. In comparison to previous experiments with the RQ135 scaffold, it appears that the formation of the parasite did not lead to a decrease in yields of the specific replicon.

After confirming the functionality of replicon MDV-1_F30Bro, a pRNA sequence was inserted between the F30Bro sequence and the (+) strand MDV-1 3'UTR (MDV-1_F30Bro_pRNA$_{ExAb}$) and a final length of 475 nt **(fig. 22)**. We previously explained that the recognition mechanisms of Qβ are primarily structural. Therefore, we utilized the RNAVienna Fold to confirm that each component of the newly designed replicon could

maintain its structure when a new sequence was added **(fig. 23)**. It should be noted that, similar to the F30-Broccoli aptamer, the pRNA sequence was added in the opposite direction and thus will only be functional if the (-) strand is synthesized by the replicase. The ExAb sequence of the pRNA list **(table 8.3)** was selected.

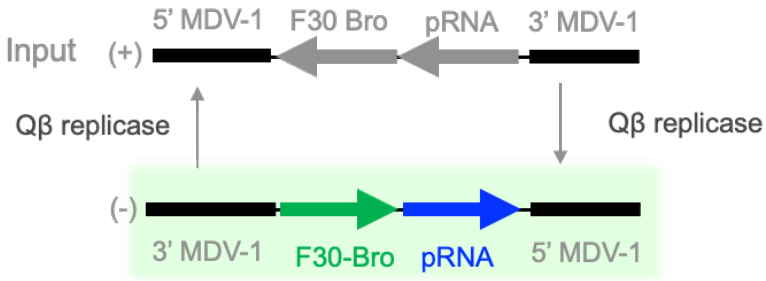

Figure 22: Replication mechanism of the MDV-1 _F30Broccoli_pRNA replicon. *The (+) strand of the MDV-1 _Bro template is added to the reaction and the (-) strand is synthetised by the Qβ replicase. The F30-Broccoli aptamer is functional when the (-) strand is produced, making it a suitable read-out to test the success of the replication reaction by Qβ. The same thing occurs with the pRNA sequence, when the (-) strand is produced, it can be in the correct orientation to obtain the correct fold for the assembly.*

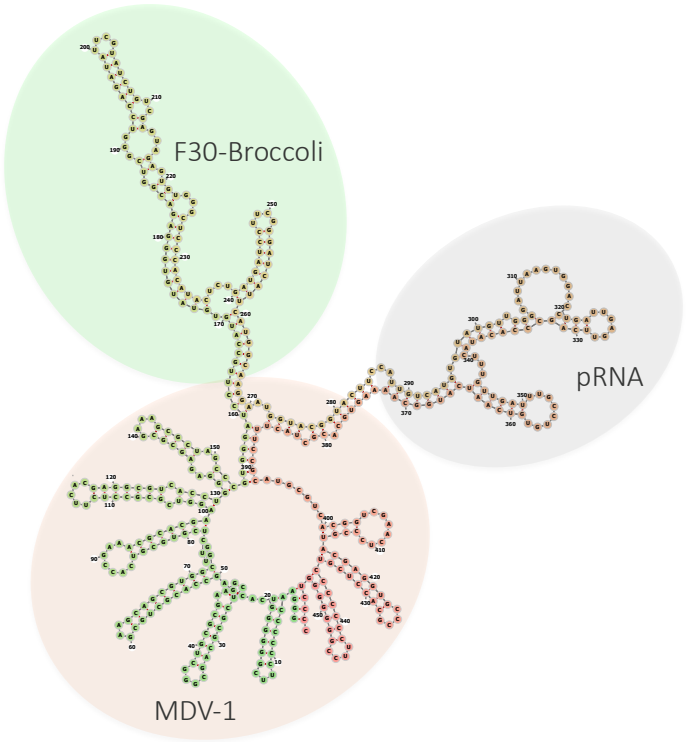

Figure 23: (-) MDV-1 _F30Bro_pRNA. *RNAfold Vienna in-silico folding prediction of the (-) strand of the MDV-1 _F30Bro_pRNA replicon. F30-Broccoli: fluorescent unit. MDV-1: replication unit. pRNA: structural unit.*

It was possible to see **(fig. 24)** that the replicon was recognized and replicated by the replicase. This means, that increasing the size of the previous replicon doesn't impact the recognition and replication ability by the Qβ. The presence of the bands at 0 hours in both the previus **(fig. 21)** and this gel **(fig. 24)** could be explained by the fact that when bringing the 0 hour sample to the thermocycler for the denaturation of the Qβ, and therefore to stop the replication, Qβ can synthesize a small amount of (-) RNA in that short amount of time. This RNA becomes visible on the gel if stained. It needs to be remembered that the kinetic of replication of the Qβ replicase is very fast since the enyme is extremly processive (Hosoda *et al.*, 2007).

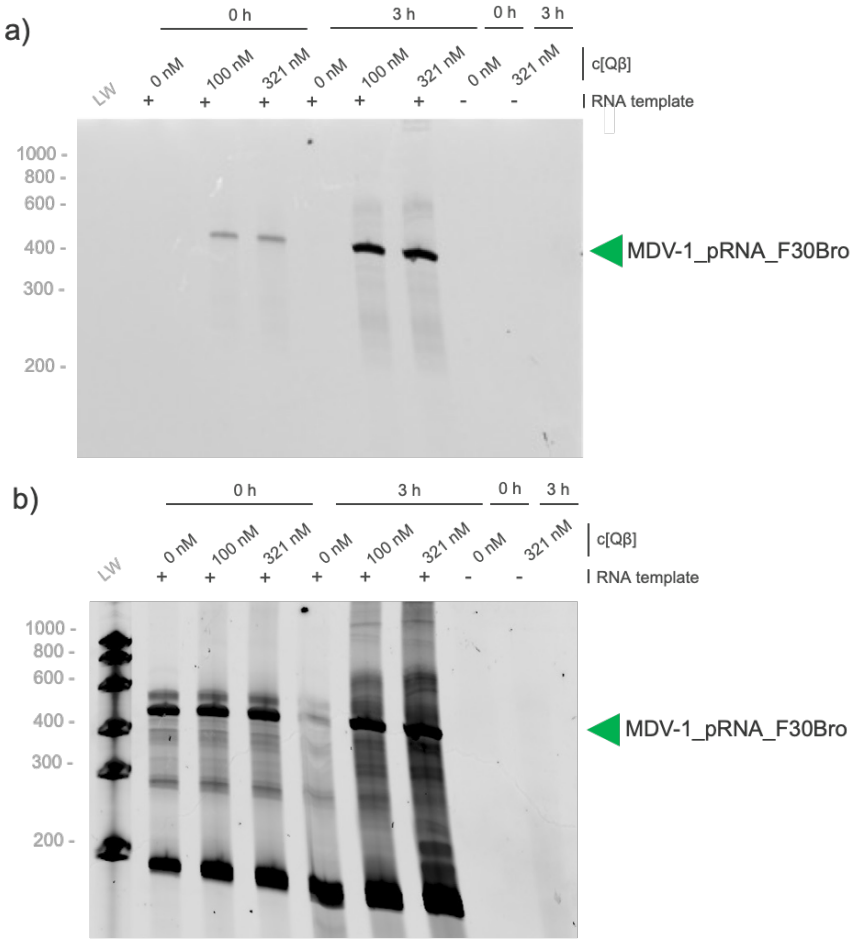

Figure 24: Replication assay of MDV-1 _pRNA_F30Broccoli replicon. *8% urea-PAGE of the replication assay for the MDV-1 _pRNA_F30Broccoli template (475 nt).* ***The RNA template was*** *incubated with 0, 10, or 321 nM of Qβ replicase at 37°C in a water-oil emulsion system, as described in the Materials and Methods section. Controls without the RNA template were also run. Samples were taken at 0 and 3 hours.* ***a)*** *DFHBI stain,* ***b)*** *SYBR Gold stain. LW: RiboRuler Low Range ssRNA Ladder (nt) (Thermo).*

Self-replication assays of co-replication of two MDV-1-based replicons in water-oil emulsion. To assess the possibility of co-replication of two replicons with similar cargos by Qβ within a single reaction, a replicon with a different pRNA sequence (ExBa) and another aptamer was constructed. Since there is no overlap with the emission spectrum of the F30-Broccoli aptamer, The F30-mango aptamer were selected for its short sequence and strong fluorescence enhancement upon ligand binding (Autour *et al.*, 2018). The ExBa sequence have complementary D-loop and CE-and therefore when add together to the same reaction, if the (-) strand is produced, they should drive the self-assembly of the two replicons. Furthermore, the presence of two loop complementary sequences on each pRNA enables the dimer nanoring to assemble if both are added to the same replication reaction, and if the (-) strand is produced starting from the (+) as template. It's important to undelight also that the Mango aptamer differs in primary, secondary and tertiary structure form the previously used F30-Broccoli (Trachman *et al.*, 2018) and therefore it's addition to the replicon required to be tested in silico and in vitro.

As previously done, the newly designed sequence of the replicon MDV-1_F30Mango_pRNA$_{ExBa}$ (475 nt) was tested in-silico using RNAFold Vienna to confirm the retention of each component structure. This was followed by a replication assay. The conditions and experimental design were identical to those used for the MDV-1_F30Bro_pRNA replicon. An 8% urea-PAGE gel was utilized to run the samples collected at both 0 and 3 hours. In order to confirm replication, a staining protocol adapted for the

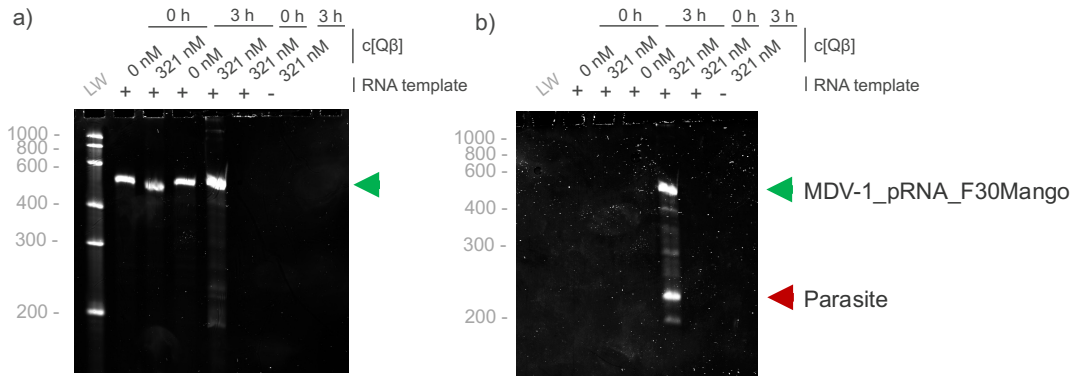

Figure 25: Replication assay of MDV-1 _pRNA$_2$_F30Mango replicons. *8% urea-PAGE of the replication assay for the MDV-1 _pRNA$_2$_F30Mango template (475 nt). The RNA template was incubated with 0 and 321 nM of Qβ replicase at 37°C in a water-oil emulsion system, as described in the Materials and Methods section. Controls without the RNA template were also run. Samples were taken at 0 and 3 hours.* ***a)*** *SYBR Gold stain,* ***b)*** *TO1-B stain. LW: RiboRuler Low Range ssRNA Ladder (nt) (Thermo).*

Mango aptamer and was employed to visualize the fluorescent signal given by the formation of the (-) strand **(fig. 25)**. Changing the aptamer did not affect recognition by the replicase and formation of the (-) strand. However, **fig. 25** shows that a shorter sequence was also produced, indicating the presence of a potential parasite that retains the F30-Mango sequence and therefore could be detected after staining.

After verifying the replication capabilities of the two replicons, MDV-1_F30Bro_pRNA$_{ExAb}$ and MDV-1_Mango_pRNA$_{ExBa}$, a co-replication experiment was performed to verify the co-recognition and co-replication by the replicase of the two replicons in a single reaction, thus validating the feasibility of adding more replicons carrying a pRNA structural motif in a single reaction and the possibility of separately detecting the formation of both their (-) strand **(fig. 26)**. In addition, this would make it possible to verify that two different replicons can be encapsulated in water-oil emulsion system and replicated by the replicase at the same time.

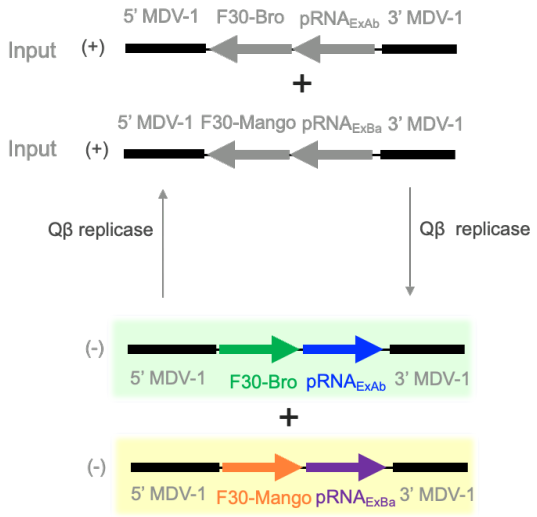

Figure 26: Coreplication of the MDV-1 _F30Bro_pRNA$_1$ and MDV-1 _F30Mango_pRNA$_2$ replicons. *Both the (+) strand of the MDV-1 _F30Bro_pRNA$_1$ and MDV-1 _F30Mango_pRNA$_2$ templates are added to the reaction, and the (-) strands are synthesized by the Qβ replicase. The success of the replication reaction by Qβ of both templates is detected through the read-out, as the two aptamers, F30-Broccoli and F30-Mango, can fold when in the correct orientation.*

Three reactions were set-up. The main reaction contains 100 nM of each replicon (co-replication reaction) and the other two positive controls reactions contain each 100 nM of just one of the replicons. 321 nM of Qβ PB2 was added to the reaction and samples at 0 hours and 3 hours were taken and two 8% urea-PAGE gel were run with the same sample

to stan specifically each of them with the DHFBI ligand for visualize the replicon carrying the Broccoli aptamer and the TO1 for visualize the replicon carrying the Mango aptamer.

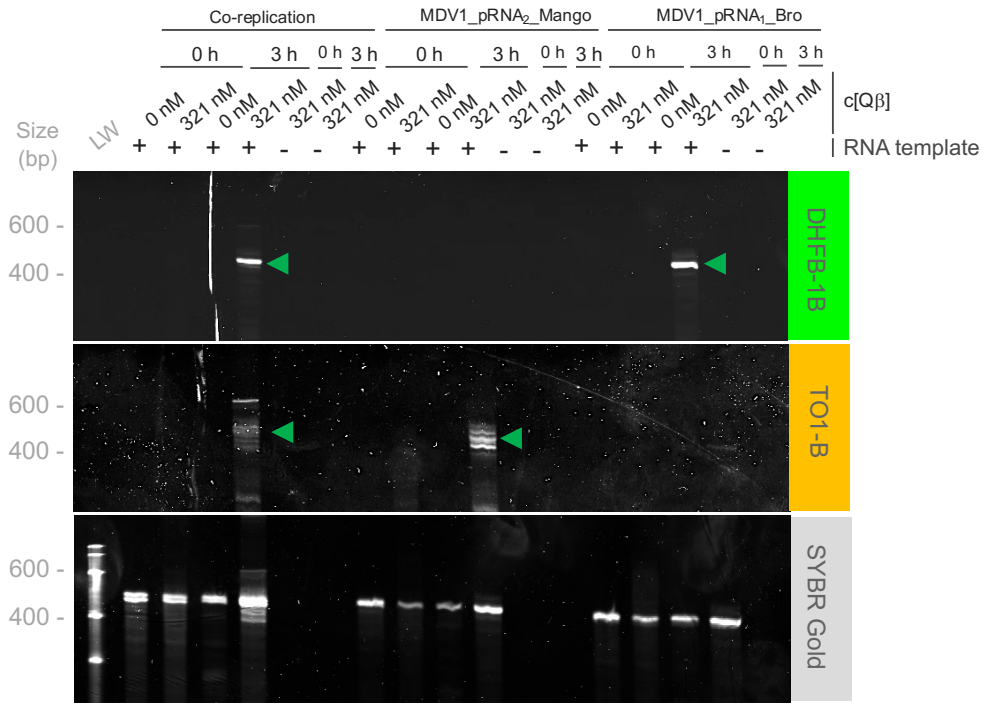

Figure 27: Co-replication of MDV-1 _F30Bro_pRNA$_1$ and MDV-1 _F30Mango_pRNA$_2$ replicons. *8% urea-PAGE of the assay for the co-replication of MDV-1 _F30Bro_pRNA$_1$ (475 nt) and MDV-1 _F30Mango_pRNA$_2$ (475 nt) replicons. The two RNA templates (co-replication), the single MDV-1 _F30Bro_pRNA$_1$ template and the MDV-1 _F30Mango_pRNA$_2$ template were incubated with 0 and 321 nM of Qβ replicase at 37°C in a water-oil emulsion system, as described in the Materials and Methods section. Controls without the RNA template were also run. Samples were taken at 0 and 3 hours. From the top - First gel: DHFB stain. Second gel: TO1-B stain. Third gel: SYBR Gold stain. LW: RiboRuler Low Range ssRNA Ladder (nt) (Thermo).*

Co-replication of the two replicons was successfully carried out by the Qβ in droplets with different efficiencies. As we can see from **fig. 27**, the (-) strand of the MDV-1_F30Bro_pRNA$_{ExAb}$ was produced in higher yields compared to the MDV-1_Mango_pRNA$_{ExBa}$ replicon. The presence of the Mango aptamer and the final replicon structure may hinder recognition and replication by the replicase, resulting in a slower production of the (-) strand and therefore lower yields. Since both replicons were present in the same reaction and possess different recognition and replication kinetics, the production of the (-) strand seemed asymmetric. Specifically, the MDV-1_F30Bro_pRNA$_{ExAb}$ was more likely to be replicated at a faster rate due to its structure.

Since our main objective was to assemble several replicons in nanorings and fuel their replication by the addiction of the replicase, this co-replication experiment confirmed the feasibility of adding multiple replication units to the reaction. As a result, the focused was on to the next section of the project, which involved testing the optimal conditions for assembling replicons in nanorings of increasing dimensions.

3.1.3. Summary and conclusions

The main aim of this section was to design and test replicating scaffolds that could be recognised and replicated by Qβ replicase. To begin, Qβ replicase was overexpressed and purified to obtain the necessary amount for future replicon tests. Next, RQ135-based replicons were designed to carry a pRNA sequence as cargo. This structural motif will allow several replicons to be assembled in a nanoring later in the project. To test the replication capability of the newly designed replicons, a tailored replication assay was set up and different concentrations of Qβ replicase were tested. The assays demonstrated that the replicase effectively replicated the RQ135_pRNA replicon, but non-specific product formation, also known as parasite, was observed, as previously reported in the literature (Kita *et al*., 2008; Matsumura *et al*., 2016; Koonin, Wolf and Katsnelson, 2017; Furubayashi and Ichihashi, 2018; Mizuuchi and Ichihashi, 2018). The other replicon, RQ135_sfGFP_pRNA, showed replication after 1 hour, but stopped after 4 hours.

To contain or even completely inhibit the formation of the parasite and achieve higher yields of replication of the desired replicon, compartmentalization was adopted as an effective parasite containment method, as previously done by Matsumura *et al*., 2016. The reaction was encapsulated in droplets within a water-oil emulsion. To confirm that the replicase was able to recognize and replicate our new replicon, the inverted sequence of a fluorescent aptamer, F30-Broccoli, was inserted as cargo into the (+) strand of the MDV-1 replicon and verified by in-silico prediction that the folding of each component was retained. Encapsulation in droplets improved yields and contained parasite formation. The $pRNA_{Ab}$ sequence was then incorporated into the MDV-1_F30Bro replicon. The successful replication of the newly designed MDV-1_F30Bro_$pRNA_{Ab}$ was achieved through encapsulation in water-oil emulsion. To test the possibility of co-replicating two replicons in a single reaction, MDV-1_Mango_$pRNA_{Ba}$ replicons were designed with a different aptamer sequence (Mango aptamer) and a complementary pRNA sequence $pRNA_{Ba}$ to $pRNA_{Ab}$. Co-replication of the two replicons was confirmed.

A potential improvement for the systems developed for both RQ135 and MDV-1 based replicons could be the implementation of a protocol for a controlled compartmentalization to generate smaller compartments. Until now, the general “scratching” protocol adopted in this work made it impossible to determine the size of the generated droplets. However, with a proper microfluidic setup, it is possible to generate controlled size compartments, which can help reduce the size of the droplets in a controlled manner. This reduction can aid in reducing non-specific products and maintaining specific replication dynamics. This could be an efficient method for containing parasites since, as previously shown by Bansho *et al*., (2012), the smaller the compartment, the lower the chance of parasites emerging and taking over the reaction.

Furthermore, looking at the system itself, altering the replicase and replicon scaffold could be beneficial in reducing parasite formation. In this regard, the MS2 system could be advantageous since it has been shown to be less prone to generating parasites in self-replication reactions and therefore more specific in replicating towards non-genomic templates (Wagner, Weise and Mutschler, 2022). Additionally, its replication kinetics are more relaxed compared to the highly processive Qβ replicase. One potential challenge to the use of MS2 is the need to retest if structural elements, such as pRNA, can be inserted as cargo. However, it has recently been demonstrated that fluorogenic aptamers can be inserted without compromising the system's efficiency (Weise *et al.*, 2019).

As the final potential improvement of the system, it's the optimisation of RNA sequence and structure based on *in vivo* kinetic evaluations. The experiments aim to comprehend the kinetics of RNA replication and the replicase's inclination towards specific parts of the RNA sequence, particularly the 3' end. This information can aid in the design of RNA sequences that replicate with greater specificity. The replication efficiency of each replicon can be improved by optimizing its CG content. This is based on the 'fewer unpaired GC rule', which states that replicons with lower GC content in their secondary structure are replicated more efficiently and specifically by the replicase, resulting in less dsRNA formation (Mizuuchi, Usui and Ichihashi, 2020).

3.2. Self-assembly of RNA replicons into nanorings

3.2.1. Background and concept

This chapter explores the possibility of designing and building nanorings based on the assembly properties of heterologous replicons carrying synthetic pRNA motifs. It also aims to identify and optimise key parameters that influence the assembly process, with the aim of establishing a universal technology capable of building RNA genomes of increasing dimension. The Guo group previously established this technology, characterised it, and used it for various applications in biosensing and biomedicine (D. Shu *et al*., 2011; Y. Shu *et al*., 2011; Shu, Shu, *et al*., 2013; Zhang *et al*., 2013; Shu *et al*., 2014; Guo *et al*., 2018). Each pRNA is described with a specific annotation. The annotation consists of 'Ex' followed by a capital letter indicating the sequence of the CE-loop and a lowercase letter indicating the sequence of the D-loop, for example ExAb, where A is the name of the CE-loop and b the name of the D-loop **(fig. 28)**.

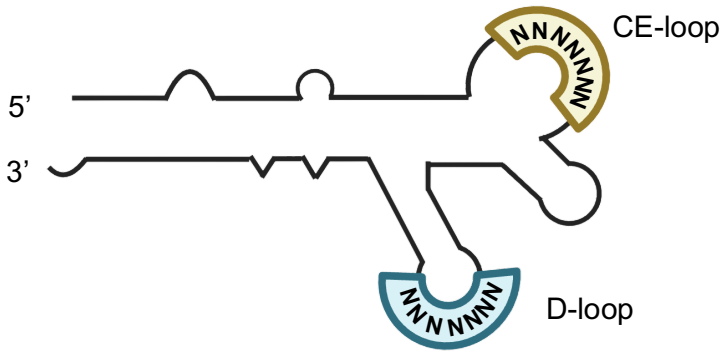

Figure 28: Synthetic pRNA. *The CE-loop and D-loop each carry seven nucleotides that are essential for specific binding in trans with another pRNA molecule. These nucleotides can be reprogrammed to enable interaction with a different pRNA molecule. Adapted from Shu Y et al., 2013.*

The nanostructures based on the pRNA motif can be design in a modular way and bigger nanorings can be formed by adding more and different pRNA monomers to the assembly reaction **(fig. 29)**. As demonstrated in literature, the addition of more pRNA monomers to the self-assembly reaction results in an increase in the number of side-products formed. This is due to the promiscuity of the sequences of the CE-loop and D-loops (Shu, Haque, *et al.*, 2013; Shu, *et al.*, 2013).

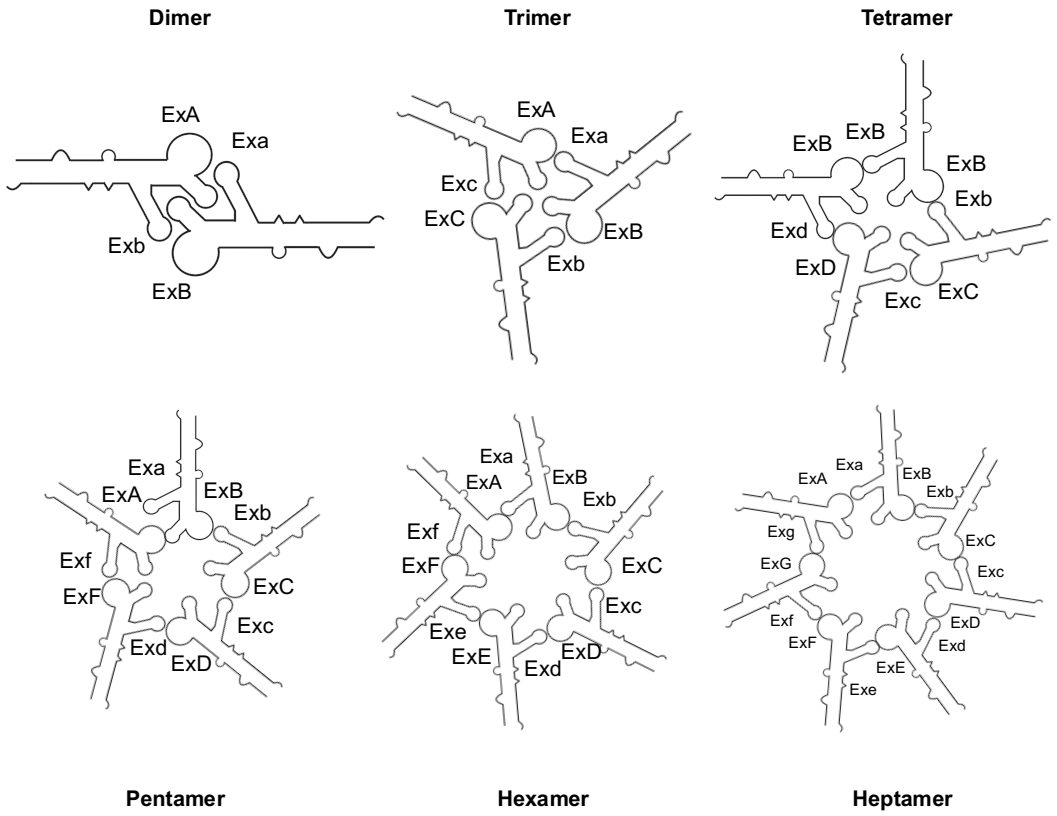

Figure 29: Self-assembly of nanorings starting from single pRNA monomers. *Addition of a single pRNA to the reaction leads to an increase in the dimensions of the nanoring. Nanostructure formation is visualized by Native PAGE at the end of the self-assembly reaction to preserve its folding.*

At the start of this chapter, larger nanorings were assembled from pRNA-only monomers to confirm system reproducibility. Next, the pRNA sequence was integrated as cargo into the replication sequence of MDV-1 replicons to enable assembly into nanorings. A Mg^{2+} screening was conducted to determine the optimal salt concentration for forming nanorings with this novel and larger monomer. As previously reported, Mg^{2+} is an essential ion that influence the folding of the monomer and therefore can heavily impact the assembly (Fang *et al.*, 2008). After screening, the size of MDV-1-based nanorings was increased by attempting to form larger nanorings through the addition of more monomers. The buffer parameters and protocol for ideal stabilization were before fixed. Additionally, to reduce the amount of non-specific products during assembly, the pRNA structural sequence was included as cargo into RQ135-based replicons. For the last experiment, each monomer was fluorescently tagged to visualise specifically the monomers involved in the assembly and to follow them in the context of the assembly.

3.2.2. Results

Self-assembly of simple pRNA motifs into nanorings. As starting point for the testing of the assembly of the replicons, single pRNA fragments were used in order to replicate the conditions used previously by Shu *et al*., 2013. ssDNA oligos were ordered from IDT, by fill-in the whole dsDNA pRNA fragment was obtained and then the RNA was produced by IVT as reported in material and methods. As a first test, several nanorings were assembled in increasing dimensions: dimers, trimers, tetramers, pentamers, hexamers and heptamers **(fig. 30)**.

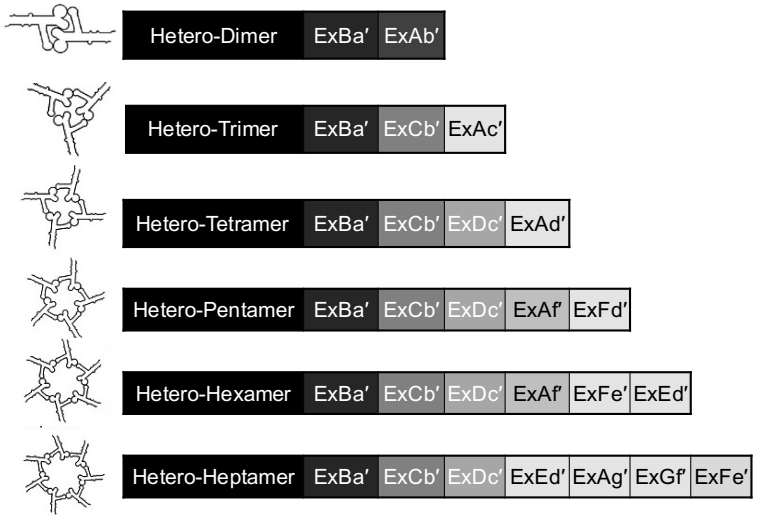

Figure 30: Hand-in-hand pRNA nanoparticles forming nanorings. *Increasing the number of monomers in the reactions lead to an increase of the dimension of the nanoring.*

The dimension of the nanoring is direct proportional to the number of pRNA added to the assembly reaction and each pRNA was added in equimolar amount in TMS buffer (10 mM $MgCl_2$, 100 mM of NaCl and 50 mM Tris-HCl (pH 8.0). It is important to note that the presence of magnesium chloride ($MgCl_2$) and sodium chloride (NaCl) influences the assembly of pRNA. Thus, adding an appropriate amount to the assembly mix is crucial for enhancing the assembly's stability, promoting necessary conformational changes, and facilitating proper pRNA functionality (Gu and Schroeder, 2011).

To visualize the formation of rings, a custom native PAGE gel system was established, as described in the Materials and Methods. The gel was run in TBM running buffer for 4 hours at 70V and keeping a constant temperature of 4 °C. To achieve a clear depiction of the pRNA assemblies, numerous gel optimizations were necessary. It was observed that maintaining a temperature of 4 °C plays a crucial role in the quality of the resulting bands,

decreasing the smearing and obtaining more definition. **Fig. 31** shows one of the initial PAGEs. It's possible to see that larger rings are formed with an increase in the number of monomers added to the reaction. It is important to note that as the dimension increases, there is also an increase in the formation of nonspecific assemblies due to a lack of orthogonality between the complementary sequences of the D-loop and of the CE-loop. Since each loop consists of only 5 nucleotides, it is possible that undesired cis- and trans- interactions may occur, leading to the formation of these "side-products". However, this does not compromise the specific assembly, as evidenced by the presence of a well-defined and thick band in the gel.

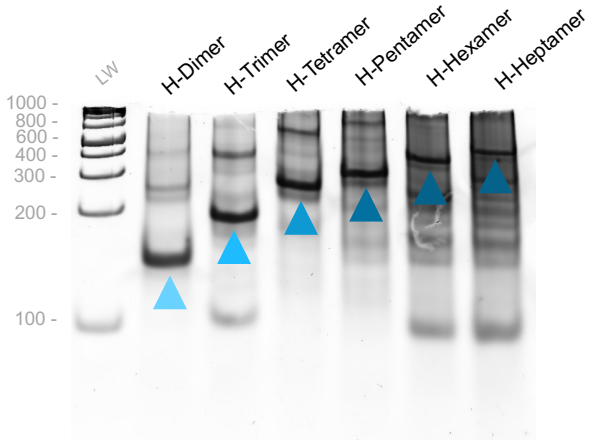

Figure 31: pRNA-only nanoring self-assembly. *Native 6% PAGE gel run in TBM buffer for 4 hours at 4 °C of the self-assembly of H-dimer, H-trimer, H-tetramer, H-pentamer, H-hexamer and H-heptamer nanorings (arrows). H-: hetero. For each self-assembly reaction, an equimolar concentration of pRNA was added and incubated at 37°C for 1 hour. LW: RiboRuler Low Range ssRNA Ladder (nt) (Thermo).*

Self-assembly of MDV1_pRNA replicons into dimeric and trimeric nanorings. Since one of the main goals is to build segmented and replicating RNA nanoring, tests were conducted to assemble previously designed MDV-1_pRNA replicons, taking in consideration that their replication ability was previously verified. As previously demonstrated, each structural section of these replicons maintains the desired fold and therefore they can be functional. This means that the 5' and 3'UTR sections of the MDV-1 will form a double strand and form the replicating unit that will enable the recognition and replication by the Qβ replicase, while the pRNA section will allow to structure assembly multiple monomers containing complementary pRNA into rings of increasing dimension **(fig. 32)**. The focus of this chapter is the structural motif of the pRNA.

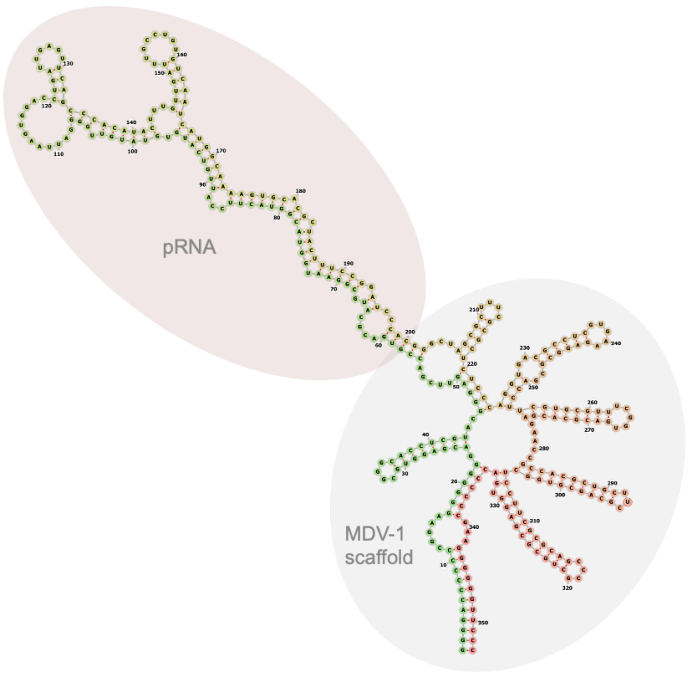

Figure 32: MDV-1 _pRNA replicon. *RNAvienna Fold in-silico prediction of the MDV-1 _pRNA replicon folding with its pRNA structural section and the RQ135 replicative sequence.*

As previously mentioned, the presence of $MgCl_2$ is a critical factor in stabilizing the pRNA structure, a well-documented phenomenon (Binzel, Khisamutdinov and Guo, 2014). However, the impact of $MgCl_2$ on the secondary and tertiary structure, and whether it affects the replication of MDV-1 and RQ135 while carrying a structural pRNA motif by Qβ replicase is still undocumented. Therefore, further investigation is necessary.

To determine how different concentrations of $MgCl_2$ affect ring assembly, we tested dimer formation starting from the (-) strands of the MDV-1_pRNA$_{ExAb}$ and MDV-1_pRNA$_{ExBa}$ monomers in TMS buffer with varying $MgCl_2$ concentrations: 0 mM, 1 mM, 3 mM, 5 mM, 7 mM, 8 mM, 9 mM, and 10 mM. The functional pRNA was obtained by PCR of the (-) strand of each MDV-1_pRNA replicon and subsequential IVT, as the functional sequence is solely available on this strand and therefore only two (-) can assemble in the ring. It is crucial to note that each monomer underwent PAGE purification after the IVT. It is necessary to obtain a pure sample containing only the desired monomer and not the whole population of side products arising from the IVT. This is important because the side products could hinder the assembly and make visualization of the assembly challenging, as demonstrated by experiments in the exploratory phase of this section. Equimolar concentrations of both MDV-1_pRNA replicons were added to the reaction. A refolding protocol was conducted prior to incubation to ensure the correct refolding of each monomer

following gel extraction. It is known that the purification steps performed after PAGE extraction have the potential to cause RNA unfolding. Therefore, a refolding step was necessary to restore proper folding. The refolding steps consisted of first heating the RNA at 80 °C for 2 min and slowly cooling to 37 °C at 1 °C/min. Then, when reached 37 °C, the assembly reaction was incubated at 37 °C for 1 hour. Afterwards a 5% Native PAGE gel was run with TBM as running buffer **(fig. 33)**.

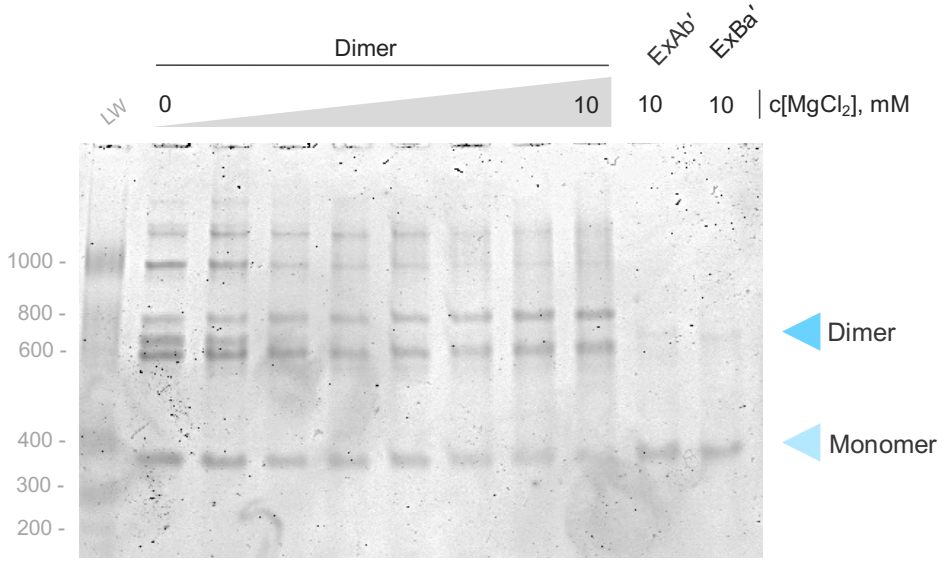

Figure 33: $MgCl_2$ titration of MDV-1 _pRNA replicons dimer nanoring self-assembly: *5% Native PAGE run in TBM buffer showing the effect of increasing $MgCl_2$ concentration the self-assembly of MDV-1 _pRNA dimers (706 nt). Reactions contain equimolar concentration of each monomer and were firstly refolded heating them at 80 °C for 2 min and slowly cooling to 37 °C at 1 °C/min in TMS buffer at 0, 1, 3, 5, 7, 8, 9, and 10 mM $MgCl_2$. Then incubated at 37 °C for 1 hour. MDV-1 _pRNA monomers (each 353 nt) containing the pRNA ExAb and ExBa were run as control. LW: RiboRuler Low Range ssRNA Ladder (nt) (Thermo).*

Multiple bands were visible at 0 mM, indicating that the replicons were not correctly folded in the absence of $MgCl_2$ and could be assembled into various non-specific isoforms. Out of all those bands, it could also be noted that specific band corresponding to the dimer nanoring becomes visible at 706 nt. Increasing the concentration from 0 to 10 mM corresponded to a gradual disappearing of the bands over 1000 nt and an increasing in intensity of the bands at 706 and 600 nt. The presence of these two bands could be explained by the formation of two similar but different isoforms, assembled in dimers. Since a native PAGE gel was used to visualize the assembly, the sample was not heat-treated and therefore the fold should have been maintained. It is possible that the dimer assembly formed two distinct folding isoforms with different patterns, leading to slight differences in their

running. The 600 nt isoform is more "linear" and can run through the channels of the gel more quickly than the other isoform.

It is evident that not all the monomers have participated in forming the nanorings as there are bands present at 353 nt. This indicates the presence of some unreacted product. It is possible that the assembly kinetics require more than an hour to convert all monomers into dimers, providing a potential explanation for the retention of monomers. It is possible to understand that the assembly of the dimer seems to occur optimally in the presence of 10 mM $MgCl_2$, despite the existence of two isoforms.

A new assembly experiment was conducted to explore whether the same $MgCl_2$ concentration would be optimal for trimer assembly. To assemble the trimer nanoring, three monomers with pRNA sequences suitable for assembly (MDV-1_$pRNA_{ExAc}$, MDV-1_$pRNA_{ExBa}$, MDV-1_$pRNA_{ExCb}$) were selected and their RNA produced by IVT and then PAGE purified. The three monomers were incubated in TMS containing 10 mM $MgCl_2$ for 1 hour at 37 °C. Subsequently, they were analysed by running a Native PAGE using the previously established protocol **(fig. 34)**. To enable clear visualization of the dimer and trimer differences, a separate dimer assembly reaction was also run on the same gel. The band corresponding to the newly assembled trimer run at 1059 nt while the dimer run at 706 nt, which confirmed the successful assembly of the nanorings.

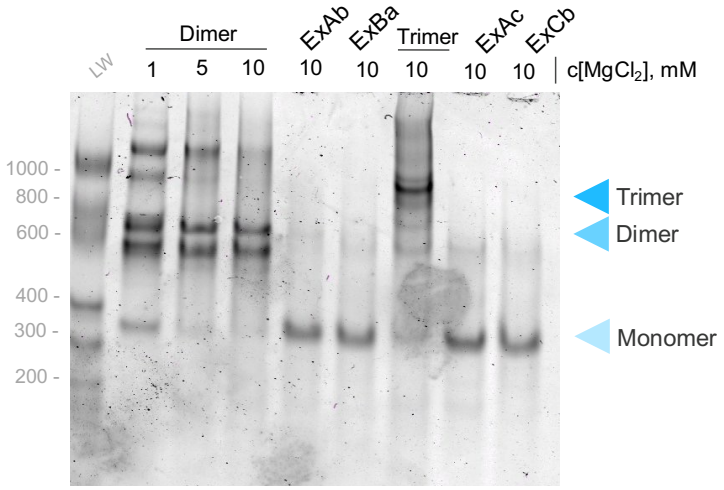

Figure 34: MDV-1 _pRNA replicons dimers and trimers nanoring self-assembly. *5% Native PAGE run in TBM buffer of the self-assembly of MDV-1 _pRNA dimers (706 nt) and trimers (1055 nt). Reactions contain equimolar concentration of each monomer and were firstly refolded heating them at 80 °C for 2 min and slowly cooling to 37 °C at 1 °C/min in TMS buffer at 1, 5, and 10 mM $MgCl_2$ for the dimer and 10 mM $MgCl_2$ for the trimer. Then incubated at 37 °C for 1 hour. MDV-1 _pRNA monomers (each 353 nt) containing the pRNA ExAb, ExBa, ExAc and ExCb were run as control. LW: RiboRuler Low Range ssRNA Ladder (nt) (Thermo).*

Self-assembly of MDV-1 _F30_pRNA replicons into dimeric and trimeric nanorings. To achieve a more precise assembly and enhance the stability of the pRNA structure while distancing it from the MDV-1 replication section, a F30 scaffold was introduced upstream and downstream of the pRNA sequence. The F30 scaffold has been utilized by multiple research groups to stabilize the Broccoli aptamer. The new design allows for the aptamer to maintain its structure in various buffer conditions, leading to a stronger fluorescence signal and increased stability (Filonov *et al*., 2015). This could potentially apply to our pRNA replicon and decrease isoforms formation.

MDV-1-based dimers and trimers, with a pRNA located between two F30 sequences, were incubated separately in TMS buffer with 0, 5, and 10 nM $MgCl_2$. Each monomer was PAGE purified and added in equal quantities to the reaction. Before incubating at 37°C for one hour, we utilized the previously established refolding protocol in this experiment. Following, a 5% Native PAGE was executed to visualize the assembly results. As seen in **Fig. 35**, the addition of the F30 scaffold did not improve the results.

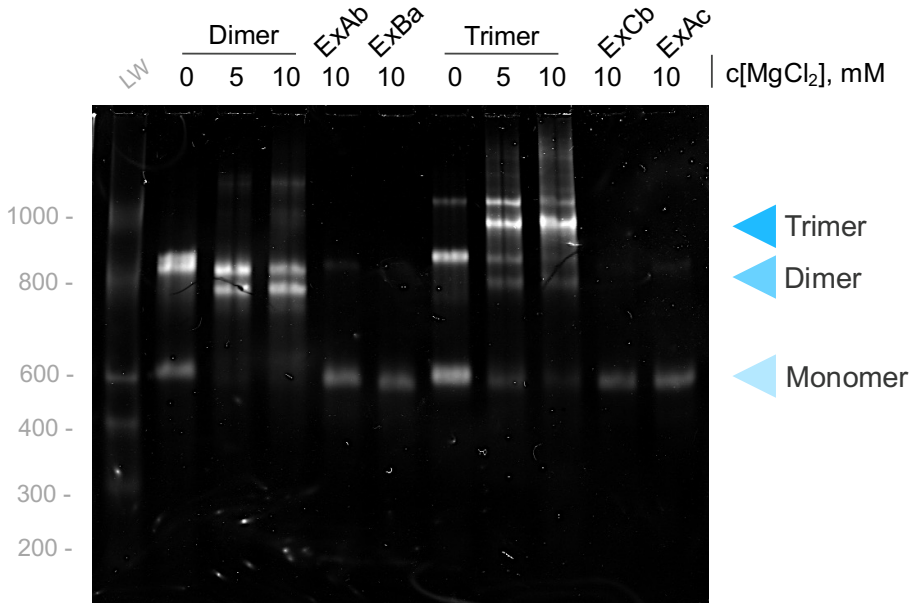

Figure 35: MDV-1 _F30_pRNA replicons dimer and trimer nanoring self-assembly. *5% Native PAGE run in TBM buffer of the self-assembly of MDV-1 _F30_pRNA dimers (822 nt) and trimers (1233 nt). Reactions contain equimolar concentration of each monomer and were firstly refolded heating them at 80 °C for 2 min and slowly cooling to 37 °C at 1 °C/min in TMS buffer at 0, 1, 5, and 10 mM $MgCl_2$ for the dimer and the trimer. Then incubated at 37 °C for 1 hour. MDV-1 _F30_pRNA monomers (each 353 nt) containing the pRNA ExAb, ExBa, ExCb and ExAc were run as control. LW: RiboRuler Low Range ssRNA Ladder (nt) (Thermo).*

Self-assembly of RQ135_pRNA replicons into dimeric, trimeric, tetrameric nanorings. The next step was to minimize the presence of non-specific assemblies and avoid the presence of isoforms during the assemblies as noticed from the MDV-1_pRNA dimer. Since the RQ135 replication scaffold exhibits a more linear folding pattern, as predicted by RNA Fold Vienna **(fig. 36)**, it was selected for testing its assembly in nanorings.

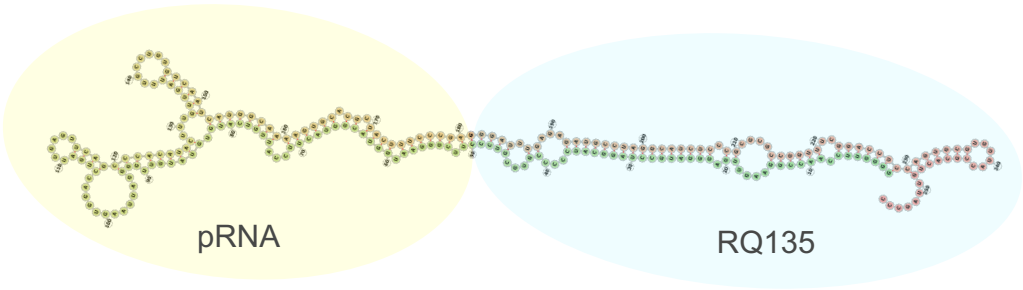

Figure 36: RQ135_pRNA replicon. *RNAvienna Fold in-silico prediction of the RQ135_pRNA replicon folding with its pRNA structural section and the RQ135 replicative sequence.*

Dimers, trimers, and tetramers were assembled from the (-) strand of the RQ135_pRNA replicon using the same refolding and incubation protocol as the MDV-1_pRNA assemblies. Three salt condition were tested: 0, 3, 10 mM $MgCl_2$. The results were then analysed using a 5% Native PAGE and as shown in **fig. 37**. At 10 mM $MgCl_2$ the dimer only presented one band on the gel indicating at the desired size of 512 nt and the absence of other undesired assembly products. As previously mentioned, the two binding sequences of the pRNA structure in the loops differ by only a few nucleotides. Therefore, what may appear to be highly specific in silico may not hold true in experimental conditions where there may be undesired complex formation due to alternative tertiary interactions based on Watson-Crick base pairing from other conformers. As a result, sequences that were not expected to bind each other may actually bind and form unexpected structures due to promiscuous binding. Furthermore, it could be observed that there was no unassembled monomer at approximately 300 nt, indicating that the two monomers, ExAb and ExBa, added in the reaction had successfully assembled. In the case of the trimer, the desired single band at approximately 1024 nt could only be observed in the 10 mM sample. At 3 mM $MgCl_2$, there are two bands present, one specific and one non-specific, while at 0 mM $MgCl_2$, the band at 1024 nt corresponding to the trimer wasn't present. There were also

some unreacted monomers at about 300 nt. The same could be said for the tetramer, indicating that longer incubation times may be necessary to convert all monomers into the nanoring and form the trimer and tetramer. Apart from that, it was confirmed that a dimer, trimer, and tetramer nanoring could be formed from RQ135_pRNA monomers. Thus, this scaffold could be considered for testing the coupled assembly and replication, elaborated upon in chapter 3.

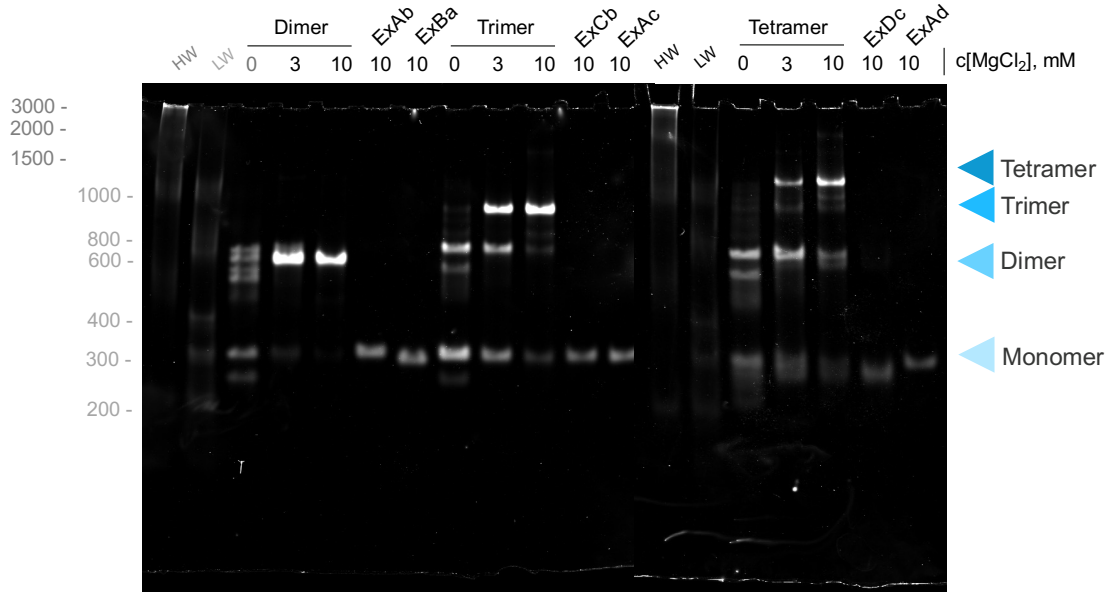

Figure 37: RQ135_pRNA replicons dimer, trimer, tetramer nanoring self-assembly. *5% Native PAGE run in TBM buffer of the self-assembly of RQ135_pRNA dimers (512 nt), trimers (768 nt) and tetramers (1024 nt). Reactions contain equimolar concentration of each monomer and were firstly refolded heating them at 80 °C for 2 min and slowly cooling to 37 °C at 1 °C/min in TMS buffer at 0, 3, 10 mM $MgCl_2$ for dimers, trimers and tetramers. Then incubated at 37 °C for 1 hour. RQ135_pRNA monomers (each 256 nt) containing the pRNA ExAb, ExBa, ExCb, ExAc, ExDc and ExAd were run as control. HW: RiboRuler High Range ssRNA Ladder (nt). LW: RiboRuler Low Range ssRNA Ladder (nt) (Thermo).*

Nanoring self-assembly visualization by replicon fluorescent labelling. After assessing the feasibility of building nanorings from MDV-1_pRNA and RQ135_pRNA monomers, it was necessary to better understand the assembly dynamic and experimentally visualize it. Three fluorescent UTP analogues (Cy3-UTP, Cy5-UTP, FAM-UTP) were selected in order to label four different RNA replicons during IVT. MDV-1_pRNA$_{ExAb}$ and MDV-1_pRNA$_{ExCb}$ were labelled with Cy3, MDV-1_pRNA$_{ExBa}$ with Cy5 and MDV-1_pRNA$_{ExAc}$ FAM as reported in material and methods. The refolding and assembly protocol used for the unlabelled assemblies was also used for this experiment. Subsequently, a 5% Native PAGE was run and during the image analysis at Sapphire four different channels

(Cy3 λ_{exc}= 550 nm λ_{em}= 570 nm, Cy5 λ_{exc}= 649 nm λ_{em}= 670 nm, FAM λ_{exc}= 492 nm λ_{em}= 517 nm) were used to observe to visualize specifically each replicon on the gel, as a monomer or as part of the assembly.

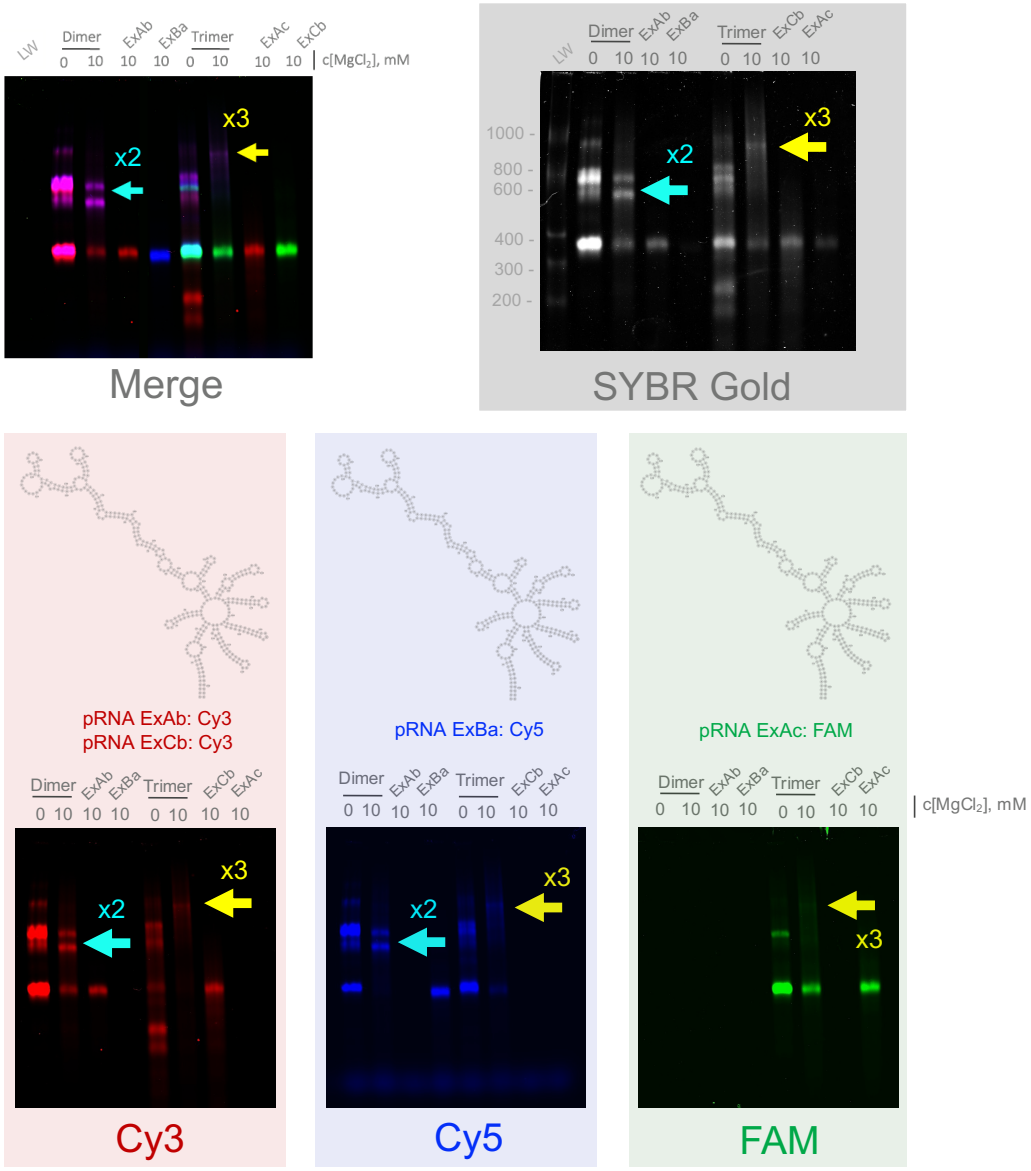

Figure 38: Fluorescent labeled MDV-1_pRNA replicons dimers and trimers nanoring self-assembly. *5% Native PAGE of the self-assembly reaction of the dimer (706 nt, indicated as x2) and trimer (1059 nt, indicated as x3) starting from fluorescently labelled MDV-1 _pRNA monomers (each 353 nt). Channels used for the visualization at the Sapphire. Merge: Cy3, Cy5 and FAM channels. SYBR Gold:* λ_{em} *539 nm. Cy3:* λ_{em} 570 nm. *Cy5:* λ_{em} 670 nm. *FAM:* λ_{em} 517 nm. *Reactions contain equimolar concentration of each monomer and were firstly refolded heating them at 80 °C for 2 min and slowly cooling to 37 °C at 1 °C/min in TMS buffer at 0, 10 mM* $MgCl_2$ *for dimers and trimers. Then incubated at 37 °C for 1 hour. RQ135_pRNA monomers containing the pRNA ExAb, ExBa, ExCb, ExAc were run as control. HW: RiboRuler High Range ssRNA Ladder (nt). LW: RiboRuler Low Range ssRNA Ladder (nt) (Thermo).*

Upon examining the gel **(fig. 38)**, it was evident that even at 10 mM $MgCl_2$, two distinct bands were visible at both Cy3 and Cy5 channels at approximately 600 and 800 nt, indicating the presence of the MDV-1_pRNA dimer and its isoform. However, it was noteworthy that at 400 nt, there is still some unassembled $pRNA_{ExAb}$ monomer present. As for the $pRNA_{ExBa}$, all the monomers have been assembled into dimeric nanorings.
In the case of the MDV-1_pRNA trimer, at 10 mM $MgCl_2$ it was possible to visualise the band at about 1000 nt corresponding to the trimer formed by the monomers Cy3-MDV-1_$pRNA_{ExCb}$, Cy5-MDV-1_$pRNA_{ExBa}$, and FAM-MDV-1_$pRNA_{ExAc}$ **(fig. 38)**. When visualising each channel separately to visualise the single replicon as a monomer and as part of the trimer, the band is faint, and this makes it difficult to visualise the assembly. This occurs despite the SYBR staining image provide the visualization of the trimer's presence and it could be due to less efficient assembly caused by the labelled UTP bases potentially interfering with the binding, resulting in less assembly product. This hypothesis was further supported by the fact that at 10 mM $MgCl_2$ many monomers did not assemble.

Self-assembly of MDV1_pRNA replicons into dimeric, trimeric, tetrameric and pentameric nanorings. After confirming and visualizing the formation of an MDV-1 dimer and tetramer, the expansion of the complexity of the assembly was attempted by building higher-level structures, such as tetramer (ExBa-ExCb-ExDc-ExAd) and pentamer (ExBa-ExCb-ExDc-ExFd-ExAf) rings. Additionally, the formation of dimers and trimers was retested using the same experimental procedure as before. The results were visualized on a 4% Native PAGE **(fig. 39)**. The dimer and trimer exhibited identical bands, while the tetramer and pentamer displayed multiple bands at 10 mM $MgCl_2$. A faint band was observed at 1412 nt for the tetramer, which was mostly obscured by a smear. Similarly, the desired band at 1756 nt for the pentamer was faint but still visible, and also hidden by smearing. The smearing observed in the experiment could be explained by the degradation of RNA while incubated with $MgCl_2$ at temperatures starting from 37 °C. This phenomenon has been previously observed by Abouhaidar & Ivanovb, 1999. The study investigated the degradation of RNA in the presence of $MgCl_2$ at 37°C and found that RNA degradation is promoted by the combined catalytic activity of buffers and magnesium ions. The degradation of RNA begins at 37°C and becomes extensive at 55°C in the presence of Mg^{2+}. The study demonstrates that the combination of Mg^{2+} with common buffers, such as Tris and sodium borate, is a potent catalyst for RNA degradation, and this can potentially explain the presence of the smearing and the decrease of efficiency of the self-assembly.

Overall, seems that the formation of the tetramer and pentamer is possible even if the assembly efficiency is not so high as for the tetramer formation starting from the RQ135_pRNA scaffold. The folding of the MDV-1 sequence presents more loops and structures that can potentially bind complementary or similar sequences on the other monomers. This phenomenon is similar to when the D-loop of the pRNA of a replicon binds the complementary CE-loop of the corresponding pRNA present on another replicon. This could also explain why at higher nt, it is possible to observe the formation of a band above the specific one.

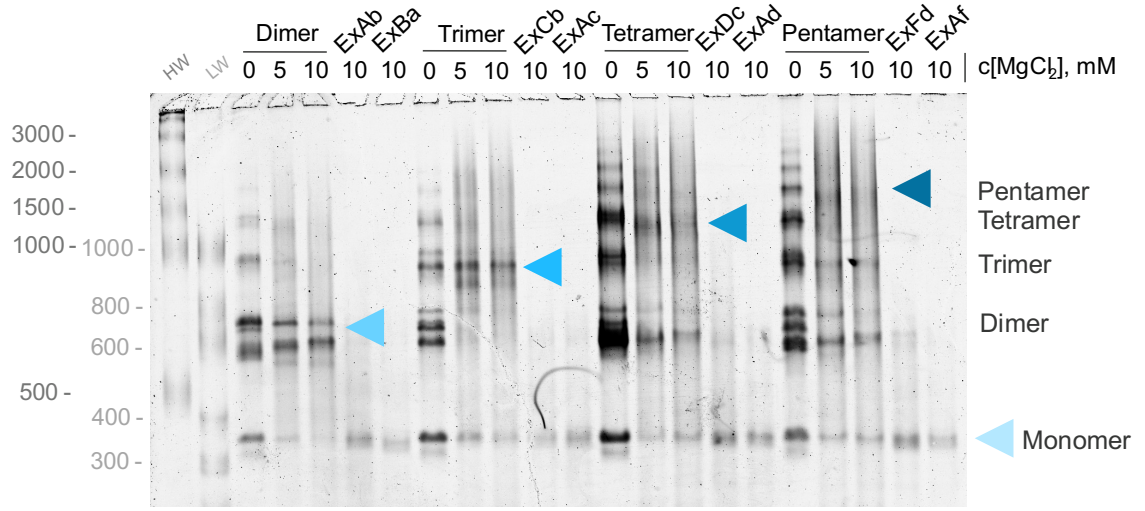

Figure 39: MDV-1_pRNA replicons dimer, trimer, tetramer and pentamer nanoring self-assembly. *4% Native PAGE run in TBM buffer of the self-assembly of MDV-1 _pRNA dimers (706 nt), trimers (1059 nt), tetramers (1412 nt) and pentamers (1765 nt) nanorings. Reactions contain equimolar concentration of each monomer and were firstly refolded heating them at 80 °C for 2 min and slowly cooling to 37 °C at 1 °C/min in TMS buffer at 0, 5, 10 mM $MgCl_2$ for dimers, trimers, tetramers and pentamers. Then incubated at 37 °C for 1 hour. MDV-1 _pRNA monomers (each 353 nt) containing the pRNA ExAb, ExBa, ExCb, ExAc, ExDc, ExAd, ExFd and ExAf were run as control. HW: RiboRuler High Range ssRNA Ladder (nt). LW: RiboRuler Low Range ssRNA Ladder (nt) (Thermo).*

3.2.3. Summary and conclusions

This section focuses on identifying and optimizing key parameters that influence the assembly of previously designed replicons into nanorings. The aim was to explore the most favourable conditions for assembly and stability.

Initial testing of single pRNA fragments was conducted to replicate the conditions from Shu *et al.*, (2013) for assembly into nanorings. The formation of these nanorings is influenced by the concentrations of $MgCl_2$ and NaCl in the TMS buffer (Binzel, Khisamutdinov and Guo, 2014). Nanorings of increasing dimensions, including dimers,

trimers, tetramers, pentamers, hexamers, and heptamers, were assembled and visualized using a custom Native PAGE gel system. It was noticed that non-specific assemblies were present, increasing the number of monomers in the solution.

Tests were conducted to assemble MDV-1_pRNA-based nanorings. Dimer and trimer formation was observed with varying $MgCl_2$ concentrations, with the optimal concentration being 10 mM $MgCl_2$. Then, F30 scaffold was introduced to enhance stability and prevent isoform and non-specific assembly formation. Results show no improvement in assembly of the replicons carrying the additional F30 scaffold.

After testing the assembly of MDV-1_pRNA replicons, we proceeded to test the RQ135_pRNA replicons to determine their assembly capabilities and potential for lower non-specific assembly formation. We successfully assembled RQ135_pRNA-based dimers, trimers, and tetramers nanorings with varying $MgCl_2$ concentrations. Notably, non-specific assembly formation was contained, as evidenced by a single visible band on the Native PAGE gel for each dimer and trimer at 10 mM $MgCl_2$.

To visualize the assembly of the two selected scaffold systems, a fluorescent technique was used to separately visualize MDV-1_pRNA in each assembled monomer. This allowed to determine which monomers fully participated in the assembly and which ones only partially participated.

Finally, the assembly of higher-level structures was attempt in order to build tetramer and pentamer rings using MDV-1_pRNA replicons. The results showed the formation of multiple isoforms and non-specific assemblies at 10 mM $MgCl_2$, indicating possible formation of larger nanorings, but the efficiency was not high and the specific band corresponding to the pentamer and tetramer was poorly visible. It was suggested that the folding complexity, which is both highly folded and very loopy, of the specific MDV-1-only sequence may have contributed to these results.

In summary, the assembly of nanorings was successful by carefully adjusting the amount of $MgCl_2$, temperature, and sequence complexity. However, further research is required to improve the replicability of the process, ensure the stability of the structures, and determine the optimal assembly conditions.

To optimize the self-assembly of the replicon, it may be beneficial in future experiments to optimize the reaction conditions by screening temperatures, pH, and salt concentration. Additionally, to eliminate non-specific assembly caused by potential complementary sequences, novel and more diverse sequences could be designed, tested, and checked for any secondary structures that may hinder assembly (Hata, Sawada and Serizawa, 2018).

Any necessary modifications to the sequence can then be made. One way to increase the efficiency of self-assembly could also be represented by the use molecular crowding agents. These agents can promote closer and more frequent interactions between each pRNA monomer, thereby improving self-assembly efficiency.

3.3. Replication & Assembly: towards replicon assembly-coupled-replication

3.3.1. Background and concept

The objective of this final section is to combine the RNA replicons ability to replicate in the presence of the Qβ replicase and to assemble into nanorings when multiple replicons carrying complementary pRNA sequences are present in the reaction. As stated in the introduction, the project aims to rationally design and assemble RNA genomes for genomic transplantation in *E. coli* but also to generate the first replicative RNA nanostructures with defined geometry and stoichiometry. The ultimate goal is to create an organism capable of storing genetic information on both DNA and RNA and successfully retaining and transferring the RNA-stored genetic information through cell division. Since replicative RNAs cannot exceed 30,000 nucleotides (Smith, Sexton and Denison, 2014), the genetic information is segmented by the self-assembly of multiple replicons into nanorings, which is necessary to transfer all the genetic information partially stored on each replicon. When looking at nature, segmented RNA viruses are a natural example of segmentation. (McDonald *et al.*, 2016). Therefore, it is necessary to test whether the newly designed replicons can replicate and assemble in multipartite nanorings in an *in vitro* setting to determine their feasibility and optimal conditions.

The initial step was to select a new buffer that could be compatible for both efficient replication by Qβ replicase and pRNA-based self-assembly. Subsequently, the (+) and (-) strands of MDV-1 and RQ135 replicons carrying pRNA sequences as cargos were tested for replication and simultaneous self-assembly into dimers and trimers in bulk. After observing the emergence of parasites, the previous replication coupled assembly protocol was modified in order to perform the reaction in a water-oil emulsion. Several reaction protocols were tested to achieve the goal and to improve the efficiency of the system.

3.3.2. Results

After validating the ability of our RQ135 and MDV-1 replicons to replicate and assemble in nanorings of increasing dimensions, the aim was to couple these two abilities to obtain nanorings able to be replicated by the Qβ replicase *in vitro*.

Novel buffer formulation for assembly-coupled-replication assays. As the replication and assembly reactions occur in two different buffers, it was important to determine if they could occur in a compatible buffer. To accomplish this, the common components of each buffer were identified and a suitable buffer was developed, which was named the Assembly-Coupled-Replication buffer (ACR). Both buffers contain 10 mM $MgCl_2$ and 50 mM Tris-HCl (pH 7.5/8). However, the TMS buffer for the pRNA assembly contains 10 mM NaCl, while the Qβ replication buffer contains 0.10% (w/v) Pluronic F-68. Both were added to the ACR buffer while retaining the common components **(fig. 40)**.

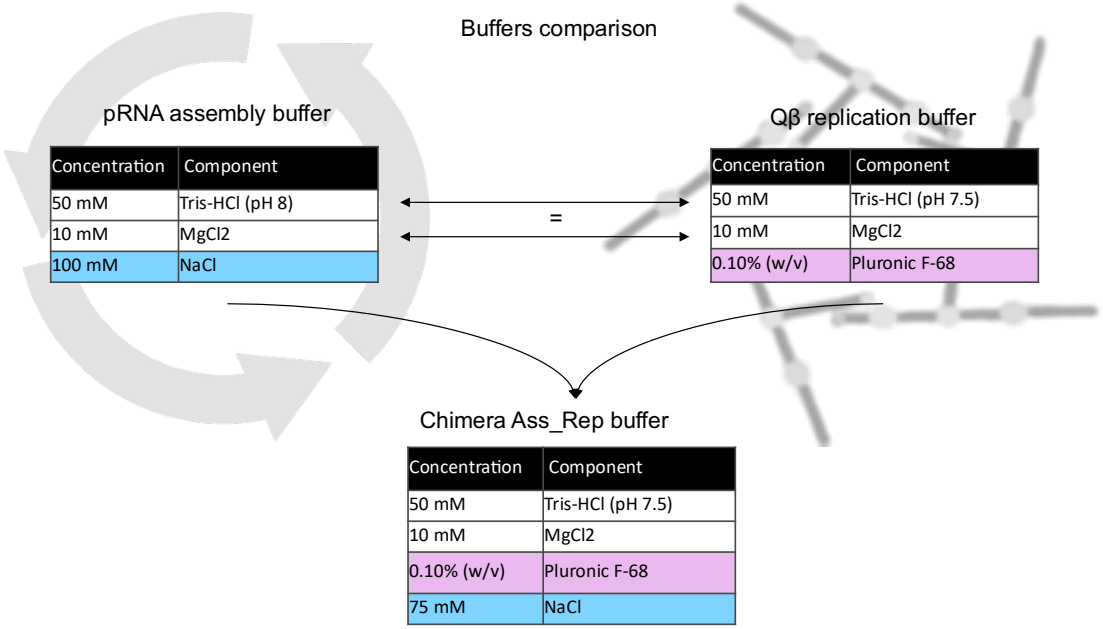

Figure 40: Generation of the ACR buffer. *Comparison between the pRNA assembly buffer (TMS buffer) and the Qβ replication buffer (MDV-1 buffer) and generation of a suitable buffer for testing the assembly-coupled-replication reaction of the replicons.*

To test the possibility of both assembly and replication in bulk, a new protocol was designed **(fig. 41)**. Each monomer was added in equimolar concentration to the reaction mix composed of the ACR buffer. Then, a refolding protocol was performed by heating the mixture to 80°C for 2 minutes and cooling it down at a rate of 1 °C per minute until it reached 37 °C. Subsequently, the re-folded replicons were incubated at 37 °C for 30 minutes to allow them to assemble into nanorings. Finally, the assembled nanorings were kept at 4°C, where rNTPs and the Qβ PB2 were added, and a t_0 sample was taken. Then the reaction was incubated at 37 °C for 3 hours and then the t_0 sample was taken. The t_0 and t_3 samples were run on a 5% Native PAGE for 70 V at 4 °C for 4 hours and SYBR gold

stained before visualizing them at the Sapphire. The protocol was repeated for the assembly of the dimer and trimer, starting from the (+) and (-) strands of the MDV-1_pRNA and the (+) and (-) strands of the RQ135_pRNA replicons.

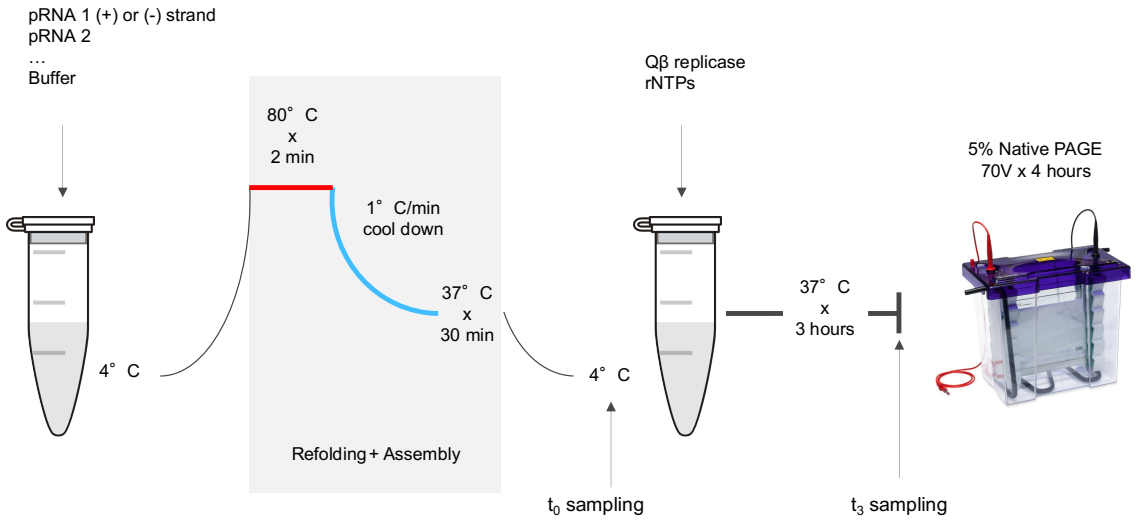

Figure 41: Assembly-coupled-replication in batch reactions. *Schematic representation of the protocol followed for the assembly-coupled-replication reaction in bulk. Dimers or trimers were assembled by adding each replicon carrying a pRNA sequence as cargo to a single Eppendorf tube and at first, a refolding and assembly step was performed. Then, while on ice, Qβ replicase and rNTPs were added to the reaction and incubated at 37°C for 3 hours while on ice. The samples were run on a 5% Native PAGE.*

Assembly-coupled-replication of MDV-1_pRNA replicons in bulk. The first series of experiments were conducted in bulk. Both MDV-1_pRNA replicon dimers and trimers exhibited similar gel patterns. In the case of the (-) dimer **(fig. 42)**, the formation of the nanoring was visible at approximately 706 nt at t_0. It is unclear whether the replicase recognized and amplified the dimer. After 3 hours of incubation, in the sample were the replicase was added, multiple bands began to appear, indicating that the Qβ was active. However, it did not appear to selectively replicate the target replicon, but instead produced a smear representing the formation of various RNA species. Furthermore, the formation of parasites was visible at approximately 100 nt. It could be understood that the replicase was able to replicate the monomers in the new ACR buffer, but there was no clear evidence of dimer replication.

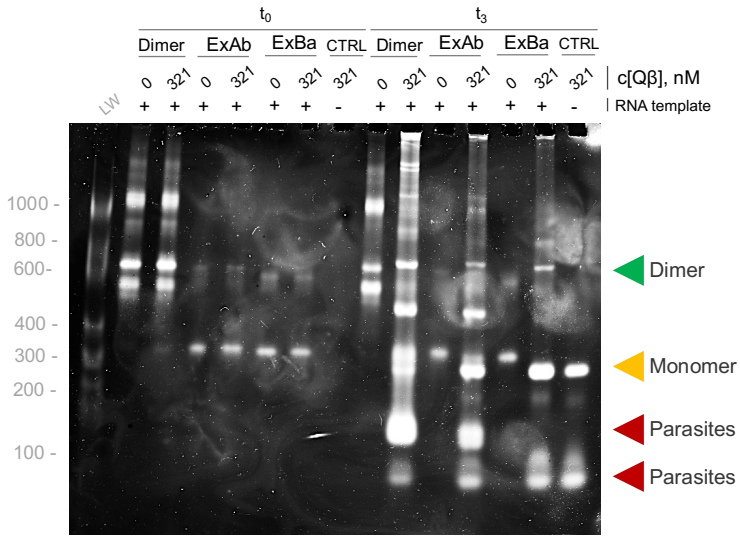

Figure 42: Assembly-coupled-replication assay of (-) MDV-1 _pRNA replicon dimer in bulk. *5% Native PAGE of the assembly-coupled-replication reaction of the (-) MDV-1 _pRNA replicon dimer (706 nt) in bulk, as described in material and methods. Concentrations of 0 and 321 nM of Qβ replicase were tested, and samples were taken at 0 hours (t_0) and 3 hours (t_3). In addition, control reactions were carried out using monomers ExAb and ExBa (each 353 nt), as well as a reaction without the RNA template (CTRL), following the same protocol as for the dimer. LW: RiboRuler Low Range ssRNA Ladder (nt) (Thermo).*

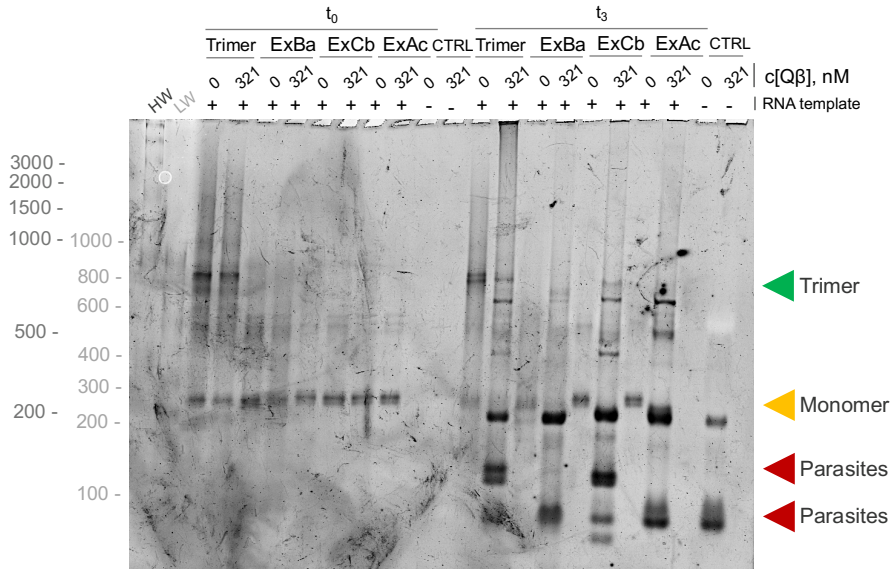

Figure 43: Assembly-coupled-replication assay of (-) MDV-1_pRNA trimer in bulk. *5% Native PAGE of the assembly-coupled-replication reaction of the (-) MDV-1_pRNA replicon trimer (1059 nt) in bulk, as described in material and methods. Concentrations of 0 and 321 mM of Qβ replicase were tested, and samples were taken at 0 hours (t_0) and 3 hours (t_3). In addition, control reactions were carried out using monomers ExAb, ExCb, ExAc (each 353 nt), as well as a reaction without the RNA template (CTRL), following the same protocol as for the trimer. HW: RiboRuler High Range ssRNA Ladder (nt). LW: RiboRuler Low Range ssRNA Ladder (nt) (Thermo).*

In the case of the trimer **(fig. 43)**, it was possible to observe the formation of the trimer at t_0, at about 1000 nt. Upon adding the Qβ PB2 replicase, the band at 300 nt became more intense, similar to the bands corresponding to the monomers used as controls. However, the expected band at 1059 nt became less intense, making it impossible to verify the replication of the trimer nanoring. This could potentially represent a disrupting activity of the replicase towards the assembly. Additionally, the band at t_3 at about 300 nt representing the monomers became more intense, which could indicate that the replicase disrupted the nanoring and carries on the replication of only each single replicon, thereby interfering with the assembly.

Assembly-coupled-replication of RQ135_pRNA replicons in bulk. The RQ135_pRNA replicons were also assayed for their ability to assemble and replication. When considering the RQ135_pRNA trimer nanoring starting from the (+) strands of the RQ135_pRNA replicons, the addition of Qβ PB2 to the reaction resulted in the disappearance of the band corresponding to the trimer nanoring, previously visible in the first two lanes of the t_0 samples, and the appearance of a smear **(fig. 44)**. This could be interpreted as evidence of replicase activity, while the smear may be attributed to uncontrolled and untargeted replication ability of the replicase. Also, in the case of the RQ135_pRNA assembly it was possible to see the formation of parasites below 200 nt at t_3.

When starting from the (-) strand of the RQ135_pRNA replicon as input **(fig. 45)**, a side product can be observed at t_0, potentially formed by the self-assembly of the monomers. At approximately 256 nt, the monomers become visible. When adding the Qβ PB2 replicase, at t_3 it's possible to see that multiple bands started to appear meaning that multiple products were synthesized by the replicase. At about 700 nt it was possible to see that two close bands were present, and they could possibly be attributed to the replication of the trimer, since the dimension of the trimer is of 768 nt. However, it was also possible to see the presence of the two similar bands at about the same nt at t_3 of the $pRNA_{ExAb}$ and $pRNA_{ExBa}$ monomers, questioning the formation of the trimer. At approximately 1500 nt in the trimer assembly reaction, a new band appeared. This new band was likely due to the assembly of the trimer and its association with the Qβ replicase. As the samples were not denaturated before loading onto the Native PAGE following the replication-coupled assembly reaction, it was possible that the replicase was still bound to the trimer, causing a shift in the band to

higher sizes and representing a potential proof of the replication and self-assembly of the nanoring.

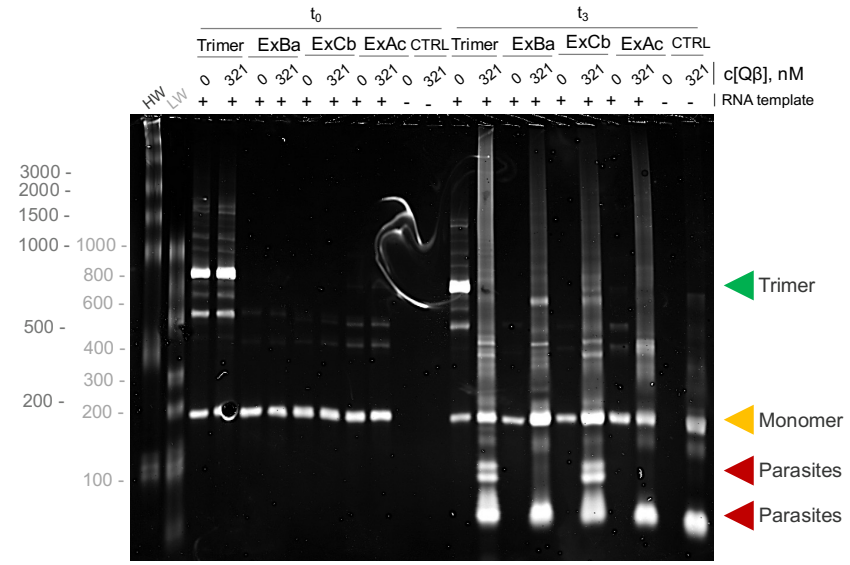

Figure 44: Assembly-coupled-replication assay of (+) RQ135_pRNA trimer in bulk. *5% Native PAGE of the assembly-coupled-replication reaction of the (+) RQ135_pRNA replicon trimer (768 nt) in bulk, as described in material and methods. Concentrations of 0 and 321 mM of Qβ replicase were tested, and samples were taken at 0 hours (t_0) and 3 hours (t_3). In addition, control reactions were carried out using monomers ExAb, ExCb, ExAc (each 256 nt), as well as a reaction without the RNA template (CTRL), following the same protocol as for the trimer. HW: RiboRuler High Range ssRNA Ladder (nt). LW: RiboRuler Low Range ssRNA Ladder (nt) (Thermo).*

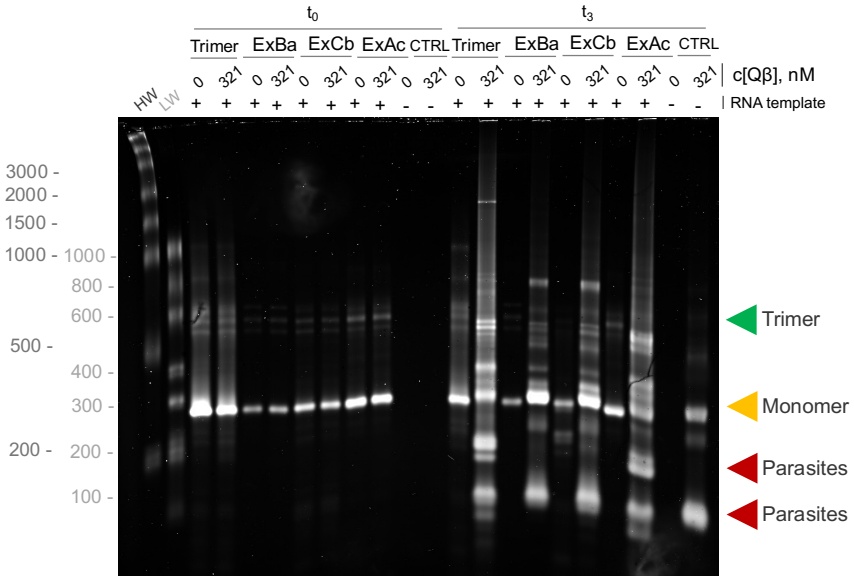

Figure 45: Assembly-coupled-replication assay of (-) RQ135_pRNA trimer in bulk. *5% Native PAGE of the assembly-coupled-replication reaction of the (-) RQ135_pRNA replicon trimer (768 nt) in bulk, as described in material and methods. Concentrations of 0 and 321 mM of Qβ replicase were tested, and samples were taken at 0 hours (t_0) and 3 hours (t_3). In addition, control reactions were carried out using monomers ExAb, ExCb, ExAc (each 256 nt), as well as a reaction without the RNA template (CTRL), following the same protocol as for the trimer. HW: RiboRuler High Range ssRNA Ladder (nt). LW: RiboRuler Low Range ssRNA Ladder (nt) (Thermo).*

Assembly-coupled-replication of MDV-1_pRNA replicons in water-oil emulsion. To address the difficulty of understanding whether bulk assembly-coupled replication could occur, it was decided to encapsulate the reaction in a water-oil emulsion system, since encapsulating the reaction in droplets contained parasite formation and enhanced the production of the desired replicon, as previously demonstrated in Chapter 1.

To benefit from the emulsion properties, an encapsulation step was added to the previous assembly-coupled replication protocol as follows **(fig. 46)**. The initial steps, up until the cooldown to 4°C, remained unchanged. As previously, each MDV-1_pRNA replicon or the RQ135_pRNA replicon was added in equimolar concentration to the reaction in ACR buffer. The reaction was then heated to 80°C for 2 minutes and gradually cooled at a rate of approximately 1°C/min until it reached 37°C. This was followed by a 30 minute incubation at 37°C, a cooled down to 4°C, and storage on ice. rNTPs were added to the reaction, followed by the Qβ replicase PB2 and 2% Pico-Surf w/w in Novec 7500 in order to generate the emulsion, as described in the Materials and Methods section. The t_0 samples were taken while still on ice. The reaction was then incubated at 37°C for 3 hours, and finally, the emulsion was broken following the general protocol present in material and methods and the t_3 sample was collected. Both t_0 and t_3 samples were run on a 5% Native PAGE at 70V for 4 hours at 4°C, stained with SYBR gold, and visualized using an Azure Sapphire Biomolecular Imager.

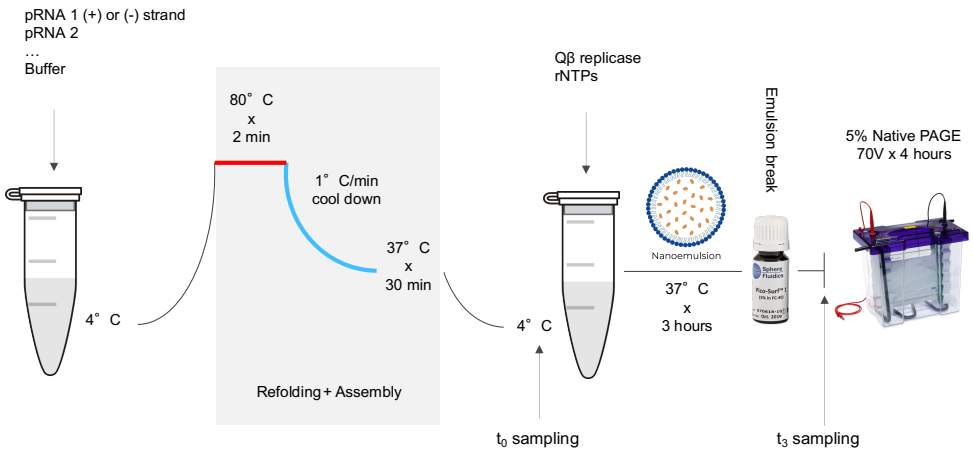

Figure 46: Assembly-coupled-replication in water-oil emulsion. *Schematic representation of the protocol followed for the assembly-coupled-replication reaction in water-oil emulsion. Trimers were assembled by adding each replicon carrying a pRNA sequence as cargo to a single Eppendorf tube and at first, a refolding and assembly step was performed. Qβ replicase and rNTPs were added to the reaction while on ice. The emulsion was generated by scratching the tube on a tube rack and then incubated at 37°C for 3 hours. At the end of the 3 hours, the emulsion was broken as explained in the material and methods. The samples were run on a 5% Native PAGE.*

Several optimization tests were necessary to achieve proper compartmentalization. The optimal concentration of surfactant for efficient encapsulation of the reaction was found to be 2% (w/w) PicoSurf. Subsequently, the previously described assembly-coupled replication in droplets protocol was tested. **Fig. 47** shows that the trimer was correctly assembled at t_0, at about 800 nt. After incubating in the emulsion for 3 hours and breaking it, the addition of the Qβ replicase PB2 to the assembly resulted in the disappearance of the band corresponding to the trimer. Additionally, the single band corresponding to each monomer also disappeared after the addition of replicase potentially representing RNA degradation during the reaction.

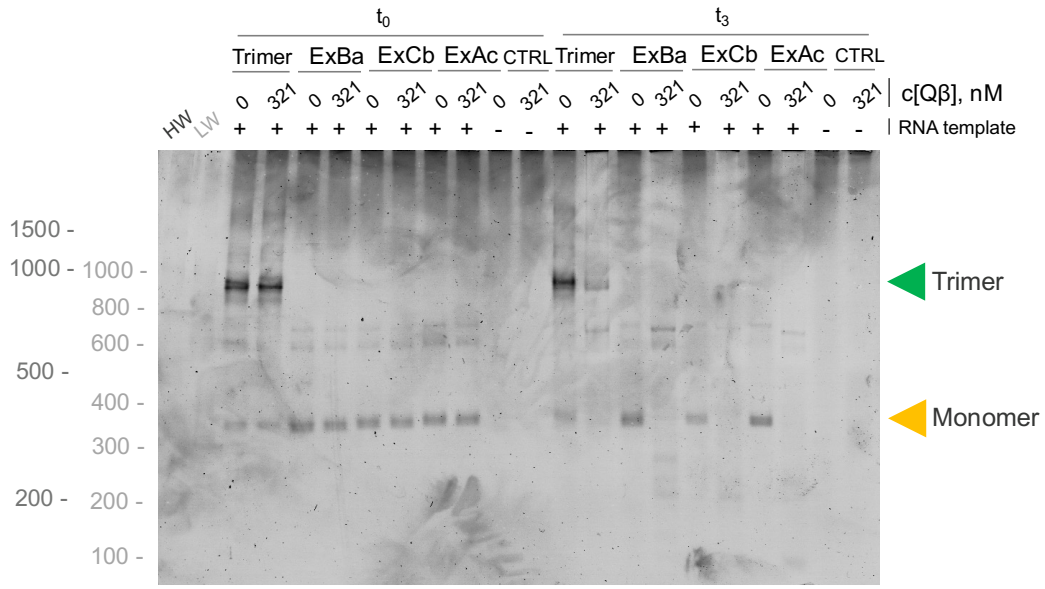

Figure 47: Assembly-coupled-replication assay of (-) MDV-1 _pRNA trimer assembly in water-oil emulsion. *5% Native PAGE of the assembly-coupled-replication reaction of the (-) MDV-1 _pRNA replicon trimer (1059 nt) in water-oil emulsion, as described in material and methods. Concentrations of 0 and 321 mM of Qβ replicase were tested, and samples were taken at 0 hours (t_0) and 3 hours (t_3). In addition, control reactions were carried out using monomers ExAb, ExCb, ExAc (each 353 nt), as well as a reaction without the RNA template (CTRL), following the same protocol as for the trimer. HW: RiboRuler High Range ssRNA Ladder (nt). LW: RiboRuler Low Range ssRNA Ladder (nt) (Thermo).*

Experiments based on the RQ135_pRNA scaffold yielded comparable results **(fig. 48)**. The trimer assembled at t_0, but upon addition of the replicase and subsequent emulsion formation and incubation, the band corresponding to the trimer at about 768 nt disappeared, and a lower band at about 600 nt emerged. The same outcome was observed with the single monomers used as positive controls. The addition of Qβ resulted in an output that remains

unclear when the replicase is added in the reaction, it seemed that the previously assembled nanoring is dismantled and there was a formation of an unexpected band pattern.

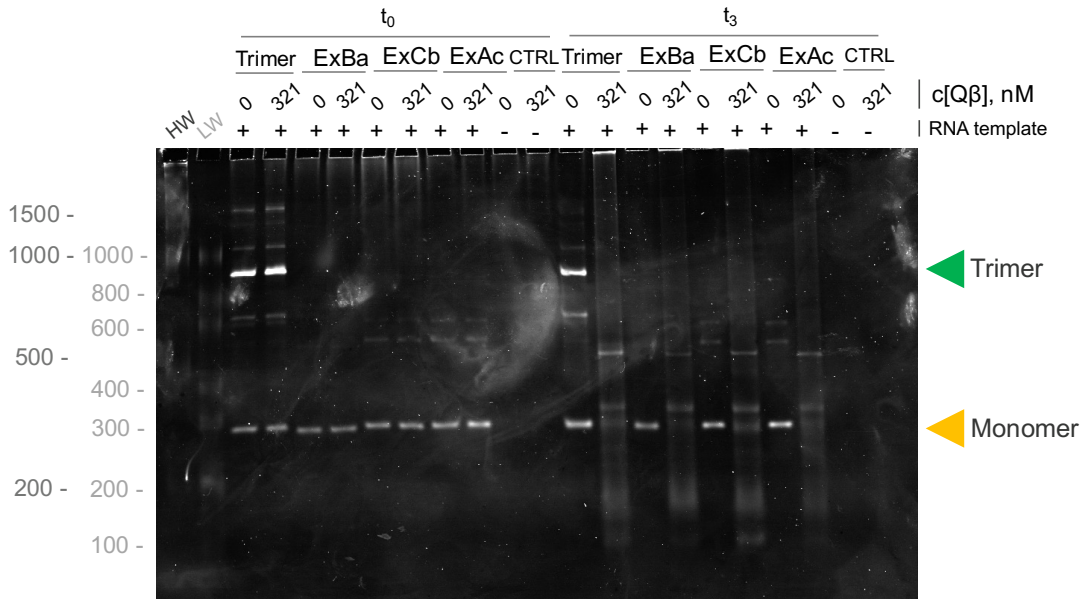

Figure 48: Assembly-coupled-replication assay of (+) RQ135_pRNA in water-oil emulsion. *5% Native PAGE of the assembly-coupled-replication reaction of the (+) RQ135_pRNA replicon trimer (768 nt) in water-oil emulsion, as described in material and methods. Concentrations of 0 and 321 nM of Qβ replicase were tested, and samples were taken at 0 hours (t_0) and 3 hours (t_3). In addition, control reactions were carried out using monomers ExAb, ExCb, ExAc (each 256 nt), as well as a reaction without the RNA template (CTRL), following the same protocol as for the trimer. HW: RiboRuler High Range ssRNA Ladder (nt). LW: RiboRuler Low Range ssRNA Ladder (nt) (Thermo).*

Protocol variation for assembly-coupled-replication of MDV-1_pRNA and RQ135_pRNA replicons in water-oil emulsion. After the unsuccessful attempts to replicate both the MDV-1_pRNA and RQ135_pRNA replicon assemblies described above, a new protocol was designed and tested for both scaffold systems **(fig. 49)**. Each monomer was refolded separately in ACR buffer, using the same method as in the previous assembly-coupled replication protocols. After refolding, the monomers were combined in equimolar amounts in a single Eppendorf tube and kept on ice. The RNase inhibitor was added to prevent potential RNase contamination that would lead to RNA degradation. Next, Qβ PB2 and rNTPs were added while keeping the tubes on ice. A t_0 sample was taken before forming the emulsion and encapsulating the reaction. The emulsion was then incubated at 37°C for 3 hours. Finally, the emulsion was broken and the t_0 and t_3 samples were analysed using 5% Native PAGE and 5% urea-PAGE.

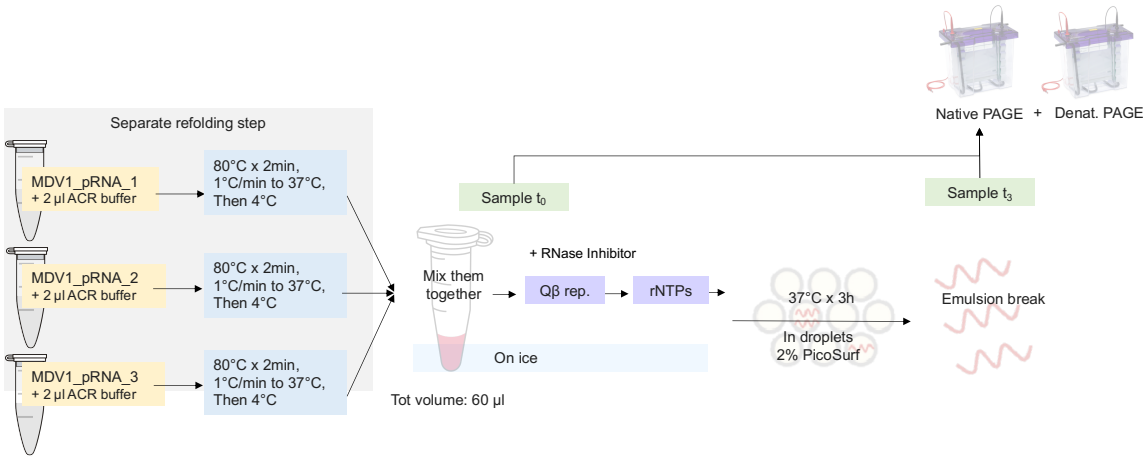

Figure 49: Alternative protocol for the assembly-coupled-replication in water-oil emulsion of trimers. *Schematic representation of the alternative protocol followed for the assembly-coupled-replication reaction of trimers replicons in water-oil emulsion. Each replicon carrying a pRNA sequence as cargo underwent a separate refolding step. Afterwards, while on ice, they were added to an Eppendorf tube. At this point, Qβ replicase, rNTPs and RNase inhibitor were added to the reaction while still on ice. The emulsion was generated by scratching the tube on a tube rack and then incubated at 37°C for 3 hours, as explained in the Materials and Methods. At the end of the 3 hours, the emulsion was broken down, as explained in the Materials and Methods. The samples were then run on a 5% Native PAGE and a 5% urea-PAGE.*

The (-) strand MDV-1_pRNA replicons were the first to be tested using the new protocol. As expected at t_0 there was no formation of the trimer, as evident by the bands in the native gel at about 350 nt corresponding to the monomers, since the monomers were refolded separately and then stored at 4 °C before the incubation at 37 °C, the optimal temperate for the assembly formation. As it possible to see in the native PAGE, when Qβ PB2 replicase was added, a band at approximately 500 nt appeared in the t_3 sample and the monomers previously present at 350 nt disappeared **(fig. 50a)**. This could indicate the production of the (-) strand by Qβ, but the band was not present at the expected size, meaning that it may have adopted a different fold that makes it moved faster in the native PAGE gel **(fig. 50a)**. Upon addition of the replicase, a band potentially corresponding to a trimer at a size of approximately 1000 nt was observed in the t_3 sample. The identity of this band remains unclear. Upon analysing samples t_0 and t_3 on denaturant PAGE **(fig. 50b)**, single bands corresponding to the monomers were observed at 353 nt. Upon addition of replicase at t_3, a smear was present, and bands at about 190 nt appeared, indicating the possibility of parasite formation. It is unclear why this lower band appeared only in the denaturing gel and not in the native gel. There is a possibility that the monomers interacted with the assembly, causing a shift in their position on the gel. However, there is no evidence of the

actual formation of the assembly and therefore it can be concluded that no replication of the trimer was detected.

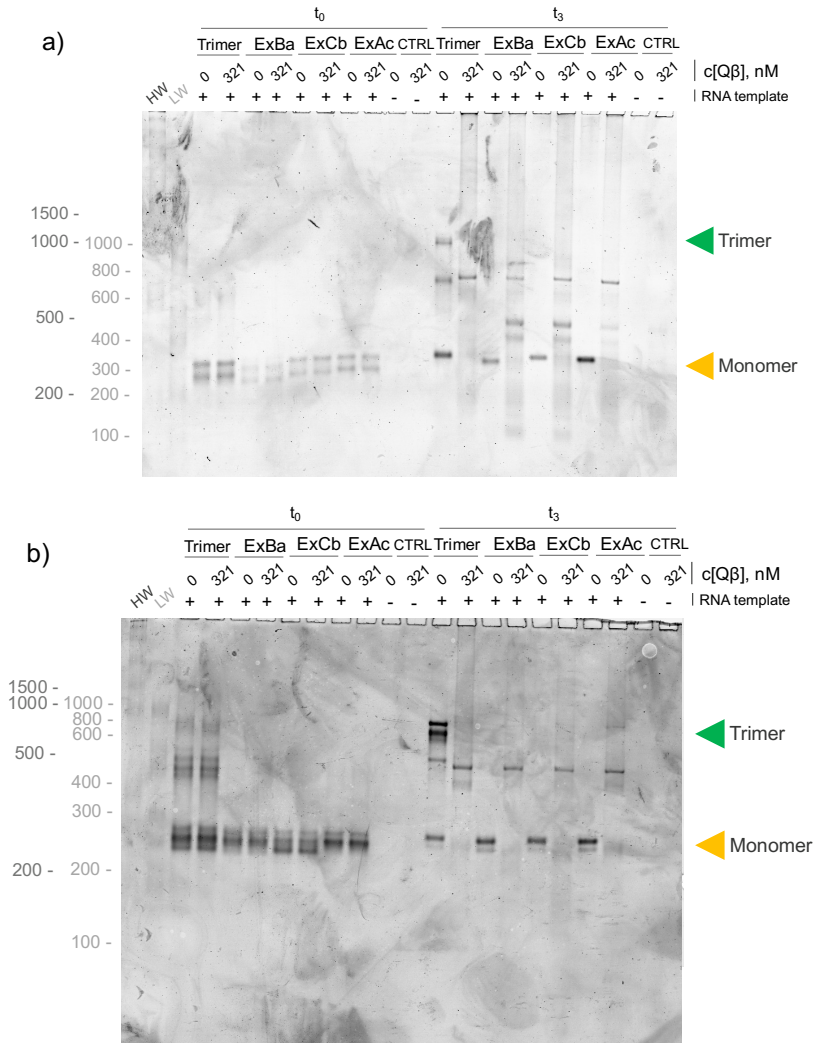

Figure 50: Alternative protocol of the assembly-coupled-replication assay of the (-) MDV-1 _pRNA trimer in water-oil emulsion. *5% Native PAGE of the assembly-coupled-replication reaction of the (-) MDV-1_pRNA replicon trimer (1059 nt) in water-oil emulsion, as described in material and methods. Concentrations of 0 and 321 nM of Qβ replicase were tested, and samples were taken at 0 hours (t_0) and 3 hours (t_3). In addition, control reactions were carried out using monomers ExAb, ExCb, ExAc (each 353 nt), as well as a reaction without the RNA template (CTRL), following the same protocol as for the trimer.* ***a)*** *5% Native PAGE* ***b)*** *5% urea-PAGE. HW: RiboRuler High Range ssRNA Ladder (nt). LW: RiboRuler Low Range ssRNA Ladder (Thermo).*

After the (-) strand MDV-1_pRNA replicons, the (+) strand RQ135_pRNA were tested. The replication protocol used previously was also adopted for these replicons. Considering the native PAGE **(fig. 51a)**, looking at the t_0 sample where all the three monomers were added, there was a slight formation of trimer at approximately 650 nt even when the sample was kept on ice at 4°C. After incubating the reaction for 3 hours at 37°C in the absence of Qβ replicase, it was observable that the trimer assembled and become visible at

approximately 1000 nt in the absence of replicase. However, upon addition of replicase to the reaction, the band corresponding to the trimer disappeared and a lower band at around 650 nt appeared. This lower band was also present in the t_3 control samples containing only the monomers and was therefore suggestive of non-templated parasite formation.

When analysing the samples on a denaturant PAGE **(fig. 51b)**, a smear appeared at t_3, which was consistent with previous observation for MDV-1 replicons in the assembly-couple-replication in emulsion, upon addition of the replicase to the reaction. Additionally, bands at lower nucleotides were observed, suggesting the formation of parasites or potentially

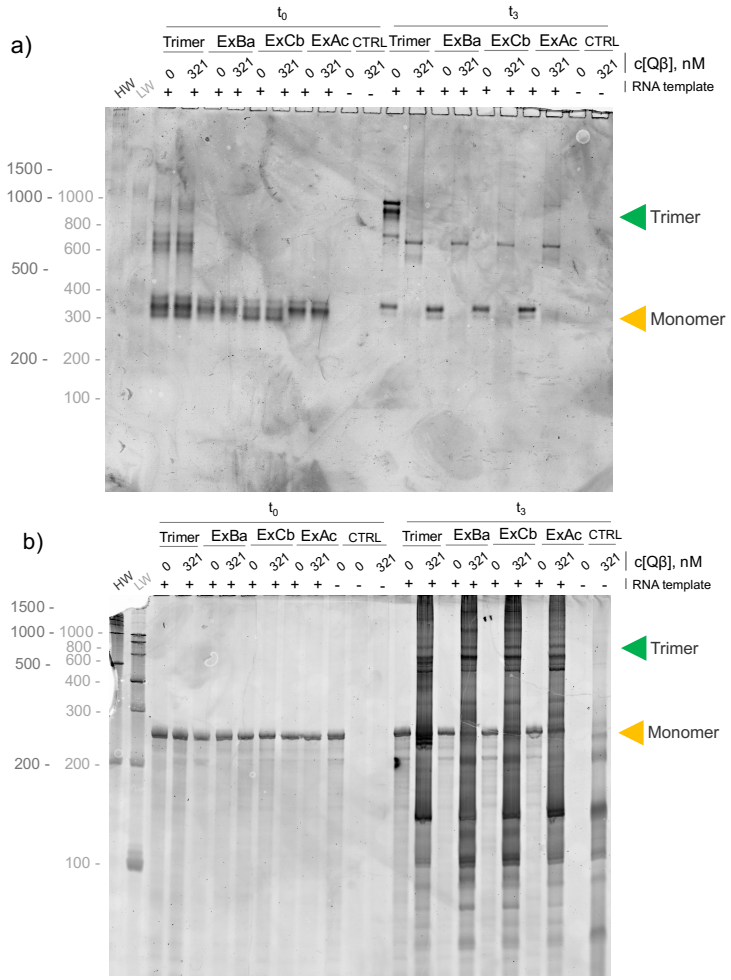

Figure 51: Alternative protocol of the assembly-coupled-replication assay of the (+) RQ135_pRNA trimer in water-oil emulsion. *5% Native PAGE of the assembly-coupled-replication reaction of the (+) RQ135_pRNA replicon trimer (768 nt) in water-oil emulsion, as described in material and methods. Concentrations of 0 and 321 mM of Qβ replicase were tested, and samples were taken at 0 hours (t_0) and 3 hours (t_3). In addition, control reactions were carried out using monomers ExAb, ExCb, ExAc (each 256 nt), as well as a reaction without the RNA template (CTRL), following the same protocol as for the trimer.* ***a)*** *5% Native PAGE* ***b)*** *5% urea-PAGE. HW: RiboRuler High Range ssRNA Ladder (nt). LW: RiboRuler Low Range ssRNA Ladder (nt) (Thermo).*

degraded product. Similarly to the MDV-1 based replicons, it could be concluded for the RQ135_pRNA replicons that no replication and assembly of the trimer from newly generated plus strands occurred.

Proposed experiments for assembly-coupled-replication of MDV-1_pRNA and RQ135_pRNA replicons in water-oil emulsion. To assess the ability of our replicons to assemble and replicate, new protocols were designed and proposed. This was done to identify potential solutions to previous failures. However, due to time constraints, these protocols were not tested.

The proposed protocol **(fig. 52)** suggests a separate refolding step for each replicon, MDV-1_pRNA or RQ135_pRNA, and a separate incubation with the Qβ PB2 replicase in droplets. After a 3-hour incubation at 37°C, each emulsion containing the individual replicons are broken, and combined with the other reactions in a single tube. The mixture is then incubated for an additional 30 minutes at 37 °C to assemble the potentially replicated monomers into the nanoring. The samples t_0, t_3, and the sample mix are loaded and visualized on a native and denaturant PAGE.

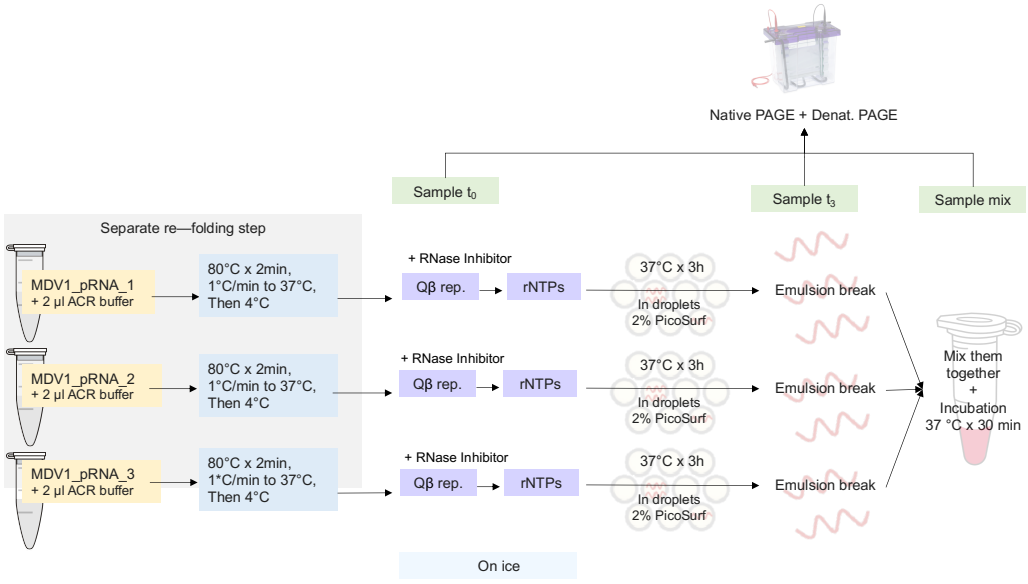

Figure 52: Proposed experiment for trimer assembly-coupled-replication in water-oil emulsion. *Schematic representation of the proposed protocol for the assembly-coupled replication reaction of MDV-1_pRNA and RQ135_pRNA trimers replicons in a water-oil emulsion. Each replicon carrying a pRNA sequence as cargo undergoes a separate refolding step. Afterward, Qβ replicase, rNTPs, and RNase inhibitor are added to each tube while on ice. The emulsion is then generated by scratching the tube on a tube rack and incubated at 37°C for 3 hours, as explained in the Materials and Methods. At the end of the 3-hour incubation period, the emulsion was broken down, as described in the Materials and Methods. The resulting samples were combined into a single tube and incubated at 37°C for 30 minutes. Subsequently, the samples were run on a 5% Native PAGE and a 5% urea-PAGE.*

Another proposed protocol is called “replication and assembly in cycles” **(fig. 53)**. In this protocol, each replicon follows a separate refolding step. At the end of this step, they are mixed together while keeping the tube on ice. Then, Qβ PB2 replicase, rNTPs, and the RNase inhibitor are added. The sample t_0 is taken while still on ice. This is followed by incubation in droplets for 3 hours at 37 °C, after which the emulsions are broken and the t_3 sample can be taken. Here, a new step is added. After collecting the t_3 sample, heat it to 95 °C for 4 minutes to denature Qβ replicase and disassemble the assembly. Then rapidly cool it down to 4 °C and keep it on ice. Next, fresh ACR buffer, Qβ replicase, rNTPs, and RNase inhibitor are added. Another cycle of assembly and replication can then be performed. For each cycle, t_0 and t_3 are taken and run on the gel to visualize any potential replication of the nanoring and a potential increase in yields resulting from refuelling the reaction with fresh components.

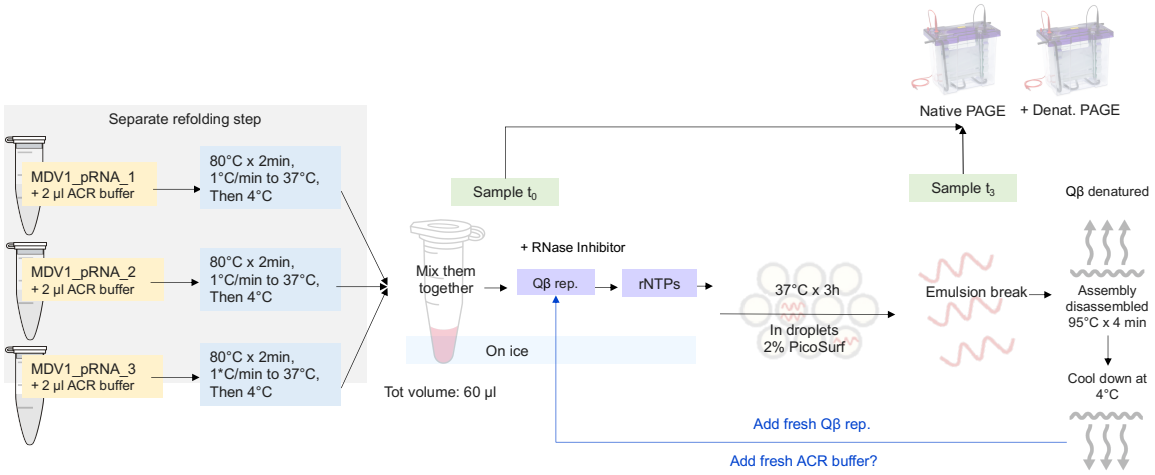

Figure 53: Proposed experiment for replication and assembly in cycles in water-oil emulsion. *Schematic representation of a proposed experiment for the assembly-coupled-replication reaction of trimers replicons emulsion in cycles. Each replicon carrying a pRNA sequence as cargo underwent a separate refolding step. Afterwards, while on ice, they are added to an Eppendorf tube. At this point, Qβ replicase, rNTPs and RNase inhibitor is added to the reaction while still on ice. The emulsion was generated by scratching the tube on a tube rack and then incubated at 37°C for 3 hours, as explained in the Materials and Methods. At the end of the 3 hours, the emulsion is broken down, as explained in the Materials and Methods. Then, the sample is heated at 95 °C for 4 min and then cool down at 4 °C. Fresh Qβ replicase and ACR buffer is then added and then another cycle is performed as before. After several cycles, all the samples are then run on a 5% Native PAGE and a 5% urea-PAGE for the analysis.*

3.3.3. Summary and conclusions

In this section, the main goal was to couple the assembly and replication of the previously designed and tested replicons based on the MDV-1 and RQ135 scaffold, in order to build

replicating nanorings of increasing dimensions. This is the first attempt to build, test, and understand the potential requirement for an RNA nanostructure capable of replicating *in vitro.*

The first step was to decide a potential buffer that would allow the replication of the desired MDV-1 and RQ135 RNA replicons carrying the pRNA sequence, and at the same time allow the formation of self-assembled nanorings by adding more replicons to the reaction. Therefore, the Assembly-coupled-replication (ACR) buffer was used, which contains common components of replication and assembly buffers, make the coupling of the two abilities feasible. Next, a proper protocol was designed to test the MDV-1_pRNA dimer and trimer and RQ135_pRNA trimer in bulk. The MDV-1_pRNA replicon dimers showed inconclusive evidence of replication, while trimer replication remained unclear. Conversely, RQ135_pRNA trimer replication suggested replicase activity, but the evidence was unclear. Furthermore, as noted in the single replicon test, short parasites emerge during incubation, necessitating the use of compartmentalization and the setup of the reaction in a water-oil emulsion. The previous protocol was revised to include the water-oil emulsion system, as previously done in this work for the replication of MDV-1 by the Qβ single replicons. Trimer assembly was observed at t_0, but the trimer band disappeared after 3 hours in the emulsion. Therefore, a modified protocol was used to separately refold the replicon monomers before incubation in emulsion. However, even with this modification, no clear evidence of trimer replication was observed for both MDV-1_pRNA and RQ135_pRNA replicons. Overall, a possible explanation for this observation is that the Qβ replicase may disrupt the nanoring, thereby preventing replication, as indicated by the results showing the formation of a smear after 3 hours of incubation and disappearing of the band representing the nanoring. Overall, although the replication of our nanorings remains unclear and potentially unfeasible in our experimental conditions, we were able to confirm once again that the use of a water-oil emulsion system was effective in preventing parasite formation.

In conclusion, the presented data indicates that our attempt to build replicating nanostructures based on our design of MDV-1 and RQ135 was inconclusive and need more investigation in order to understand if MDV-1 and RQ135 are not a suitable scaffold for the purpose. Potentially, Qβ is not the best system for this purpose due to the too high replicability and formation of parasitic species. Further investigation and a potential change in direction are necessary, but this work represented perhaps the first experimental evidence of how a structural RNA motif such as the pRNA could be coupled to the replication activity of a viral replicase.

One potential improvement for this system could be to test the assembly-coupled replication experiment in a lysate system. The lysates would allow for prototyping the replicating system without the need to transplant it directly into *E. coli*, while retaining most of the properties of living cell. This would enable the self-replication system previously constructed to interact with unknown mechanisms present in a living cell, which could significantly impact its assembly and replication abilities. This interaction could potentially involve host factors that contribute to or regulate the replication process.

Another potential solution to make the system replicate could be the adoption of the MS2 virus self-replicating system, as previously mentioned. As the MS2 system can replicate its own RNA at a slower rate, this could provide an advantage in terms of reducing parasites (Wagner *et al.*, 2022) and obtain a targeted and specific replication of the desired MS2 adapted replicon by the MS2 replicase what wasn't possible with the Qβ system.

4. Closing Remarks

The recreation of LUCA (Koonin *et al.*, 2020) is seen as an important milestone in the field of origin of life research, since it could provide valuable insights into how genetic information is passed from RNA to DNA and has potential biotechnological applications. To achieve this goal, the viral world could offer a vast array of pre-existing and evolutionary optimised technologies that are ready to be implemented using the latest synthetic biology techniques. Starting from this concept, this work explored the initial stages of creating synthetic RNA alongside the DNA genome of *E. coli*, setting up the replication, based on the Qβ replicase system, and assembly technology, based on the pRNA based nanorings, of such RNA genome. In addition, the ability to replicate conferred to the nanorings, and possibly other RNA-based structures based on different motifs, could have potential applications in the field of RNA nanotechnology and may represent a first ever attempt in conferring replicability properties to previously static molecules.

The aim of this work was to establish a first *in vitro* technology that can be exploited in an *in vivo* setting in the future, such as *E. coli*. Although the assembly-coupled replication experiments yielded inconclusive results and need further investigation, a system based on Qβ and its two replicons, RQ135 and MDV-1, was successfully established and tested. This system incorporates useful sequence information for the read-out of the replication reaction, given integration of fluorogenic aptamer, and pRNA sequences that can drive the self-assembly of multiple replicons. This provided feature enables the RNA genome to be divided into subunits, each of which can carry distinct information and be condensed in a circular manner for greater efficiency and modularity. Furthermore, the addition of a pRNA motif to the replicons and their assembly into nanorings has not been previously reported in the field, but has been successful, since the assembly or the replicons that were designed works in the tested conditions. This approach may also be applicable to other self-replicating systems, such as MS2 (Wagner *et al.*, 2022), which could be a preferable option for building a synthetic self-replication system compared to Qβ, that, based on the assembly-coupled-replication series, results quite unpredictable and unstable.

One important finding from this work, which confirms previous observations by other groups (Lehman, 2012; Matsumura *et al.*, 2016), is that encapsulating the heterologous replicon and Qβ replicase in compartments, such as the one adopted in the work, water-oil emulsion, prevents the emergence of parasitic species. These species can pose a significant issue for the reaction's sustainability of the RQ135 and MDV-1-based due to their high

replication rate and buffer exhaustion. Beside the encapsulation, another important factor that was confirmed to prevent parasite formation was the use of a highly purified replicase to eliminate nucleic acid contamination, as shown by use of the Qβ PB2 in this work. Qβ binds RNA strongly, so potential DNA and RNA contamination from the *E. coli* expression system could be present in the downstream batch during the purification process and this contamination could represent a seed for parasite production, starting from non-specific binding and replication by Qβ.

If further optimization will be adopted for the novel designed self-replication *in vitro* system discussed in this work, this could form the basis for translation into an in vivo setting by building the first hybrid organism carrying its genetic information on both DNA and RNA. This could shed light on a missing link in the evolution towards a life-like entity on this planet and add new potential applications in the modern synthetic biology field and RNA nanotechnology.

5. Materials and Methods

5.1. Laboratory equipment

- ÄKTA Start Chromatographic System (Cytiva)
- Benchtop Centrifuge 5425 and 5425 R (cooled) (Eppendorf)
- Blue light scanner BIO-1000F (Microtek)
- Concentrator plus (Eppendorf)
- Dry block Thermomixer C (Eppendorf)
- EasyPhor PAGE maxi WAVE electrophoresis (20 x 20 cm) (Biozym)
- Heater (Heidolph)
- Magentic stirrer (Heidolph)
- Nanodrop one^{c} (Thermo Fisher Scientific)
- Owl Easycast B1 mini gel electrophoresis system (Thermo Fisher Scientific)
- Ph/mv meter FiveEasy (Mettler Toledo)
- Power supply EV3330 (Consort)
- PowerEase Touch 120W (Invitrogen) (Thermo Fisher Scientific)
- Proflex PCR systems from Applied Biosystems (Life Technologies)
- Rocking platform (VWR)
- Sapphire Biomolecular Imager (Azure Biosystems)
- Sonopuls HD 4100 with Sonotrode TS106 (Bandelin)
- Standard incubator model B 28 (Binder)
- UV light source UVLS-26 EL (Analytic Jena)
- X-cell surelock Mini-Cell Electrophoresis (10 x 10 cm) (Thermo Fisher Scientific)

5.2. Consumables

- 2-propanol (Isopropanol) (Sigma)
- Absolute ethanol (Sigma)
- Agar (Becton, Dickinson and Company)
- All DNA oligonucleotides (IDT)
- Amicon UF 3 KDa MWCO rigenerate cellulose spin filters (Merck)
- Aminoallyl-UTP-Cy3 (Jena bioscience)
- Aminoallyl-UTP-Cy3 (Jena bioscience)

- Aminoallyl-UTP-Cy5 (Jena bioscience)
- Ammonium persulfate (APS) (Carl Roth)
- Boric acid (Sigma)
- Bromophenol blue sodium salt (Carl Roth)
- Calcium chloride ($CaCl_2$) (Carl Roth)
- Carbenicillin (Carl Roth)
- Cellulose acetate filter spin columns (spin-x) (Costar)
- Chloroform (Carl Roth)
- DHFBI (Jean bioscience)
- Dimethyl sulfoxide (DMSO) (Carl Roth)
- Dithiothreitol (DTT)
- DNase I (RNase-free)
- DpnI (NEB)
- EcoRV (NEB)
- *E. coli* inorganic pyrophosphatase (IPP) (NEB)
- *E. coli* Top10 competent cells (NEB)
- Ethylenediaminetetraacetic acid (EDTA) (Carl Roth)
- Fluorescein-12-UTP (Jena bioscience)
- Gel Loading Buffer II (Thermo Fisher)
- Gibson assembly HiFi (NEB)
- Glycerol (99%) (Carl Roth)
- GoTaq G2 Hot-Start green master mix (Promega)
- High and low range ladder (Thermo Fisher)
- Imidazole (Carl Roth)
- Imidazole (Sigma)
- Magnesium Chloride ($MgCl_2$) hexahydrate and Tris(hydroxymethyl)aminomethane (Tris) (Th.Geyer)
- Magnesium sulfate ($MgSO_4$) heptahydrate (Carl Roth)
- Megashortscript kit (Thermo Fisher)
- Micro-granulated yeast extract (Carl Roth)
- Monarch DNA cleanup kit (5 µg) (NEB)
- Monarch RNA cleanup kit (10 µg and 50 µg) (NEB)
- N, n, n′, n′-tetramethylethylendiamin (TEMED) (Carl Roth)
- Nickel-NTA affinity resin (Sigma)

- Nucleospin plasmid EasyPure miniprep kit (Machery-Nagel).
- Picobreak (Sphere Fluidics)
- Picosurf (2% w/w) in Novec 7500 (Sphere Fluidics)
- Pluronic F-68 (Thermo)
- Potassium chloride (KCl) (Sigma)
- Pre-coated TLC plates (Machery-Nagel)
- Q5 High Fidelity DNA polymerase 2x master mix (NEB)
- RNA-grade glycogen (Thermo Fisher)
- RNase I (Thermo Fisher)
- rNTP (Jena Bioscience)
- Rotiphorese 40% 19:1 acrylamide:bis-acrylamide ready-to-use solution (Carl Roth)
- Rotiphorese 40% 29:1 acrylamide:bis-acrylamide ready-to-use solution (Carl Roth)
- Sodium acetate (NaOaC) (Carl Roth)
- Sodium chloride (NaCl) (Sigma)
- Spermidine (Thermo Fisher)
- Standard agarose (Carl Roth)
- SYBR Gold (Thermo Fisher)
- SYBR Safe (Thermo Fisher)
- TO1-B
- Triton x-100 (Carl Roth)
- Ultrapure Milli-Q water (Millipore) was used for all experiments in this study.
- Urea (Carl Roth)
- Vivaspin 20 polyethersulfone (Pes) 30 kda mwco centrifugal filters (Vivascience AG)
- Xylene cyanol sodium salt (Carl Roth)

5.3. Media and Buffers

- 10X Tris-Borate-EDTA (TBE): 0.89 M tris, 0.89 M boric acid, 20 mM EDTA pH 8.0.
- 50X Tris-Acetate-EDTA (TAE): 2 M tris, 1 M acetic acid, 50 mM EDTA pH 8.0.
- 20% urea-PAGE: 48% w/v urea (8 M), 1X TBE, 20% 19:1 acrylamide:bisacrylamide.
- 0% urea-PAGE: 48% w/v urea (8 M), 1X TBE.
- LB Media: 1% w/v peptone-tryptone, 0.5% w/v yeast extract, 100 mM NaCl.
- LB plates: LB media with 1.5% w/v bactoagar, supplemented with 100 µg/mL carbenicillin.

- SOC media: 2% w/v peptone-tryptone, 0.5% w/v yeast extract, 10 mM NaCl, 2.5 mM KCl, 5 mM $MgCl_2$, 5 mM $MgSO_4$, 20 mM glucose.
- RQ135 buffer: 1 mM Tris-Cl pH 7.5, 100 mM $MgCl_2$, 5 mM EDTA and 1% Triton X-100, 0.25 mM each rNTP (1 mM in total).
- MDV-1 buffer: Tris-HCl pH 7.5, 10 mM $MgCl_2$, 0.10 (w/v) Pluronic F-68, 1.25 mM each rNTP (5 mM in total).
- 1X Tris-magnesium saline (TMS): 50 mM Tris-HCl pH 8.0, 100 mM NaCl and 10 mM $MgCl_2$.
- 1X Tris-borate magnesium (TBM): 89 mM Tris base, 200 mM boric acid and 5 mM $MgCl_2$.
- Assembly-coupled-replication (ACR) buffer: 50 mM Tris-HCl pH 7.5, 10 mM $MgCl_2$, 75 mM NaCl, 0.10% (w/v) Pluronic F-68.
- DHFBI staining buffer: 10 µM DHFBI, 40 mM HEPES pH 7.4, 100 mM KCl, 1 mM $MgCl_2$.
- TO1-B staining buffer: 100 nM TO1-B, 40 mM Tris-HCl pH 8, 50 mM KCl, 22 mM $MgCl_2$.
- Qβ protein purification buffers

  Protocol 1, adapted from Kita et al., 2006:

  - Lysis buffer I: 0.1 M Na_2PO_4 at pH 7,0, 0.5 M NaCl, 20% glycerol, 5 mM MgCl2, 0.005% TWEEN 100 and 5 mM mercaptoethanol).
  - Buffer II: 50 mM Tris-HCl pH = 7,8, 0,2 M NaCl, 5 mM $MgCl_2$, 5 mM mercaptoethanol and 1 mM EDTA).

  Protocol 2_ as used from the MPI protein purification facility:

  - Buffer 1: Lysis / Binding Buffer: (50 mM Na-P pH 8, 500mM NaCl, 20 mM imidazole, glycerol 10%, 5 mM $MgCl_2$, 1 mM TCEP, 0,005% Tween).
  - Buffer 2: Elution Buffer: Na-P 50 mM pH 8, NaCl 500 mM, 250 mM imidazole, glycerol 10%, 5 mM $MgCl_2$, 1 mM TCEP, Tween 0,005%.
  - Buffer 3: IEX Buffer A: Bis-Tris 50 mM pH 6,5, NaCl 0 mM, glycerol 10%, EDTA 0.1 mM, TCEP 1 mM, Tween 0,005%.
  - Buffer 4: IEX Buffer B: 50 mM Bis-Tris pH 6,5, 1000 mM NaCl, glycerol 10%, 0.1 mM EDTA, 1 mM TCEP, Tween 0,005%.
  - Buffer 5: SEC Buffer: Tris 50 mM pH 7,5, NaCl 100 mM, EDTA 0.1 mM, DTT 1 mM, Triton 0.10%, glycerol 30%.

5.4. Antibiotics

The media used for *E. coli* growth in liquid cultures and plates was Lysogeny Broth (LB Lennox). Plates were prepared using BD Difco Bacto Agar (Fisher Scientific).

The liquid cultures and plates were supplemented with antibiotics based on the antibiotic resistance of the desired plasmids carried by the TOP10 *E. coli* cells. Chloramphenicol (Cam) was added to the media at a final concentration of 34 μg/mL for the chloramphenicol-resistant strains, and Carbenicillin (Carb) was added at a final concentration of 100 μg/mL for the ampicillin-resistant strains.

5.5. Software

The following online software were used:

- SnapGene (software) and Benchling (online – https://www.benchling.com/): visualization, design and storage of nucleic acid sequences and plasmids.
- RNAFold Vienna (online – http://rna.tbi.univie.ac.at/cgi-bin/RNAWebSuite/RNAfold.cgi): prediction of secondary structures of single stranded RNA or DNA sequences.
- OligoCalc (online – http://biotools.nubic.northwestern.edu/OligoCalc.html): for calculating the physical properties of DNA and RNA oligonucleotides including melting temperature, molecular weight, %GC content and absorbance coefficient for a given oligonucleotide sequences in order to find the concentration.
- ProtParam (online – https://web.expasy.org/protparam/): Calculate physical and chemical parameters for a Swiss-Prot or TrEMBL protein, or for a user-entered protein sequence.
- ImageJ (software): visualization, editing and analysis of agarose and PAGE gels.
- Sapphire Capture (software): visualization, editing and analysis of agarose and PAGE gels.

5.6. General Methods

Plasmids construction, preparation, and validation. If the plasmids containing the replicons with the desired cargos have not already been ordered from IDT, they were

assembled using Gibson assembly. To prepare the inserts, primers with a complementary region at the 5' end of the final backbone region should have been designed according to the NEBuilder HiFi DNA Assembly Cloning Kit, and the steps should have been performed according to the kit. At the end of the Gibson Assembly protocol, the plasmids were transformed into *E. coli* strain Top10 (Invitrogen).

The plasmid *1.3_Assembled_pgemt_rq135notiecorv + pRNA* was produced as followed. The *pgemt_rq135notiecorv_sfGFPwt* vector template was amplified via PCR using the Vector_pgemt_rq135notiecorv_1.REV and Vector_pgemt_rq135notiecorv_1.FOR primers. The resulting product was then subjected to DpnI (NEB) digestion. The pRNA dsDNA sequence was previously generated via fill-in, as described in the materials and methods section. To obtain sequence overlaps, it was subsequently amplified via PCR using the Fragment_RQ135_ExXy'.REV and Fragment_RQ135_ExXy'.FOR primers. Then the vector and the fragments were added together in the same reaction and assembled using the NEBuilder HiFi DNA Assembly Cloning Kit (NEB).

The plasmid *1.6_Assembled_pgemt_rq135notiecorv+pRNA+sfGFP* was produced as follows to insert the pRNA sequence into a vector that previously contained the RQ135 replication sequences and the sfGFP sequence. The template vector pgemt_rq135notiecorv_sfGFPwt was linearized by digestion with the EcoRV (NEB) restriction enzyme. The dsDNA of the pRNA sequence was prepared by fill-in as described in Materials and methods and amplified by PCR using the primers Fragment_3'RQ135_ExXy'.REV and Fragment_sfGFP_ExXy'.FOR to obtain 5' and 3' overlaps. The backbone and fragments were then combined in the same reaction and assembled using the NEBuilder HiFi DNA Assembly Cloning Kit (NEB).

The plasmids series from *pDR57* to *pDR64*, containing the MDV-1 sequence and a pRNA sequence, were produced as followed. The backbone was obtained by PCR of the plasmid *pDR40* using primers 164 and 165, followed by DpnI (NEB) digestion. The dsDNA of each single pRNA insert was previously produced by fill-in, as described in the Materials and Methods section. Then, the amplified backbone and the pRNA fragment were added together in the same reaction and assembled by the NEBuilder HiFi DNA Assembly Cloning Kit (NEB), producing respectively the plasmid *pDR57*, *pDR58*, *pDR59*, *pDR60*, *pDR61*, *pDR62*, *pDR63*, *pDR64*.

The plasmids series from *pDR79* to *pDR84*, containing the RQ135 sequence and a pRNA sequence, were produced as followed. The backbone was obtained by PCR of the plasmid pgemt_rq135notiecorv with primers 178 and 179 and followed by DpnI (NEB) digestion. The dsDNA of the single pRNA insert was previously produced by fill-in, as described in the Materials and Methods section. Then, the amplified backbone and the pRNA fragment were added together in the same reaction and assembled by the NEBuilder HiFi DNA Assembly Cloning Kit (NEB), producing respectively the plasmid *pDR79*, *pDR80*, *pDR81*, *pDR82*, *pDR83*, *pDR84*.

The cloning by Gibson assembly, plasmid propagation or for storage, a general protocol to transform chemically competent *E. coli* cells was used. About 30-50 ng of plasmid was added to a 50 µl of competent TOP10 *E. coli* cells in one tube for 5 min incubation on ice. The mixture was then heat shocked at 42°C for 45 seconds and incubated again on ice for 5 minutes. For plasmids carrying Ampicillin or Carbenicillin resistance, plate cells directly on pre-warmed LB agar supplemented with 100 µg/mL of the corresponding antibiotic. For plasmids carrying other resistance genes, dilute *E. coli* cells in 1 mL of pre-warmed SOC media and incubate for 1 hour at 37 °C at 900 rpm on a thermoblock before plating. The cells were then centrifuged at 12,000 g for 2 minutes. After centrifugation, 900 µL of supernatant was discarded, and 100 µL of cells were plated onto a pre-warmed LB agar plate supplemented with the antibiotic. The plate was then incubated overnight at 37°C in a static incubator supplemented with the corresponding selection marker.
The following day, the plasmid was isolated from the transformed *E. coli* cells using the NucleoSpin Plasmid Mini Kit (Macherey & Nagel). Subsequently, the plasmid was eluted in nuclease-free H_2O. After screening the correct built plasmids by colony PCR, their concentration was determined by measuring the absorbances at 260 nm for RNA and DNA, and checking for possible protein contamination by measuring the 280 nm value. The plasmids that tested positive were sent to Microsynth Seqlab GmbH (Göttingen, Germany) for confirmation through Sanger sequencing. To ensure complete coverage of the insert sequence, specific sequencing primers were designed.

Nucleic acids and protein quantification and storage. The absorbance and concentrations of DNA, RNA, and protein were measured using a NanoDrop One (Thermo Scientific). Concentration Values: The 260 nm value was used for both DNA and RNA. For DNA concentration, no further calculation was necessary (1 A_{260nm} was approximated

to correspond to ~40 ng/µL). For RNA concentration, the 260 nm value was used to calculate the concentration, taking into consideration the length of the molecule using Oligo Calc190. DNA and RNA was conserved at -20 °C for daily use, and -80 °C if long term storage.

The ProtParam191 online tool was used for protein analysis, with calculations based on the 280 nm value. Concentrations were then determined using the Lambert-Beer law, which describes the correlation between absorbance A_λ at wavelength λ, absorption coefficient ε_λ (Mol^{-1} cm^{-1}), optical pathlength d (cm), and concentration c (mol L^{-1}). Proteins were aliquoted and frozen in liquid nitrogen for short and long term storage if freshly purified.

Purification of recombinant Qβ replicase

Qβ PB1 expression and purification, as adapted from Kita *et al*. (2006). His-tagged Qβ replicase expression plasmid pBAD33tutsfusion (P_{bad}-inducible promoter) was previously build and stored in the lab. Transformation was carried out by adding 50 ng of plasmid (miniprep purity) to 50 µL of competent TOP10 *E. coli* cells, then mixed and incubated for 5 minutes on ice. Heat shocked was performed for 45 second at 42 °C, and the cells were cooled on ice for 5 minutes. The cells were diluted in 1 mL of pre-warmed (37 °C) SOC media and recovered by growing for 1 hour at 37 °C and 900 rpm on a thermoblock. After recovery, cells were pelleted by spinning 2 minutes at 12,000 g, 900 µL of supernatant was discarded, the pellet was resuspended and 100 µL of cells was plates on pre-warmed LB agar plate supplemented with 25 µg/mL of chloramphenicol and left to grow overnight in a static incubator at 37 °C. The next day, single colonies were picked and used to inoculate 5 L of LB media supplemented with chloramphenicol, 0.5% glycerol, 0.05% glucose, and the expression was induced with 0.2% arabinose and grow overnight in a shaker incubator at 30 °C, 240 rpm. The next day, the culture was harvested by centrifugation at 3200 rpm for 20 min in cold room. The pellet was dissolved in 20 mL of Lysis Buffer I (0.1 M Na_2PO_4 at pH 7.0, 0.5 M NaCl, 20% glycerol, 5 mM $MgCl_2$, 0.005% TWEEN 100 and 5 mM mercaptoethanol). Then, it was sonicated on ice using the following settings: 70% amplitude, 6 cycles for 10 minutes. Follow a centrifugation at 10000 rpm for 30 min. At this point the supernatant was ready for leading in onto a His-trap FF column. After sonification, the column was equilibrated with H_2O, then with Buffer I (100 mM Na-P buffer pH 7.0, 500 mM NaCl, 20% glycerol, 5 mM $MgCl_2$, 0.005 % TWEEN 100, 5 mM mercaptoethanol). The clarified lysate was loaded onto the column and flow through twice to ascertain resin saturation with His-tagged Qβ replicase and prevent non-specific protein

binding. After binding, the resin was subjected to high salt washing steps to elute non-specific protein: a first wash with Buffer I with addition of 20 mM imidazole, a second wash with Buffer I with addition of 4 M urea, and a third with Buffer I with addition of 20 mM imidazole. Then, in the end, the protein of interest was eluted with Buffer I with addition of 250 mM of imidazole and fractionated in 15 samples of 1 mL size. SDS-PAGE were run to verify the presence of the desired protein. After identified the positive fractions, they were concentrated in a SPIN-X-UF concentrator at 3260 g at 4 °C until the total volume was reduced to 2 mL. After that, follows a purification with S200-16-20 column. First, the column was washed with H_2O and then calibrate over-night with Buffer II (50 mM Tris-HCl pH = 7.8, 200 mM NaCl, 5 mM $MgCl_2$, 5 mM mercaptoethanol and 1 mM EDTA). The day after the sample was loaded in the column and fractionate automatically by the Äkta start chromatographic system (Cytiva). Fractions were collected and the presence of the polished verified by SDS-PAGE. As last step, the positive fractions were concentrated via Vivaspin 20 GE Healthcare 100 kDa and then glycerol was added in order to conserve them at -80 °C. Protein concentration was determined as previously described. The purified Qβ replicase was used in initial self-replication assays when indicated.

Qβ PB2 expression and purification. This Qβ replicase purification batch was obtained in collaboration with the MPI of Biochemistry Protein Purification facility. His-tagged Qβ replicase expression plasmid pBAD33tutsfusion (P_{bad}-inducible promoter) was previously built and stored in the lab. Transformation was carried out by adding 50 ng of plasmid to 50 µL of competent TOP10 *E. coli* cells, and then mixed and incubated for 5 minutes on ice. Heat shocked was performed for 45 second at 42 °C, and the cells were cooled on ice for 5 minutes. The transformed cells were diluted in 1 mL of pre-warmed (37 °C) SOC media and recovered by growing for 1 hour at 37 °C and 900 rpm on a thermoblock. After recovery, cells were pelleted by spinning 2 minutes at 12,000 g, 900 µL of supernatant was discarded, the pellet was resuspended and 100 µL of cells was plates on pre-warmed LB agar plate supplemented with 34 µg/mL of chloramphenicol and left to grow overnight in a static incubator at 37 °C. After recovery, cells were pelleted by spinning 2 minutes at 12,000 g, 900 µL of supernatant was discarded, the pellet was resuspended and 100 µL of cells was plates on pre-warmed LB agar plate supplemented with 34 µg/mL of chloramphenicol and left to grow overnight in a static incubator at 37 °C. The next day, single colonies were picked and used to inoculate 10 mL of YG media and supplemented with 34 µg/mL chloramphenicol, 0.05% glucose 80g/l $MgSO_4$ x $7H_2O$, K_2HPO_4 x $3H_2O$

allowed to grow overnight in a shaker incubator at 37 °C at 220 rpm. On the following day, the fermenter was inoculated with the entire 10 mL of the previous preculture and incubated at 37 °C and 800 rpm. Once the OD_{600} reached 8.9, 0.2% arabinose was added to induce growth at 24 °C and 800 rpm. The culture was then harvested the next day by centrifugation at 8000 rpm and 4 °C when the OD_{600} reached 15.6, resulting in a biomass of 30 g. For the cell lysis Buffer 1 at pH 8 (Na-P 50 mM, NaCl 500 mM, imidazole 20 mM, glycerol 10%, TCEP 1 mM, Tween 0,005%) and 100 mL of an enzyme cocktail (AEBSF-HCl 1 mM, Aprotinin 2 µg/mL, Leupeptin 1 µg/mL, Pepstatin 1 µg/mL) was added. 5mM $MgCl_2$ was added to the Buffer 1 after the lysis. The sample was centrifuged at 20500 rpm for 30 minutes at 4 °C using a Beckman Coulter centrifuge. After that, PEI 5% was added to achieve a final concentration of 0.1% and stirred for 10 minutes. The first purification step involved Ni-NTA Agarose purification with Ni-Sepharose (High Performance) beads. Buffer 1 was used as the equilibration buffer and centrifuged at approximately 1500 rpm for 5 minutes. Then, 100 mL of the sample was loaded into the column at 4 °C for 1.5 hours and rotated on a wheel. The column was first washed with Buffer 1 containing 4 M urea at 4 °C, followed by a wash with Buffer 1 without urea at 4 °C. Finally, elution was performed with Buffer 2 at pH 8 (Na-P 50 mM, NaCl 500 mM, 250 mM imidazole, 10% glycerol, 5 mM $MgCl_2$, 1 mM TCEP, 0.005% Tween) for 10 minutes at 4 °C. It was observed that there was a significant nucleic acid contamination at this step, indicating the need for further purification. The second purification step involved cation exchange chromatography using a HiS-creen SP HP column filled with 6% highly cross-linked agarose beads with a pore size of 34 mm (GE) and a bed volume of 4.7 mL. The column was first equilibrated with H_2O for 5 column volumes (CV) and then with Buffer 3 at pH 6.5 (50 mM Bis-Tris, 0 mM NaCl, glycerol 10%, 0.1 mM EDTA, 1 mM TCEP, 0.005% Tween) for 10 CV. The previous sample from the previous treatment was diluted 1:10 and 90 mL of the diluted sample was added to the column. The gradient elution was performed starting with Buffer 3 and then Buffer 4 at pH 6.5 (50 mM Bis-Tris, 1000 mM NaCl, glycerol 10%, 0.1 mM EDTA, 1 mM TCEP, Tween 0.005%). The gradient length was about 5 CV, and the flow rate was 0.5 mL/min pressure. Fractionation volumes of 1 mL were collected. After the analysis at the spectrophotometer at 260/280, it was observed that nucleic acids were still present. Therefore, a subsequent purification step was necessary. As third step, an Heparin column purification was performed. The column used in this study was an Heparin Sepharose 6 Fast Flow, which contains beads made of highly cross-linked 6% Agarose/Heparin (GE). The bed volume was 1 mL and the void volume was 4mg

bovine/mL (maximum pressure 0.3 MPa). To equilibrate the column, 5 CV of H_2O were used, followed by 10 CV of Buffer 3. Then, sampled from the previous purification was diluted 1:10 in Buffer 3 and loaded onto the column. Then Buffer 3 was added and followed the addition of Buffer 4 in gradient from 5% to 100%. The gradient length was of 10 CV and the flow rate of 1 mL/min. The fractionation volume was of 1 mL. Unfortunately, the spectrophotometer analysis showed still the presence of nucleic acids. In order to get the purest Qβ replicase sample possible and to get rid of the nucleic acids, another step of purification was adopted. Size exclusion was performed using a HiLoad 16/60 Superdex 200 column packed with cross-linked agarose and dextran beads (GE) with a fractionation range of 10-600 kD and a bed volume of 120 cm and height of 60 cm. Equilibration was achieved using 1 CV of H_2O, followed by 1 CV of Buffer 5 at pH 7.5 (50 mM Tris, 100 mM NaCl, 0.1 mM EDTA, 1 mM DTT, 0.10% Triton, 30% glycerol). Next, 6 mL of the previous sample was loaded onto the column. For the elution Buffer 5 was used, and a fractionation volume of 2 mL was adopted with a flow rate of 1 mL/min. Fractions of 6 mL were taken. After pooling, Triton and glycerol were added. The sample was then concentrated to a volume of 1.3 mL using an Amicon Ultra 15 (Eppendorf) Healthcare 30 kDa concentrator at 3000 rpm and 4°C. To confirm the presence of Qβ replicase and its co-factors (Ef-Tu and Ef-Ts), liquid chromatography-mass spectrometry (LC-MS) was used. The expected masses for the following proteins are: 66353 Da for RNA-directed polymerase subunit, 61158 Da for the 30S ribosomal protein rpsA (S1), 43314 Da for Ef-Tu, and 30423 Da for Ef-Ts. After SEC purification, the sample underwent dialysis using Buffer 5 with added glycerol and triton in a volume of 1 L in a D-Tube Dialyser Mega of MWCO 3.5 kD. The sample was left at 4°C overnight and then recovered and stored at -80°C.

Preparation of DNA templates. Prior to RNA production via IVT, the DNA template was prepared using the following methods. For RNAs of 70-120 nucleotides, the fill-in protocol was followed. A double-stranded DNA template was created by annealing two complementary oligos at the T7 promoter region. The promoter was then extended using the Taq G2 hot start master mix (Promega) to generate. For the fill-in, the total volume of the reaction was set up to 50 µL and to the reaction was added 25 µL of H_2O, 1 µM of each oligonucleotide and 25 µL GoTaq G2 hot start master mix. After the set-up of the reaction in the tube, the reaction was incubated in a thermocycler for 2 minutes at 98 °C, 2 cycles comprising denaturation for 5 seconds at 98 °C, annealing at 54 °C for 15 seconds and

extension at 72 °C for 2 minutes, and a final extension at 72 °C for 2 minutes. For the purification of the reaction, the silica column of the Monarch DNA & PCR clean-up kit (NEB) and the kit protocol were used with a final elution in 15 µL H_2O, then stored at -80 °C. To produce the dsDNA of each pRNA sequence by fill-in, the following primers were used: primers 16 and 28 for $pRNA_{ExAb}$, primers 15 and 23 for the $pRNA_{ExBa}$, primers 14 and 22 for the $pRNA_{ExCb}$, primers 16 and 27 for the $pRNA_{ExAc}$, primers 13 and 21 the $pRNA_{ExDc}$, primers 16 and 26 for the $pRNA_{ExAd}$, primers 11 and 19 for the $pRNA_{ExFd}$, primers 16 and 25 for the $pRNA_{ExAf}$.

For the production of RNA bigger than 120 nt, the sequence was ordered already cloned by Gibson assembly or synthetically produced by IDT, and then the specific section amplified by PCR. Primers were designed accordingly for the selected template sequences in order to amplify the desired replicons as in **table 8.3**. For these PCR reactions, the Q5 High fidelity master mix (NEB) was used. A reaction of 50 µL were set up and 1 µM of each primer and the template plasmid was added to the reaction. Then the cycling was set up as follows: initial denaturation at 98°C for 30 seconds, 35 cycles of denaturation at 98°C for 10 seconds and annealing at a temperature depending on the tm of the primers used and for 20 seconds, an extension at 72°C for a number of seconds depending on the size in bp of the template, followed by a final extension step at 72°C for a number of seconds depending on the size in bp of the template. PCR purification was performed by Monarch DNA & PCR clean-up kit (NEB) with a final elution step of 10-15 µL in H_2O. For the quantification (ng/µL), Nanodrop was used for quantifying the samples and check their purity. For checking the product of the PCR, agarose gel was run as describe in the following chapter.

For all designed and tested RQ135 replicons, whether with added cargo or just the single scaffold, primers T7_RQ_fw and RQ_rev was used to amplify the (+) strand and primers 180 and 181 to amplify the (-) strand to produce the dsDNA before the following IVT step. Notably, primer 181 includes the T7 promoter at the 5' end to promote transcription of the (-) strand during IVT.

For all designed and tested MDV-1 replicons with added cargo, primers 86 and 87 were used to amplify the (+) strand and primers 136 + 141 to amplify the (-) strand to produce the dsDNA before the following IVT step. Primer 141 incorporates the T7 promoter at the 5' end to promote transcription of the (-) strand during in vitro transcription (IVT).

Agarose gel electrophoresis. For the preparation of the 1% agarose gels, 1% TAE was used by heating up and melting the agarose powered in a Erlenmeyer flask in the microwave. Followed the cooling down of the flask to ~65 °C and then the addition of 3-5 µL of SYBR Safe. The gel added to a casting station of 10x10 cm and a 14-well comb was used. For PCR, usually 5 µL of PCR reaction products were adding with the addition of 1 µL of 6X DNA Loading Dye. In the case of the fill-in reaction, they were added at a volume of 6 µL directly after since the reaction buffer contains already the dye. To estimate the size of the amplicon, several weight marker were used depending on the application: for DNA, 1 Kb Plus DNA Ladder was used, for RNA RiboRuler High and RiboRuler Low Range RNA Ladders were used, all from Thermo Fisher. The gels were usually run at 80-100 V for 60-80 minutes and the Blue Light Scanner BIO-1000F from Microtek was used for visualization.

Preparation of RNA and sequence design. In vitro transcription (IVT) RNA was prepared through in vitro transcription (IVT) by T7 RNA polymerase kits or custom formulations was used to transcribe all the RNA used in this work. T7 promoter was placed upstream of each target transcription template and GpGpG sequence was added, if not present, in between the T7 promoter and the sequence to transcribe to enhance the transcription yields by the T7 RNA polymerase. Fill-in derived DNA templates were added in full volume for the IVT after the column purification. Typical reactions volumes were 100 µL, however for large scale production of RNAs the reaction was scaled up (between 200 – 300 µL transcriptions). For short templates (less than 300 nt) and difficult templates, the MEGAshortscript T7 Transcription Kit from Thermo Fisher was used (see kit protocol for details). For all the other templates, an in-house protocol was used. The reaction conditions for the in-house protocol were: DNA template, 30 mM Tris-HCl pH 7.8, 30 mM $MgCl_2$, 10 mM DTT, 2 mM spermidine, 5 mM of each NTP, 1 U/mL *E. coli* inorganic pyrophosphatase, 0.5 µM T7 RNA polymerase from NEB. The reaction was incubated for 2-6 hours at 37 °C, and then 0.1 volumes of DNase I (Thermo) was added and further incubated for 30-60 minutes at 37 °C. For the purification procedure, Monarch RNA clean-up kit (NEB) following manufacturer's instructions was used with a final elution step of, 30-40 µL of H_2O. For the quantification of the RNA produced by IVT and purified. It is important to remember that the set-up of the transcription reactions should be carried out at room temperature to avoid precipitation of reagents (especially NTPs).

Preparative urea polyacrylamide gel electrophoresis (PAGE). In order to purify the RNA produced by IVT, 5-8% PAGE were set-up, and concentration decided based on the length of the transcript. To obtain the gel polyacrylamide percentage needed, 20% and 0% acrylamide gel solutions were mixed with fixed rations. Then, to the solution, 0.001 volumes of TEMED and 0.01 volumes of 10% APS (for 70 mL gel solution, 70 µL TEMED and 700 µL 10% APS) were added to catalyse the polymerization reaction. 2- or 1-mm spacer and large-well combs. After polymerization of the gel, it was mounted in the running chamber filled with 1X TBE as running buffer. Then the comb was removed and the well flushed with a syringe to remove the residual urea and piece of gel. The pre-run of the gel was performed at 45 mA current for 1 hour in order to heat up the gel and remove the excess of TEMED and APS. The RNA sample was prepared by diluting it in two volumes of formamide containing xylene cyanol dye and heat up at 85 °C for 3-5 minutes for denaturation before the leading it in the wells. After the loading, the gel was run at 45 mA current until the xylene cyanol dye reached 1-3 cm from the bottom of the gel. At the end of the run and removal of the gel from the apparatus, a plastic foiled was applied around the gel and then, in the dark room, the gel was positioned on a on a pre-coated TLC plate and very briefly illuminated with 254 nm UV light to visualize the band. After determinate the band and marked it, by a sterilised scalped the band was excised and place in an Eppendorf tube and crushed with the help of the plunger of a syringe. Then, a suitable volume of 0.3 M sodium acetate pH 5.2 gel elution buffer was added after determined the wright of the crushed gel. The tube was added to a rotator over-night to elute at a temperature of 4 °C. The day after, Spin-X cellulose acetate 0.45 µm filter was used to remove the gel debris. To the liquid layer then 20 ng of RNA-grade glycogen as precipitation agent was added plus 1.2 volumes of 2-propanol was added in order to precipitate the RNA and then the tube was cooled down to -20 °C for a 1 hour. Follows a spinning for 1 hour at 21,000 g at 4 °C in centrifuge to obtain the pellet. Then, supernatant was discarded and fresh 1 mL of cold 80% ethanol was added and then another 20 minutes of centrifugation at 21,000 g at 4 °C. Once again, the supernatant was discarded, and the vacuum centrifuge was used to remove the last ethanol for about 5-10 minutes. Then the sample was resuspended in 20-30 µL H_2O. Nanodrop was used to quantify the sample by collecting the absorbance at 260 nm and the concentration calculate by the online tool OligoCalc. Samples were stored at -80 °C.

Analytical urea PAGE. Electrophoretic mobility shift assays by denaturing urea-PAGE were routinely performed to analyse the purity of the IVT transcription and PAGE extractions, as well as the replication assays. As for the preparative method, the percentage of acrylamide was decide depending on the RNA size to visualize. To obtain the gel polyacrylamide percentage needed, 20% and 0% acrylamide gel solutions were mixed with fixed rations. Then, to the solution, 0.001 volumes of TEMED and 0.01 volumes of 10% APS (for 70 mL gel solution, 70 µL TEMED and 700 µL 10% APS) were added to catalyse the polymerization reaction. 2- or 1-mm spacer and large-well combs. After polymerization of the gel, it was mounted in the running chamber filled with 1X TBE as running buffer. Then the comb was removed and the well flushed with a syringe to remove the residual urea and piece of gel. The pre-run of the gel was performed at 45 mA current for 1 hour in order to heat up the gel and remove the excess of TEMED and APS. For the sample preparation, to the RNA samples were added a same volume of Gel Loading Buffer II (Thermo) and then heat up at 85 °C for 3-5 minutes followed by a fast incubation on ice, for denaturation before the leading it in the wells. When leading the samples on the gel, each well was flushed to remove leached urea from the wells. 1-3.5 µL of denatured sample was loaded per well, depending on the purpose. To get better result, such as cleared and more defined bands, it's better to add smaller volumes of sample. The gel was then run at at constant 20-25 W until the bromophenol blue reached 2-3 cm from the end of the gel.

Analytical Native PAGE of RNA. Electrophoretic mobility shift assays by native PAGE were performed to analyse the nanoring assembly formation and, later, for the replication coupled assembly assays. Native gels of 4-5 % were casted starting from a solution containing 29:1 Acrylamide:bisacrylamide 40%, 10x TBM Buffer, and H_2O. Then, 0.001 volumes of TEMED and 0.01 volumes of 10% APS (for 70 mL gel solution, 70 µL TEMED and 700 µL 10% APS) were added to catalyse the polymerization reaction. The gels were cast with 2 mm spacers with different number of wells depending on the number of samples (24, 30, 34, or 48 wells per 20 cm wide gel). After polymerization of the gel, it was mounted in the running chamber filled with 1X TBM running buffer previously cooled down to 4 °C, then the comb was removed and the well flushed with a syringe to remove the residual urea and piece of gel. The gel was then pre-run at constant wattage that results in an approximate 7W current for 45 minutes and flush out excess TEMED and APS. Meanwhile, samples were prepared in RNA Native loading buffer (TBM 5X, Glycerol 20%, Bromophenol blue 0.05%, Xylene cyanol 0.05%) and kept on ice. The wells were flushed

immediately before sample loading. 1-3.5 µL of denatured sample was loaded per well, depending on the number of teeth. The gel was run at constant 10-13 W for about 4 hours in cold room at 4 °C until the bromophenol blue reached 2-3 cm from the bottom of the gel.

Staining of PAGE gels. Most of the PAGE gels were stained with SYBR Gold. After the end of the run, the gel was placed in a staining solution where 2 µL of SYBR Gold was diluted in approximately 200 mL of 1X TBE, and then placed for the incubation in the dark for about 5-10 minutes. For destaining, the gel was washed twice in 5 minutes in ultrapure water. For the gels where no staining was needed, for example when fluorescent rNTPs incorporation was performed, 5 minutes in ultrapure water was enough. Azure Sapphire RGB laser scanner with the respective excitations (488 nm for fluorescein-based chromophores (6-FAM), 520 nm for SYBR Gold and Cyanine 3 (Cy3), 658 nm for Cyanine 5 (Cy5) was then used to scan the gel. In the case of the urea-PAGE gels where a replicon with a florescent aptamer was added, suddenly after the end of the run, the gel was incubated with DHFBI staining buffer (10 µM DHFBI, 40 mM HEPES pH 7.4, 100 mM KCl and 1 mM $MgCl_2$) if the replicon was carrying a F30-Broccoli aptamer or with TO1-B staining buffer (100 nM TO1-B, 40 mM Tris-HCl pH 8, 50 mM KCl, 22 mM $MgCl_2$) if carrying a F30-Mango aptamer. For each, in order to remove the dye, the gel was washed three times with H_2O for 5 minute to remove the staining buffer.

Oil-water emulsion protocol. The self-replication and assembly-coupled-replication reaction was encapsulated by creating a polydisperse oil-water emulsion. After preparing the reaction in a PCR tube on ice, 50 µl of 1% - 2% Pico-Surf w/w in Novec 7500 (Sphere Fluidics) was added to create the heterodisperse emulsion in the self-replication or assembly-coupled replication reaction. The tube was scratched on the surface of a tube rack to generate droplets of different sizes. The reaction was then incubated in a thermocycler at 37°C for 3 hours. After incubation, the tube was spun to separate the two phases. The PicoSurf oil, which is the bottom layer, was carefully removed using a standard plastic pipette tip to minimize the amount of Pico-Break needed to break the emulsion. After removing the oil phase, the volume of the water phase was measured. Then, two times the total volume of the previous solution of Pico-Break (Sphere Fluidics) were added to the solution and gently agitated. The tube was then spun in a micro-centrifuge for a maximum of 1 minute at RCF 100-1000 x g to completely disperse the emulsion and separate the two phases. Two layers should be visible after phase separation. The bottom layer, which is

orange in colour, is the undesired fluorous phase. The tube was then tilted at a 45° angle, and the top aqueous layer was removed carefully using a pipette. The layer was then transferred to a clean microcentrifuge tube and stored directly at -80°C.

5.7. Specific Methods

MDV-1 replicon RNA labelling. To visualize the self-assembly of the nanorings on a Native PAGE gel, fluorescent-labelled RNA replicons were obtained through IVT reactions. Modified UTP was randomly incorporated internally in the RNA sequence using a T7 RNA polymerase and a DNA template. The assembly of dimers and trimers from MDV-1_pRNA monomers was tested by labelling four different monomers: MDV-1_pRNA$_{Ab}$ was labelled with Aminoallyl-UTP-Cy3 (Jena Bioscience), MDV-1_pRNA$_{Ba}$ was labelled with Aminoallyl-UTP-Cy5 (Jena Bioscience), MDV-1_pRNA$_{Cb}$ was labelled with Aminoallyl-UTP-Cy3 (Jena Bioscience), and MDV-1_pRNA$_{Ac}$ (Jena Bioscience) was labelled with fluorescein-12-UTP (Jena Bioscience). The fluorescent-labelled UTP transcription reactions were carried out by adding the DNA template obtained by PCR to a buffer containing 30 mM Tris-HCl pH 7.8, 30 mM $MgCl_2$, 10 mM DTT, 2 mM spermidine, and a total of 2.5 mM rATP, rCTP, and rGTP, along with 0.2 mM of rUTP and 0.1 mM of labelled rUTP, 1 U/mL *E. coli* inorganic pyrophosphatase, and 0.5 µM T7 RNA polymerase from NEB. The reactions were incubated at 37°C for 4 hours. At the end of the 3-hour reaction, DNase I (Thermo Fisher) was added at a concentration of 0.1 volumes and incubated for 30-60 minutes at 37°C. T The monomers were purified using PAGE, as previously described. An analytic urea-PAGE was then used to confirm the correct incorporation of the fluorinated nucleotides. The gel was subsequently imaged on the Azure Sapphire RGB laser scanner using the respective excitations: 488 nm for fluorescein-based chromophores (6-FAM) and Cyanine 3 (Cy3), and 658 nm for Cyanine 5 (Cy5). Samples were stored at -80°C for future use.

RQ135 self-replication assay. The self-replication assay using RQ135-based replicons was conducted as follows: Reactions were prepared at 4°C in a small PCR tube containing 5-8 nM of the RNA template and the RQ135 reaction buffer composed of 0.25 mM of each rNTP (1 mM in total), 1 mM Tris-HCl (pH 7.5), 100 mM $MgCl_2$, 5 mM EDTA, and 1% Triton X-100 in a total volume of 50 µl. For each RNA template, two different concentrations of Qβ replicase were tested: 10 and 100 nM. The reactions were incubated

for three hours at 37°C, and samples were taken at time 0, 1, 2, and 3 hours. Each experiment included controls containing either 5 or 8 nM of the RNA template (depending on the experiment) and 0 nM of Qβ replicase, or 0 nM of RNA template and 100 nM of Qβ replicase. Replication was characterised using 1% denaturing agarose gel electrophoresis, running at 80-100 V for 60-80 minutes. The gel was then stained with SYBR Gold and imaged directly on the Blue Light Scanner BIO-1000F from Microtek.

MDV-1 self-replication assay in water-oil emulsion. The self-replication assay was performed on MDV-1 templates carrying a fluorescent aptamer sequence (F30-Broccoli or F30-Mango) and a fluorescent aptamer plus a pRNA sequence in a water-oil emulsion, following the same procedure. Reactions were prepared at 4°C in a small PCR tube containing 100 nM of the RNA template and the MDV-1 reaction buffer composed of 50 mM Tris-HCl (pH 7.5), 1.25 mM of each (total 5 mM), 10 mM $MgCl_2$, and 0.10% (w/w) Pluronic F-68 (Gibco) in a total volume of 50 µl. Two different concentrations of Qβ replicase (100 and 321 nM) were tested for each RNA template. Each experiment included controls with either 100 nM of RNA template (depending on the experiment) and 0 nM of Qβ replicase, or 0 nM of RNA template and 321 nM of Qβ replicase. After adding all components on ice, 50 ul of 2% Pico-Surf w/w in Novec 7500 (Sphere Fluidic) was added to create the emulsion. The tubes were quickly scratched on the surface of a tube rack to generate droplets. The reaction was then incubated in a thermocycler at 37°C for 3 hours, and samples were taken at time 0 and 3 hours. At the end, for each sample, the emulsion was broken by adding PicoBreak (Sphere Fluidic), as explained previously in the general methods section. Replication was characterized using 5% denaturing urea-PAGE run for 60-80 minutes at 20-25 W and subsequently stained using either the DHFBI, TO1-B, or SYBR Gold staining protocol, depending on the specific application. The stained gel was then imaged using the Azure Sapphire RGB laser scanner, as previously described.

pRNA only, MDV-1_pRNA and RQ135_pRNA based nanorings assembly. In order to create larger nanorings, additional RNA monomers were added depending on the presence of the pRNA sequence, either with the pRNA sequence alone or by incorporation into the MDV-1 and RQ135 replication scaffold: pRNA dimer ($pRNA_{ExAb}$-$pRNA_{ExBa}$), trimer ($pRNA_{ExBa}$-$pRNA_{ExCb}$-$pRNA_{ExAc}$), tetramer ($pRNA_{ExBa}$-$pRNA_{ExCb}$-$pRNA_{ExDc}$-$pRNA_{ExAd}$), pentamer ($pRNA_{ExBa}$-$pRNA_{ExCb}$-$pRNA_{ExDc}$-$pRNA_{ExFd}$-$pRNA_{ExAf}$), hexamer ($pRNA_{ExBa}$-$pRNA_{ExCb}$-$pRNA_{ExDc}$-$pRNA_{ExEd}$-$pRNA_{ExFe}$-$pRNA_{ExAf}$) and heptamer ($pRNA_{ExBa}$-

$pRNA_{ExCb}$-$pRNA_{ExDc}$-$pRNA_{ExEd}$-$pRNA_{ExFe}$-$pRNA_{ExGf}$-$pRNA_{ExAg}$). For the monomers series of MDV-1_pRNA and RQ135_pRNA the (-) strand was used as the pRNA sequence on this strand is oriented correctly and functional for the assembly. To avoid contamination by non-specific product produced by the previous IVT reaction, each RNA monomers was PAGE purified and his purity checked by a qualitative urea-PAGE. As a first step in the self-assembly process, equimolar concentrations of each monomer were added to a PCR tube containing TMS buffer (10 mM $MgCl_2$, 100 mM NaCl, and 50 mM Tris-HCl pH 8.0) and H_2O. A refolding step was then carried out by heating the RNA at 80°C for 2 minutes and slowly cooling it to 37°C at a rate of 1°C per minute. Once the temperature reached 37°C, the assembly reaction was incubated for 1 hour. Subsequently, the formation of the nanorings was observed by Native PAGE gel, as previously described.

Assembly-coupled-replication assay in bulk. The same procedure was carried out for both (+) and (-) strands of MDV-1_pRNA and (+) and (-) strands RQ135_pRNA based replicons in order to assemble and replicate dimer ($pRNA_{ExAb}$-$pRNA_{ExBa}$), trimer ($pRNA_{ExBa}$-$pRNA_{ExCb}$-$pRNA_{ExAc}$). In the ACR buffer, 80-100 nM of each monomer, previously purified by PAGE, were added in equimolar concentration to the reaction mix, resulting in a total volume of 40 µl. Controls were also created by following the same procedure for the single monomer of MDV-1_pRNA or RQ135_pRNA under the same conditions. As first step, a refolding protocol was performed by heating the mixture to 80°C for 2 minutes and cooling it down at a rate of 1 °C/min until it reached 37 °C. The solution was then incubated at 37°C for 30 minutes. The assembled nanorings were maintained at 4°C where 1.25 mM of each rNTP was added and a t_0 sample was taken. The reaction was incubated at 37°C for 3 hours, and, at the end, a t_3 sample was taken. The t_0 and t_3 samples were run on a 5% Native PAGE at 70V and 4°C for 4 hours. Afterwards, they were stained with SYBR gold and visualized by Sapphire, as previously described.

Assembly-coupled-replication assay in water-oil emulsion. The same procedure was carried out for both (+) and (-) strands of MDV-1_pRNA and (+) and (-) strands RQ135_pRNA based replicons in order to assemble and replicate dimer ($pRNA_{ExAb}$-$pRNA_{ExBa}$), trimer ($pRNA_{ExBa}$-$pRNA_{ExCb}$-$pRNA_{ExAc}$). Each monomer, previously purified by PAGE, was refolded separately in ACR buffer at a concentration of 80-100 nM. Subsequently, each monomer was heated to 80°C for 2 minutes and gradually cooled at a rate of approximately 1°C/min until it reached 37°C in a thermocycler. This was followed

by a 30-minute incubation at 37°C, a cool down to 4°C, and storage on ice. Finally, each monomer was added to a single PCR tube, resulting in a total reaction volume of 60 µl. At this point, rNTPs were added to the reaction, followed by the Qβ replicase and 50 µl 2% Pico-Surf w/w in Novec 7500 was added to encapsulate the reaction, and the encapsulation was performed as described in the general methods section. The t_0 samples were collected while still on ice to prevent the reaction from starting. The reaction was then incubated at 37°C for 3 hours. Finally, the emulsion was broken following the general protocol outlined in the Materials and Methods section, and the t_3 sample was collected. Both t_0 and t_3 samples were run on a 5% Native PAGE at 70V for 4 hours at 4°C, stained with SYBR gold, and visualized by the Sapphire, as previously described.

Alternative protocol for water-oil emulsion experiments of MDV-1_pRNA replicons. A variation for the previous protocol was also explored. The same procedure was carried out for both (+) and (-) strands of MDV-1_pRNA and (+) and (-) strands RQ135_pRNA based replicons in order to assemble and replicate dimer ($pRNA_{ExAb}$-$pRNA_{ExBa}$), trimer ($pRNA_{ExBa}$-$pRNA_{ExCb}$-$pRNA_{ExAc}$). Each RNA monomer, previously purified by PAGE, was refolded separately in ACR buffer at a concentration of 80-100 nM. Subsequently, each monomer was heated to 80°C for 2 minutes and gradually cooled at a rate of approximately 1 °C/min until it reached 37°C in a thermocycler. This was followed by a 30-minute incubation at 37 °C, a cool down to 4°C, and storage on ice. Finally, each monomer was added to a single PCR tube, resulting in a total reaction volume of 60 µl. At this point, rNTPs and RNase inhibitor, to prevent potential RNase contamination, were added to the reaction, followed by the Qβ replicase and 60 µl 2% Pico-Surf w/w in Novec 7500 was added to encapsulate the reaction, and the encapsulation was performed as described in the general methods section. The t_0 samples were collected while still on ice to prevent the reaction from starting. The reaction was then incubated at 37°C for 3 hours. Finally, the emulsion was broken following the general protocol outlined in the Materials and Methods section, and the t_3 sample was collected. Both t_0 and t_3 samples were run on a 5% Native PAGE at 70V for 4 hours at 4°C, stained with SYBR gold, and visualized by the Sapphire, as previously described.

6. Acknowledgements

As I sit at my desk reviewing the final version of my dissertation, I try to put my final thoughts into words. I can't help but think about how much I've learned and experienced during this four-year journey. There has been so much excitement, happiness, frustration, curiosity, successes, and failures. I am very grateful for the latter; they have been a source of so much growth and maturity for me. Never forget to learn from your mistakes. This is perhaps the most important message I have learnt on this journey. As I struggle to find the words to express my gratitude, I am filled with warmth and appreciation for everyone who has been a part of this four-year journey.

It all started four years ago in Munich, thanks to the most brilliant and genuine mentor I ever had: thank you Hannes. You've been my guiding star during my journey. Thank you for taking me into your group and giving me the chance to work on this project. Thank you for the help, the insights, the trust, and the energy. Thank you for believing in me. Your wisdom, guidance and patience have shaped my growth as a researcher and as a person. This PhD journey has been a rollercoaster of emotions, and your supervision has been the steady hand guiding me through every twist and turn. I will never forget how much you have done for me and I wish you every success and happiness.

Thanks also to the first MPI group for all the help, good vibes and being so good to me when I first joined the group and the TUD group when we moved to Dortmund. Thanks to Kris, Emilie, Elia, Deni, Alex, Laura, Kai, Renate, Lena, Jacopo, Corbin, Mahesh, Vanessa, Verena, Maria and Martina.

Thank you Kris, for always being supportive and friendly and creating a good atmosphere. The same goes for Emilie. Thank you both for welcoming me into the group.

Thank you Elia, for helping me when I have doubts about techniques and for being such a train of fun and inspiration. Thank you Habibi! I really enjoyed working with you.

Thank you Kai, for the cool morning talks and all the help outside of work. I really enjoyed working with you, you are such an inspiration to me and I would love to work with you again in the future.

Thank you Laura, for being so kind and helpful to me. I really missed those good times with you at the MPI. I always felt understood and helped.

Thanks to the best Italian colleague Jacopo. I really enjoyed exchanging ideas, laughing during lunch breaks and learning about tech. Keep it up, grazie di tutto e ti auguro il meglio! Te lo meriti tutto.

Thank you, Mahesh and Corbin, for being such good office mates. Thanks for the good and inspiring conversations. I wish you all the best in life and career.

Thank you, Deni, for being such a passionate and kind colleague. I appreciate all the conversations, ideas and help.

Thank you, Alex, for your technical expertise. I wish you every success and happiness.

Thank you, Lena, for your technical and logistical support and for the pleasant conversations we had.

Thank you, Verena, for being such a helpful, kind and cheerful colleague and friend. Since you joined the group two years ago, I have enjoyed our lunch breaks and talking about food and life. Thank you also for all the good times we shared outside the lab. Keep going, stay strong and believe in yourself. You're doing great! Hope to see you soon.

Thank you, Vanessa, for helping me with all the bureaucratic stuff at the TUD and for being such a lovely colleague and dancefloor partner. Looking forward to seeing you again soon.
Thank you, Maria and Martina, thank you for helping me with the TUD bureaucracy and for being such wonderful and heartful people.
Thanks to all the bachelor and master students. Especially Julius for being such a passioned and caring student; stay like that. I wish you the best of success for the Master and the future. Thanks also to Noemi and Jasmin.

Thanks to mum and dad, Milvia and Roberto. I love you. I would never have made it this far without you. You raise me and always supported me. You've been my rock. Your love, your patience and your understanding is just unvaluable. I feel so blessed to have you. Ci sarò sempre per voi, grazie di tutto!

Thank you Kevin, Anna, Gabriele, Simone, Massimo, David, Lisa, Margerita, Federico, Christian, Matthias, Ecrin. I love you all. You've been more than just companions on this journey; you've been a family to me. I'm eternally grateful for all the good moments we've shared and for the future ones.

Thank you, Fan, I will never forget the first time we met four years ago and since then I felt like I had found a partner, a friend and a family. I feel so blessed and I have so many good memories together. Thank you for being there during my struggles, during my doubts, for giving me hope and happiness, and for reminding me that with the support of loved ones, everything is possible. I'll see you very soon in Munich. I love you.

Each of you has left a mark on this work and on my soul.
Thank you all for being part of this journey. I will never forget you.

David

7. References

Abouhaidar, M. and Ivanovb, I.G. (1999) *Non-Enzymatic RNA Hydrolysis Promoted by the Combined Catalytic Activity of Buffers and Magnesium Ions*, *Z. Naturforsch*. Available at: www.znaturforsch.com.

Abouhaidar, M.G. and Ivanovb, I.G. (1999) *Non-Enzymatic RNA Hydrolysis Promoted by the Combined Catalytic Activity of Buffers and Magnesium Ions*, *Z. Naturforsch*. Available at: www.znaturforsch.com.

Afonin, K.A. *et al.* (2012) 'Attenuation of loop-receptor interactions with pseudoknot formation', *Nucleic acids research*, 40(5), pp. 2168–2180. Available at: https://doi.org/10.1093/NAR/GKR926.

Afonin, K.A. *et al.* (2014) 'Multifunctional RNA nanoparticles', *Nano letters*, 14(10), pp. 5662–5671. Available at: https://doi.org/10.1021/NL502385K.

Afonin, K.A., Cieply, D.J. and Leontis, N.B. (2008) 'Specific RNA self-assembly with minimal paranemic motifs', *Journal of the American Chemical Society*, 130(1), pp. 93–102. Available at: https://doi.org/10.1021/JA071516M.

Afonin, K.A., Lindsay, B. and Shapiro, B.A. (2013) 'Engineered RNA Nanodesigns for Applications in RNA Nanotechnology', *DNA and RNA Nanotechnology*, 1(1). Available at: https://doi.org/10.2478/RNAN-2013-0001.

Autour, A. *et al.* (2018) 'Fluorogenic RNA Mango aptamers for imaging small non-coding RNAs in mammalian cells', *Nature Communications 2018 9:1*, 9(1), pp. 1–12. Available at: https://doi.org/10.1038/s41467-018-02993-8.

Baneyx, G., Baugh, L. and Vogel, V. (2002) 'Fibronectin extension and unfolding within cell matrix fibrils controlled by cytoskeletal tension', *Proceedings of the National Academy of Sciences of the United States of America*, 99(8), pp. 5139–5143. Available at: https://doi.org/10.1073/PNAS.072650799.

Bansho, Y. *et al.* (2012a) 'Importance of parasite RNA species repression for prolonged translation-coupled RNA self-replication', *Chemistry & biology*, 19(4), pp. 478–487. Available at: https://doi.org/10.1016/J.CHEMBIOL.2012.01.019.

Bansho, Y. *et al.* (2012b) 'Importance of Parasite RNA Species Repression for Prolonged Translation-Coupled RNA Self-Replication', *Chemistry & Biology*, 19(4), pp. 478–487. Available at: https://doi.org/10.1016/J.CHEMBIOL.2012.01.019.

Bansho, Y. *et al.* (2016) 'Host-parasite oscillation dynamics and evolution in a compartmentalized RNA replication system', *Proceedings of the National Academy of*

Sciences of the United States of America, 113(15), pp. 4045–4050. Available at: https://doi.org/10.1073/PNAS.1524404113/SUPPL_FILE/PNAS.201524404SI.PDF.

Bausch, J.N. *et al.* (1983) 'Terminal adenylation in the synthesis of RNA by Q beta replicase.', *Journal of Biological Chemistry*, 258(3), pp. 1978–1984. Available at: https://doi.org/10.1016/S0021-9258(18)33084-9.

Biebricher, C.K., Diekmann, S. and Luce, R. (1982a) 'Structural analysis of self-replicating RNA synthesized by Qbeta replicase', *Journal of molecular biology*, 154(4), pp. 629–648. Available at: https://doi.org/10.1016/S0022-2836(82)80019-3.

Biebricher, C.K., Diekmann, S. and Luce, R. (1982b) 'Structural analysis of self-replicating RNA synthesized by Qβ replicase', *Journal of Molecular Biology*, 154(4), pp. 629–648. Available at: https://doi.org/10.1016/S0022-2836(82)80019-3.

Biebricher, C.K. and Luce, R. (1993) 'Sequence Analysis of RNA Species Synthesized by Qβ Replicase without Template', *Biochemistry*, 32(18), pp. 4848–4854. Available at: https://doi.org/10.1021/BI00069A021.

Bindewald, E. *et al.* (2008) 'RNAJunction: a database of RNA junctions and kissing loops for three-dimensional structural analysis and nanodesign', *Nucleic acids research*, 36(Database issue). Available at: https://doi.org/10.1093/NAR/GKM842.

Bindewald, E. *et al.* (2011) 'Multistrand RNA secondary structure prediction and nanostructure design including pseudoknots', *ACS nano*, 5(12), pp. 9542–9551. Available at: https://doi.org/10.1021/NN202666W.

Binzel, D.W., Khisamutdinov, E.F. and Guo, P. (2014) 'Entropy-driven one-step formation of phi29 pRNA 3WJ from three RNA fragments', *Biochemistry*, 53(14), pp. 2221–2231. Available at: https://doi.org/10.1021/BI4017022/ASSET/IMAGES/LARGE/BI-2013-017022_0010.JPEG.

Blumenthal, T. (1980) 'Q beta replicase template specificity: different templates require different GTP concentrations for initiation', *Proceedings of the National Academy of Sciences of the United States of America*, 77(5), pp. 2601–2605. Available at: https://doi.org/10.1073/PNAS.77.5.2601.

Blumenthal, T. and Carmichael, G.G. (1979a) 'RNA replication: function and structure of Qbeta-replicase', *Annual review of biochemistry*, 48, pp. 525–548. Available at: https://doi.org/10.1146/ANNUREV.BI.48.070179.002521.

Blumenthal, T. and Carmichael, G.G. (1979b) 'RNA replication: function and structure of Qbeta-replicase', *Annual review of biochemistry*, 48, pp. 525–548. Available at: https://doi.org/10.1146/ANNUREV.BI.48.070179.002521.

Blumenthal, T. and Carmichael, G.G. (1979c) 'RNA replication: function and structure of Qbeta-replicase.', *Annual review of biochemistry*, 48, pp. 525–548. Available at: https://doi.org/10.1146/ANNUREV.BI.48.070179.002521.

Blumenthal, T., Landers, T.A. and Weber, K. (1972) 'Bacteriophage Q replicase contains the protein biosynthesis elongation factors EF Tu and EF Ts', *Proceedings of the National Academy of Sciences of the United States of America*, 69(5), pp. 1313–1317. Available at: https://doi.org/10.1073/PNAS.69.5.1313.

Breaker, R.R. and Joyce, G.F. (1994) 'Emergence of a replicating species from an in vitro RNA evolution reaction', *Proceedings of the National Academy of Sciences of the United States of America*, 91(13), pp. 6093–6097. Available at: https://doi.org/10.1073/PNAS.91.13.6093.

Brown, D. and Gold, L. (1995a) 'Selection and Characterization of RNAs Replicated by Qβ Replicase', *Biochemistry*, 34(45), pp. 14775–14782. Available at: https://doi.org/10.1021/BI00045A019.

Brown, D. and Gold, L. (1995b) 'Selection and Characterization of RNAs Replicated by Qβ Replicase', *Biochemistry*, 34(45), pp. 14775–14782. Available at: https://doi.org/10.1021/BI00045A019/ASSET/BI00045A019.FP.PNG_V03.

Brown, D. and Gold, L. (1996a) 'RNA replication by Qβ replicase: A working model', *Proceedings of the National Academy of Sciences of the United States of America*, 93(21), pp. 11558–11562. Available at: https://doi.org/10.1073/PNAS.93.21.11558.

Brown, D. and Gold, L. (1996b) 'RNA replication by Qβ replicase: A working model', *Proceedings of the National Academy of Sciences of the United States of America* [Preprint]. Available at: https://doi.org/10.1073/pnas.93.21.11558.

Cai, R. *et al.* (2019) 'ATP/ADP modulates gp16-pRNA conformational change in the Phi29 DNA packaging motor', *Nucleic acids research*, 47(18), pp. 9818–9828. Available at: https://doi.org/10.1093/nar/gkz692.

Campbell, A. (2003) 'The future of bacteriophage biology', *Nature Reviews. Genetics*, 4(6), p. 471. Available at: https://doi.org/10.1038/NRG1089.

Chetverin, A.B. *et al.* (1997) 'Nonhomologous RNA Recombination in a Cell-Free System: Evidence for a Transesterification Mechanism Guided by Secondary

Structure', *Cell*, 88(4), pp. 503–513. Available at: https://doi.org/10.1016/S0092-8674(00)81890-5.

Chetverin, A.B. (2004) 'Replicable and recombinogenic RNAs', *Febs Letters*, 567(1), p. 35. Available at: https://doi.org/10.1016/J.FEBSLET.2004.03.066.

Chetverin, A.B. (2018) 'Thirty Years of Studies of Qβ Replicase: What Have We Learned and What Is Yet to Be Learned?', *Biochemistry (Moscow)*, 83. Available at: https://doi.org/10.1134/S0006297918140031.

Chetverin, A.B., Chetverina, H. V. and Munishkin, A. V. (1991) 'On the nature of spontaneous RNA synthesis by Q beta replicase', *Journal of molecular biology*, 222(1), pp. 3–9. Available at: https://doi.org/10.1016/0022-2836(91)90729-P.

Cruz, J.A. and Westhof, E. (2009) 'The dynamic landscapes of RNA architecture', *Cell*, 136(4), pp. 604–609. Available at: https://doi.org/10.1016/J.CELL.2009.02.003.

Dahlberg, J.E. (1968) 'Terminal sequences of bacteriophage RNAs', *Nature*, 220(5167), pp. 548–552. Available at: https://doi.org/10.1038/220548A0.

Deamer, D.W. and Fleischaker, G.R. (1994) 'Origins of life : the central concepts', p. 431. Available at: https://search.worldcat.org/title/28218773 (Accessed: 28 December 2023).

D'Hérelle F. (2007) 'On an invisible microbe antagonistic toward dysenteric bacilli: brief note by Mr. F. D'Herelle, presented by Mr. Roux', *Research in Microbiology*, 158(7), pp. 553–554. Available at: https://doi.org/10.1016/J.RESMIC.2007.07.005.

van Dijk, A.A., Makeyev, E. V. and Bamford, D.H. (2004) 'Initiation of viral RNA-dependent RNA polymerization', *The Journal of general virology*, 85(Pt 5), pp. 1077–1093. Available at: https://doi.org/10.1099/VIR.0.19731-0.

Dix, D.E. (2002) 'What is life? Prerequisites for a definition.', *The Yale Journal of Biology and Medicine*, 75(5–6), p. 313. Available at: /pmc/articles/PMC2588815/?report=abstract (Accessed: 28 December 2023).

Dobson, C.M. *et al.* (2000) 'Atmospheric aerosols as prebiotic chemical reactors', *Proceedings of the National Academy of Sciences of the United States of America*, 97(22), pp. 11864–11868. Available at: https://doi.org/10.1073/PNAS.200366897.

Draper, D.E. (2004) 'A guide to ions and RNA structure', *RNA*, 10(3), pp. 335–343. Available at: https://doi.org/10.1261/RNA.5205404.

Durzyńska, J. and Goździcka-Józefiak, A. (2015) ‘Viruses and cells intertwined since the dawn of evolution Emerging viruses’, *Virology Journal*, 12(1), pp. 1–10. Available at: https://doi.org/10.1186/S12985-015-0400-7/FIGURES/2.

Eigen, M. (1971) ‘Selforganization of matter and the evolution of biological macromolecules’, *Die Naturwissenschaften*, 58(10), pp. 465–523. Available at: https://doi.org/10.1007/BF00623322.

Ellinger, T., Ehricht, R. and McCaskill, J.S. (1998) ‘In vitro evolution of molecular cooperation in CATCH, a cooperatively coupled amplification system’, *Chemistry & biology*, 5(12), pp. 729–741. Available at: https://doi.org/10.1016/S1074-5521(98)90665-2.

Fang, Y. *et al.* (2008) ‘Modular assembly of chimeric phi29 packaging RNAs that support DNA packaging’, *Biochemical and biophysical research communications*, 372(4), p. 589. Available at: https://doi.org/10.1016/J.BBRC.2008.05.094.

Fedoroff, N. V. and Zinder, N.D. (1973) ‘Factor requirement of the bacteriophage f2 Replicase’, *Nature New Biology*, 241(108), pp. 105–108. Available at: https://doi.org/10.1038/newbio241105a0.

Filonov, G.S. *et al.* (2015a) ‘In-gel imaging of RNA processing using broccoli reveals optimal aptamer expression strategies’, *Chemistry & biology*, 22(5), pp. 649–660. Available at: https://doi.org/10.1016/J.CHEMBIOL.2015.04.018.

Filonov, G.S. *et al.* (2015b) ‘In-gel imaging of RNA processing using broccoli reveals optimal aptamer expression strategies’, *Chemistry and Biology* [Preprint]. Available at: https://doi.org/10.1016/j.chembiol.2015.04.018.

Furubayashi, T. *et al.* (2020) ‘Emergence and diversification of a host-parasite RNA ecosystem through Darwinian evolution’, *eLife*, 9. Available at: https://doi.org/10.7554/eLife.56038.

Furubayashi, T. and Ichihashi, N. (2018) ‘Sustainability of a compartmentalized host-parasite replicator system under periodic washout-mixing cycles’, *Life*, 8(1). Available at: https://doi.org/10.3390/life8010003.

Gilbert, W. (1986) ‘Origin of life: The RNA world’, *Nature 1986 319:6055*, 319(6055), pp. 618–618. Available at: https://doi.org/10.1038/319618a0.

Di Giulio, M. (2006) ‘The non-monophyletic origin of the tRNA molecule and the origin of genes only after the evolutionary stage of the last universal common ancestor (LUCA)’, *Journal of theoretical biology*, 240(3), pp. 343–352. Available at: https://doi.org/10.1016/J.JTBI.2005.09.023.

Goldberger, J. *et al.* (2003) 'Single-crystal gallium nitride nanotubes', *Nature*, 422(6932), pp. 599–602. Available at: https://doi.org/10.1038/NATURE01551.

Green, A.A. (2019) 'Synthetic bionanotechnology: synthetic biology finds a toehold in nanotechnology', *Emerging Topics in Life Sciences*, 3(5), pp. 507–516. Available at: https://doi.org/10.1042/etls20190100.

Gu, X. and Schroeder, S.J. (2011) 'Different sequences show similar quaternary interaction stabilities in Prohead viral RNA self-assembly', *Journal of Biological Chemistry*, 286(16), pp. 14419–14426. Available at: https://doi.org/10.1074/JBC.M110.191064.

Guatelli, J.C. *et al.* (1990) 'Isothermal, in vitro amplification of nucleic acids by a multienzyme reaction modeled after retroviral replication', *Proceedings of the National Academy of Sciences of the United States of America*, 87(5), pp. 1874–1878. Available at: https://doi.org/10.1073/PNAS.87.5.1874.

Guindani, C. *et al.* (2022) 'Synthetic Cells: From Simple Bio-Inspired Modules to Sophisticated Integrated Systems', *Angewandte Chemie International Edition*, 61(16), p. e202110855. Available at: https://doi.org/10.1002/ANIE.202110855.

Guo, P. (2005) 'RNA Nanotechnology: Engineering, Assembly and Applications in Detection, Gene Delivery and Therapy', *Journal of nanoscience and nanotechnology*, 5(12), p. 1964. Available at: https://doi.org/10.1166/JNN.2005.446.

Guo, S. *et al.* (2018) 'Methods for construction and characterization of simple or special multifunctional RNA nanoparticles based on the 3WJ of phi29 DNA packaging motor', *Methods*, 143, pp. 121–133. Available at: https://doi.org/10.1016/j.ymeth.2018.02.025.

Gytz, H. *et al.* (2015) 'Structural basis for RNA-genome recognition during bacteriophage Qβ replication', *Nucleic Acids Research*, 43(22), p. 10893. Available at: https://doi.org/10.1093/NAR/GKV1212.

Haque, F. *et al.* (2018a) 'RNA versatility, flexibility, and thermostability for practice in RNA nanotechnology and biomedical applications', *Wiley Interdisciplinary Reviews: RNA*, 9(1), p. e1452. Available at: https://doi.org/10.1002/WRNA.1452.

Haque, F. *et al.* (2018b) 'RNA versatility, flexibility, and thermostability for practice in RNA nanotechnology and biomedical applications', *Wiley Interdisciplinary Reviews: RNA* [Preprint]. Available at: https://doi.org/10.1002/wrna.1452.

Hata, Y., Sawada, T. and Serizawa, T. (2018) 'Macromolecular crowding for materials-directed controlled self-assembly', *Journal of Materials Chemistry B*, 6(40), pp. 6344–6359. Available at: https://doi.org/10.1039/C8TB02201A.

Hatfull, G.F. (2008) 'Bacteriophage genomics', *Current Opinion in Microbiology*, 11(5), pp. 447–453. Available at: https://doi.org/10.1016/J.MIB.2008.09.004.

Hayden, E.J., Von Kiedrowski, G. and Lehman, N. (2008a) 'Systems chemistry on ribozyme self-construction: evidence for anabolic autocatalysis in a recombination network', *Angewandte Chemie (International ed. in English)*, 47(44), pp. 8424–8428. Available at: https://doi.org/10.1002/ANIE.200802177.

Hayden, E.J., Von Kiedrowski, G. and Lehman, N. (2008b) 'Systems chemistry on ribozyme self-construction: evidence for anabolic autocatalysis in a recombination network', *Angewandte Chemie (International ed. in English)*, 47(44), pp. 8424–8428. Available at: https://doi.org/10.1002/ANIE.200802177.

Hill, A.C., Bartley, L.E. and Schroeder, S.J. (2016) 'Prohead RNA: a noncoding viral RNA of novel structure and function', *Wiley Interdisciplinary Reviews: RNA*, 7(4), pp. 428–437. Available at: https://doi.org/10.1002/wrna.1330.

Holmes, E.C. (2003) 'Error thresholds and the constraints to RNA virus evolution', *Trends in Microbiology*, 11(12), p. 543. Available at: https://doi.org/10.1016/J.TIM.2003.10.006.

Hosoda, K. *et al.* (2007) 'Kinetic analysis of the entire RNA amplification process by Qbeta replicase', *The Journal of biological chemistry*, 282(21), pp. 15516–15527. Available at: https://doi.org/10.1074/JBC.M700307200.

Ichihashi, N. *et al.* (2013) 'Darwinian evolution in a translation-coupled RNA replication system within a cell-like compartment', *Nature communications*, 4. Available at: https://doi.org/10.1038/NCOMMS3494.

Ichihashi, N. (2019) 'What can we learn from the construction of in vitro replication systems?', *Annals of the New York Academy of Sciences*, 1447(1), pp. 144–156. Available at: https://doi.org/10.1111/nyas.14042.

Ioannou, P., Baliou, S. and Samonis, G. (2023) 'Bacteriophages in Infectious Diseases and Beyond—A Narrative Review', *Antibiotics 2023, Vol. 12, Page 1012*, 12(6), p. 1012. Available at: https://doi.org/10.3390/ANTIBIOTICS12061012.

Iranzo, J. *et al.* (2016) 'Inevitability of Genetic Parasites', *Genome biology and evolution*, 8(9), pp. 2856–2869. Available at: https://doi.org/10.1093/GBE/EVW193.

Ivanov, I. *et al.* (2021) 'Bottom-Up Synthesis of Artificial Cells: Recent Highlights and Future Challenges'. Available at: https://doi.org/10.1146/annurev-chembioeng.

Jeong, Y.J., Park, K. and Kim, D.E. (2009) 'Isothermal DNA amplification in vitro: the helicase-dependent amplification system', *Cellular and molecular life sciences : CMLS*, 66(20), pp. 3325–3336. Available at: https://doi.org/10.1007/S00018-009-0094-3.

Jones, R.A.C. and Janssen, D. (2021) 'Global Plant Virus Disease Pandemics and Epidemics', *Plants 2021, Vol. 10, Page 233*, 10(2), p. 233. Available at: https://doi.org/10.3390/PLANTS10020233.

Kajitani, M. *et al.* (1994) 'Regulation of the Escherichia coli hfq gene encoding the host factor for phage Q(β)', *Journal of Bacteriology*, 176(2), pp. 531–534. Available at: https://doi.org/10.1128/JB.176.2.531-534.1994.

Kamen, R. (1970) 'Characterization of the subunits of Q-beta replicase', *Nature*, 228(5271), pp. 527–533. Available at: https://doi.org/10.1038/228527A0.

Kanavarioti, A., Monnard, P.A. and Deamer, D.W. (2001) 'Eutectic phases in ice facilitate nonenzymatic nucleic acid synthesis', *Astrobiology*, 1(3), pp. 271–281. Available at: https://doi.org/10.1089/15311070152757465.

Karimi, M. *et al.* (2016) 'Bacteriophages and phage-inspired nanocarriers for targeted delivery of therapeutic cargos', *Advanced drug delivery reviews*, 106(Pt A), pp. 45–62. Available at: https://doi.org/10.1016/J.ADDR.2016.03.003.

Kashiwagi, A. and Yomo, T. (2011) 'Ongoing phenotypic and genomic changes in experimental coevolution of rna bacteriophage qβ and escherichia coli', *PLoS Genetics*, 7(8). Available at: https://doi.org/10.1371/JOURNAL.PGEN.1002188.

Kazantsev, A. V., Krivenko, A.A. and Pace, N.R. (2009) 'Mapping metal-binding sites in the catalytic domain of bacterial RNase P RNA', *RNA*, 15(2), pp. 266–276. Available at: https://doi.org/10.1261/RNA.1331809.

Kidmose, R.T. *et al.* (2010) 'Structure of the Qbeta replicase, an RNA-dependent RNA polymerase consisting of viral and host proteins', *Proceedings of the National Academy of Sciences of the United States of America*, 107(24), pp. 10884–10889. Available at: https://doi.org/10.1073/PNAS.1003015107.

Kim, D.E. and Joyce, G.F. (2004) 'Cross-catalytic replication of an RNA ligase ribozyme', *Chemistry and Biology*, 11(11), pp. 1505–1512. Available at: https://doi.org/10.1016/j.chembiol.2004.08.021.

Kita, H. *et al.* (2006) 'Functional Qβ replicase genetically fusing essential subunits EF-Ts and EF-Tu with β-subunit', *Journal of Bioscience and Bioengineering*, 101(5), pp. 421–426. Available at: https://doi.org/10.1263/JBB.101.421.

Kita, H. *et al.* (2008a) 'Replication of genetic information with self-encoded replicase in liposomes', *ChemBioChem*, 9(15), pp. 2403–2410. Available at: https://doi.org/10.1002/cbic.200800360.

Kita, H. *et al.* (2008b) 'Replication of genetic information with self-encoded replicase in liposomes', *Chembiochem : a European journal of chemical biology*, 9(15), pp. 2403–2410. Available at: https://doi.org/10.1002/CBIC.200800360.

Kita, H. *et al.* (2008c) 'Replication of genetic information with self-encoded replicase in liposomes', *Wiley Online LibraryPaperpileH Kita, T Matsuura, T Sunami, K Hosoda, N Ichihashi, K Tsukada, I Urabe, T YomoChemBioChem, 2008•Wiley Online LibrarySign in*, 9(15), pp. 2403–2410. Available at: https://doi.org/10.1002/cbic.200800360.

Kondo, M., Gallerani, R. and Weissmann, C. (1970) 'Subunit structure of Q-beta replicase', *Nature*, 228(5271), pp. 525–527. Available at: https://doi.org/10.1038/228525A0.

Koonin, E. V. (2016) 'Viruses and mobile elements as drivers of evolutionary transitions', *Philosophical transactions of the Royal Society of London. Series B, Biological sciences*, 371(1701). Available at: https://doi.org/10.1098/RSTB.2015.0442.

Koonin, E. V. *et al.* (2020) 'The replication machinery of LUCA: common origin of DNA replication and transcription', *BMC biology*, 18(1), p. 61. Available at: https://doi.org/10.1186/s12915-020-00800-9.

Koonin, E. V. and Martin, W. (2005a) 'On the origin of genomes and cells within inorganic compartments', *Trends in genetics : TIG*, 21(12), pp. 647–654. Available at: https://doi.org/10.1016/J.TIG.2005.09.006.

Koonin, E. V. and Martin, W. (2005b) 'On the origin of genomes and cells within inorganic compartments', *Trends in genetics : TIG*, 21(12), pp. 647–654. Available at: https://doi.org/10.1016/J.TIG.2005.09.006.

Koonin, E. V., Wolf, Y.I. and Katsnelson, M.I. (2017) 'Inevitability of the emergence and persistence of genetic parasites caused by evolutionary instability of parasite-free states', *Biology direct*, 12(1). Available at: https://doi.org/10.1186/S13062-017-0202-5.

Kopsidas, G. *et al.* (2007) 'RNA mutagenesis yields highly diverse mRNA libraries for in vitro protein evolution', *BMC Biotechnology*, 7. Available at: https://doi.org/10.1186/1472-6750-7-18.

Kramer, F.R. *et al.* (1974) 'Evolution in vitro: sequence and phenotype of a mutant RNA resistant to ethidium bromide', *Journal of molecular biology*, 89(4). Available at: https://doi.org/10.1016/0022-2836(74)90047-3.

Kueppers, B. and Sumper, M. (1975a) 'Minimal requirements for template recognition by bacteriophage Qbeta replicase: approach to general RNA-dependent RNA synthesis', *Proceedings of the National Academy of Sciences of the United States of America*, 72(7), pp. 2640–2643. Available at: https://doi.org/10.1073/PNAS.72.7.2640.

Kueppers, B. and Sumper, M. (1975b) 'Minimal requirements for template recognition by bacteriophage Qβ replicase: approach to general RNA dependent RNA synthesis', *Proceedings of the National Academy of Sciences of the United States of America*, 72(7), pp. 2640–2643. Available at: https://doi.org/10.1073/PNAS.72.7.2640.

Kuhn, J.H. (2021) 'Virus Taxonomy', *Encyclopedia of Virology*, 1–5, p. 28. Available at: https://doi.org/10.1016/B978-0-12-809633-8.21231-4.

Kun, Á. *et al.* (2015) 'The dynamics of the RNA world: insights and challenges', *Annals of the New York Academy of Sciences*, 1341(1), pp. 75–95. Available at: https://doi.org/10.1111/NYAS.12700.

Kurn, N. *et al.* (2005) 'Novel isothermal, linear nucleic acid amplification systems for highly multiplexed applications', *Clinical chemistry*, 51(10), pp. 1973–1981. Available at: https://doi.org/10.1373/CLINCHEM.2005.053694.

Laing, C. and Schlick, T. (2009) 'Analysis of four-way junctions in RNA structures', *Journal of molecular biology*, 390(3), pp. 547–559. Available at: https://doi.org/10.1016/J.JMB.2009.04.084.

Lam, B.J. and Joyce, G.F. (2009) 'Autocatalytic aptazymes enable ligand-dependent exponential amplification of RNA', *Nature biotechnology*, 27(3), pp. 288–292. Available at: https://doi.org/10.1038/NBT.1528.

Lee, D.H. *et al.* (1996) 'A self-replicating peptide', *Nature*, 382(6591), pp. 525–528. Available at: https://doi.org/10.1038/382525A0.

Lee, D.H. *et al.* (1997) 'Emergence of symbiosis in peptide self-replication through a hypercyclic network', *Nature*, 390(6660), pp. 591–594. Available at: https://doi.org/10.1038/37569.

Lehman, N. (2008) ‘A Recombination-Based Model for the Origin and Early Evolution of Genetic Information’, *Chemistry & Biodiversity*, 5(9), pp. 1707–1717. Available at: https://doi.org/10.1002/CBDV.200890159.

Lehman, N. (2012) ‘Evolution Finds Shelter in Small Spaces’, *Chemistry & Biology*, 19(4), pp. 439–440. Available at: https://doi.org/10.1016/J.CHEMBIOL.2012.04.002.

Leontis, N.B., Lescoute, A. and Westhof, E. (2006) ‘The building blocks and motifs of RNA architecture’, *Current opinion in structural biology*, 16(3), pp. 279–287. Available at: https://doi.org/10.1016/J.SBI.2006.05.009.

Lescoute, A. and Westhof, E. (2006) ‘Topology of three-way junctions in folded RNAs’, *RNA (New York, N.Y.)*, 12(1), pp. 83–93. Available at: https://doi.org/10.1261/RNA.2208106.

Li, T. and Nicolaou, K.C. (1994) ‘Chemical self-replication of palindromic duplex DNA’, *Nature*, 369(6477), pp. 218–221. Available at: https://doi.org/10.1038/369218A0.

Lincoln, T.A. and Joyce, G.F. (2009a) ‘Self-sustained replication of an RNA enzyme’, *Science*, 323(5918), pp. 1229–1232. Available at: https://doi.org/10.1126/science.1167856.

Lincoln, T.A. and Joyce, G.F. (2009b) ‘Self-sustained replication of an RNA enzyme’, *Science (New York, N.Y.)*, 323(5918), pp. 1229–1232. Available at: https://doi.org/10.1126/SCIENCE.1167856.

Lincoln, T.A. and Joyce, G.F. (2009c) ‘Self-sustained replication of an RNA enzyme’, *Science (New York, N.Y.)*, 323(5918), pp. 1229–1232. Available at: https://doi.org/10.1126/SCIENCE.1167856.

De Lorenzo, V. (2018) ‘Evolutionary tinkering vs. rational engineering in the times of synthetic biology Carmen McLeod, Brigitte Nerlich’, *Life Sciences, Society and Policy*, 14(1), pp. 1–16. Available at: https://doi.org/10.1186/S40504-018-0086-X/FIGURES/5.

Luisi, P.L. (1998) ‘About various definitions of life’, *Origins of Life and Evolution of the Biosphere*, 28(4–6), pp. 613–622. Available at: https://doi.org/10.1023/A:1006517315105/METRICS.

Luisi, P.L., Walde, P. and Oberholzer, T. (1999) ‘Lipid vesicles as possible intermediates in the origin of life’, *Current Opinion in Colloid & Interface Science*, 4(1), pp. 33–39. Available at: https://doi.org/10.1016/S1359-0294(99)00012-6.

Lutay, A. V., Zenkova, M.A. and Vlassov, V. V. (2007) 'Nonenzymatic Recombination of RNA: Possible Mechanism for the Formation of Novel Sequences', *Chemistry & Biodiversity*, 4(4), pp. 762–767. Available at: https://doi.org/10.1002/CBDV.200790062.

Matsumura, S. *et al.* (2016) 'Transient compartmentalization of RNA replicators prevents extinction due to parasites', *Science*, 354(iii), pp. 4–8.

McDonald, S.M. *et al.* (2016) 'Reassortment in segmented RNA viruses: mechanisms and outcomes', *Nature reviews. Microbiology*, 14(7), p. 448. Available at: https://doi.org/10.1038/NRMICRO.2016.46.

Meile, S. *et al.* (2020) 'Reporter Phage-Based Detection of Bacterial Pathogens: Design Guidelines and Recent Developments', *Viruses*, 12(9). Available at: https://doi.org/10.3390/V12090944.

Mencía, M. *et al.* (2011) 'Terminal protein-primed amplification of heterologous DNA with a minimal replication system based on phage Φ29', *Proceedings of the National Academy of Sciences of the United States of America*, 108(46), pp. 18655–18660. Available at: https://doi.org/10.1073/PNAS.1114397108/-/DCSUPPLEMENTAL/PNAS.1114397108_SI.PDF.

Miele, E.A., Mills, D.R. and Kramer, F.R. (1983) 'Autocatalytic replication of a recombinant RNA', *Journal of molecular biology*, 171(3), pp. 281–295. Available at: https://doi.org/10.1016/0022-2836(83)90094-3.

Mills, D. R., Peterson, R.L. and Spiegelman, S. (1967a) 'An extracellular Darwinian experiment with a self-duplicating nucleic acid molecule.', *Proceedings of the National Academy of Sciences of the United States of America*, 58(1), pp. 217–224. Available at: https://doi.org/10.1073/PNAS.58.1.217/ASSET/257A40EB-3654-4182-A615-2EDF67C14F6F/ASSETS/PNAS.58.1.217.FP.PNG.

Mills, D. R., Peterson, R.L. and Spiegelman, S. (1967b) 'An extracellular Darwinian experiment with a self-duplicating nucleic acid molecule', *Proceedings of the National Academy of Sciences of the United States of America*, 58(1), pp. 217–224. Available at: https://doi.org/10.1073/PNAS.58.1.217.

Mills, D. R., Peterson, R.L. and Spiegelman, S. (1967c) 'An extracellular Darwinian experiment with a self-duplicating nucleic acid molecule.', *Proceedings of the National Academy of Sciences of the United States of America*, 58(1), p. 217. Available at: https://doi.org/10.1073/PNAS.58.1.217.

Mills, D R, Peterson, R.L. and Spiegelman, S. (1967) *An extracellular Darwinian experiment with a self-duplicating nucleic acid molecule*. Available at: https://www.pnas.org.

Mizuuchi, R. and Ichihashi, N. (2018) 'Sustainable replication and coevolution of cooperative RNAs in an artificial cell-like system', *Nature ecology & evolution*, 2(10), pp. 1654–1660. Available at: https://doi.org/10.1038/S41559-018-0650-Z.

Mizuuchi, R., Usui, K. and Ichihashi, N. (2020a) 'Structural transition of replicable RNAs during in vitro evolution with Qβ replicase', *RNA*, 26(1), pp. 83–90. Available at: https://doi.org/10.1261/RNA.073106.119.

Mizuuchi, R., Usui, K. and Ichihashi, N. (2020b) 'Structural transition of replicable RNAs during in vitro evolution with Qβ replicase', *RNA*, 26(1), pp. 83–90. Available at: https://doi.org/10.1261/RNA.073106.119/-/DC1.

Moger-Reischer, R.Z. *et al.* (2023) 'Evolution of a minimal cell', *Nature 2023 620:7972*, 620(7972), pp. 122–127. Available at: https://doi.org/10.1038/s41586-023-06288-x.

Moody, M.D. *et al.* (1994) 'Evolution of host cell RNA into efficient template RNA by Q beta replicase: the origin of RNA in untemplated reactions', *Biochemistry*, 33(46), pp. 13836–13847. Available at: https://doi.org/10.1021/BI00250A038.

Morozov, I.Y. *et al.* (1993) 'Synergism in replication and translation of messenger RNA in a cell-free system', *Proceedings of the National Academy of Sciences of the United States of America*, 90(20), pp. 9325–9329. Available at: https://doi.org/10.1073/PNAS.90.20.9325.

Moya, A., Holmes, E.C. and González-Candelas, F. (2004) 'The population genetics and evolutionary epidemiology of RNA viruses', *Nature Reviews Microbiology 2004 2:4*, 2(4), pp. 279–288. Available at: https://doi.org/10.1038/nrmicro863.

Munishkin, A. V. *et al.* (1991) 'Efficient templates for Qβ replicase are formed by recombination from heterologous sequences', *Journal of Molecular Biology*, 221(2), pp. 463–472. Available at: https://doi.org/10.1016/0022-2836(91)80067-5.

Narlikar, G.J. and Herschlag, D. (1997) 'Mechanistic aspects of enzymatic catalysis: lessons from comparison of RNA and protein enzymes', *Annual review of biochemistry*, 66, pp. 19–59. Available at: https://doi.org/10.1146/ANNUREV.BIOCHEM.66.1.19.

Nash, K., Chen, W. and Muzyczka, N. (2008) 'Complete in vitro reconstitution of adeno-associated virus DNA replication requires the minichromosome maintenance

complex proteins', *Journal of virology*, 82(3), pp. 1458–1464. Available at: https://doi.org/10.1128/JVI.01968-07.

Niemeyer, C.M. (2002) 'The developments of semisynthetic DNA-protein conjugates', *Trends in biotechnology*, 20(9), pp. 395–401. Available at: https://doi.org/10.1016/S0167-7799(02)02022-X.

Nishihara, T., Mills, D.R. and Kramer, F.R. (1983a) 'Localization of the Q beta replicase recognition site in MDV-1 RNA', *Journal of biochemistry*, 93(3), pp. 669–674. Available at: https://doi.org/10.1093/JB/93.3.669.

Nishihara, T., Mills, D.R. and Kramer, F.R. (1983b) 'Localization of the Qβ replicase recognition site in MDV-1 RNA', *Journal of Biochemistry*, 93(3), pp. 669–674. Available at: https://doi.org/10.1093/JB/93.3.669.

Notomi, T. *et al.* (2000) 'Loop-mediated isothermal amplification of DNA', *Nucleic acids research*, 28(12). Available at: https://doi.org/10.1093/NAR/28.12.E63.

Obad, S. *et al.* (2011) 'Silencing of microRNA families by seed-targeting tiny LNAs', *Nature genetics*, 43(4), pp. 371–380. Available at: https://doi.org/10.1038/NG.786.

Oliver, J. (2013) *Viruses: Essential Agents of Life*, *Journal of Chemical Information and Modeling*. Available at: https://doi.org/10.1017/CBO9781107415324.004.

Paczesny, J. and Bielec, K. (2020) 'Application of Bacteriophages in Nanotechnology', *Nanomaterials*, 10(10), pp. 1–25. Available at: https://doi.org/10.3390/NANO10101944.

Peixuan, G., Erickson, S. and Anderson, D. (1987) 'A small viral RNA is required for in vitro packaging of bacteriophage phi 29 DNA', *Science (New York, N.Y.)*, 236(4802), pp. 690–694. Available at: https://doi.org/10.1126/SCIENCE.3107124.

Pi, F. *et al.* (2017) 'RNA nanoparticles harboring annexin A2 aptamer can target ovarian cancer for tumor-specific doxorubicin delivery', *Nanomedicine : nanotechnology, biology, and medicine*, 13(3), pp. 1183–1193. Available at: https://doi.org/10.1016/J.NANO.2016.11.015.

Poteete, A.R. and Hardy, L.W. (1994) 'Genetic Analysis of Bacteriophage T4 Lysozyme Structure and Function', *JOURNAL OF BACTERIOLOGY*, pp. 6783–6788. Available at: https://journals.asm.org/journal/jb (Accessed: 26 December 2023).

Priano, C. *et al.* (1995) 'A complete plasmid-based complementation system for RNA coliphage Qβ: Three proteins of bacteriophages Qβ (Group III) and SP (Group IV)

can be interchanged', *Journal of Molecular Biology*, 249(2), pp. 283–297. Available at: https://doi.org/10.1006/JMBI.1995.0297.

Principi, N., Silvestri, E. and Esposito, S. (2019) 'Advantages and limitations of bacteriophages for the treatment of bacterial infections', *Frontiers in Pharmacology*, 10(MAY), p. 457104. Available at: https://doi.org/10.3389/FPHAR.2019.00513/BIBTEX.

Rao, V.B. and Feiss, M. (2008) 'The Bacteriophage DNA Packaging Motor', *https://doi.org/10.1146/annurev.genet.42.110807.091545*, 42, pp. 647–681. Available at: https://doi.org/10.1146/ANNUREV.GENET.42.110807.091545.

Ruiz-Mirazo, K., Umerez, J. and Moreno, A. (2008) 'Enabling conditions for "open-ended evolution"', *Biology and Philosophy*, 23(1), pp. 67–85. Available at: https://doi.org/10.1007/S10539-007-9076-8.

Saiki, R.K. *et al.* (1985) 'Enzymatic Amplification of β-Globin Genomic Sequences and Restriction Site Analysis for Diagnosis of Sickle Cell Anemia', *Science*, 230(4732), pp. 1350–1354. Available at: https://doi.org/10.1126/SCIENCE.2999980.

Salas, M. (2012) 'My life with bacteriophage phi29', *The Journal of biological chemistry*, 287(53), pp. 44568–44579. Available at: https://doi.org/10.1074/JBC.X112.433458.

Scanlan, P.D. *et al.* (2011) 'Genetic basis of infectivity evolution in a bacteriophage', *Molecular Ecology*, 20(5), pp. 981–989. Available at: https://doi.org/10.1111/J.1365-294X.2010.04903.X.

Schaerli, Y. *et al.* (2010) 'Isothermal DNA amplification using the T4 replisome: circular nicking endonuclease-dependent amplification and primase-based whole-genome amplification', *Nucleic acids research*, 38(22). Available at: https://doi.org/10.1093/NAR/GKQ795.

Schmidt, O.G. and Eberl, K. (2001) 'Nanotechnology. Thin solid films roll up into nanotubes', *Nature*, 410(6825), p. 168. Available at: https://doi.org/10.1038/35065525.

Schroeder, K.T. *et al.* (2010) 'A structural database for k-turn motifs in RNA', *RNA (New York, N.Y.)*, 16(8), pp. 1463–1468. Available at: https://doi.org/10.1261/RNA.2207910.

Schwille, P. and Diez, S. (2009) 'Synthetic biology of minimal systems', *Critical Reviews in Biochemistry and Molecular Biology* [Preprint]. Available at: https://doi.org/10.1080/10409230903074549.

Severcan, I. *et al.* (2009) 'Square-shaped RNA particles from different RNA folds', *Nano letters*, 9(3), pp. 1270–1277. Available at: https://doi.org/10.1021/NL900261H.

Shu, D. *et al.* (2011a) 'Thermodynamically stable RNA three-way junction for constructing multifunctional nanoparticles for delivery of therapeutics', *Nature nanotechnology*, 6(10), pp. 658–667. Available at: https://doi.org/10.1038/NNANO.2011.105.

Shu, D. *et al.* (2011b) 'Thermodynamically stable RNA three-way junction for constructing multifunctional nanoparticles for delivery of therapeutics', *Nature nanotechnology*, 6(10), pp. 658–667. Available at: https://doi.org/10.1038/NNANO.2011.105.

Shu, D. *et al.* (2011c) 'Thermodynamically stable RNA three-way junction for constructing multifunctional nanoparticles for delivery of therapeutics', *Nature Nanotechnology*, 6(September), pp. 1–10. Available at: https://doi.org/10.1038/nnano.2011.105.

Shu, D. *et al.* (2014) 'Programmable folding of fusion RNA in vivo and in vitro driven by pRNA 3WJ motif of phi29 DNA packaging motor', *Nucleic Acids Research*, 42(2), pp. 1–9. Available at: https://doi.org/10.1093/nar/gkt885.

Shu, Y. *et al.* (2011) 'Assembly of Therapeutic pRNA-siRNA Nanoparticles Using Bipartite Approach', *Molecular Therapy*, 19(7), p. 1304. Available at: https://doi.org/10.1038/MT.2011.23.

Shu, Y., Haque, F., *et al.* (2013a) 'Fabrication of 14 different RNA nanoparticles for specific tumor targeting without accumulation in normal organs', *Rna*, 19(6), pp. 767–777. Available at: https://doi.org/10.1261/rna.037002.112.

Shu, Y., Haque, F., *et al.* (2013b) 'Fabrication of 14 different RNA nanoparticles for specific tumor targeting without accumulation in normal organs', *RNA*, 19(6), p. 767. Available at: https://doi.org/10.1261/RNA.037002.112.

Shu, Y., Haque, F., *et al.* (2013c) 'Fabrication of 14 different RNA nanoparticles for specific tumor targeting without accumulation in normal organs', *RNA (New York, N.Y.)*, 19(6), pp. 767–777. Available at: https://doi.org/10.1261/RNA.037002.112.

Shu, Y., Shu, D., *et al.* (2013) 'Fabrication of pRNA nanoparticles to deliver therapeutic RNAs and bioactive compounds into tumor cells', *Nature Protocols*, 8(9), pp. 1635–1659. Available at: https://doi.org/10.1038/nprot.2013.097.

Siegel, R.W. *et al.* (1999) 'Use of DNA, RNA, and Chimeric Templates by a Viral RNA-Dependent RNA Polymerase: Evolutionary Implications for the Transition from the RNA to the DNA World', *Journal of Virology*, 73(8), p. 6424. Available at: https://doi.org/10.1128/JVI.73.8.6424-6429.1999.

Sievers, D. and Von Kiedrowski, G. (1994) 'Self-replication of complementary nucleotide-based oligomers', *Nature*, 369(6477), pp. 221–224. Available at: https://doi.org/10.1038/369221A0.

Silverman, P.M. (1973) 'Replication of RNA viruses: specific binding of the Q RNA polymerase to Q RNA', *Archives of biochemistry and biophysics*, 157(1), pp. 222–233. Available at: https://doi.org/10.1016/0003-9861(73)90408-6.

Singleton, R.L. *et al.* (2018a) 'Function of the RNA Coliphage Qβ Proteins in Medical In Vitro Evolution', *Methods and Protocols 2018, Vol. 1, Page 18*, 1(2), p. 18. Available at: https://doi.org/10.3390/MPS1020018.

Singleton, R.L. *et al.* (2018b) 'Function of the RNA Coliphage Qβ Proteins in Medical In Vitro Evolution', *Methods and Protocols*, 1(2), pp. 1–12. Available at: https://doi.org/10.3390/MPS1020018.

Smith, E.C., Sexton, N.R. and Denison, M.R. (2014) 'Thinking Outside the Triangle: Replication Fidelity of the Largest RNA Viruses', *https://doi.org/10.1146/annurev-virology-031413-085507*, 1(1), pp. 111–132. Available at: https://doi.org/10.1146/ANNUREV-VIROLOGY-031413-085507.

Smith, J.M. (1979) 'Hypercycles and the origin of life', *Nature*, 280(5722), pp. 445–446. Available at: https://doi.org/10.1038/280445A0.

Sun, Y., Overman, S.A. and Thomas, G.J. (2007) 'Impact of in vitro assembly defects on in vivo function of the phage P22 portal', *Virology*, 365(2), pp. 336–345. Available at: https://doi.org/10.1016/J.VIROL.2007.02.040.

Suttle, C.A. (2007) 'Marine viruses — major players in the global ecosystem', *Nature Reviews Microbiology 2007 5:10*, 5(10), pp. 801–812. Available at: https://doi.org/10.1038/nrmicro1750.

Szabó, P. *et al.* (2002) 'In silico simulations reveal that replicators with limited dispersal evolve towards higher efficiency and fidelity', *Nature*, 420(6913), pp. 340–343. Available at: https://doi.org/10.1038/NATURE01187.

Szathmáry, E. and Smith, J.M. (1995) 'The major evolutionary transitions', *Nature*, 374(6519), pp. 227–232. Available at: https://doi.org/10.1038/374227A0.

Szczepankowska, A. (2012) ‘Role of CRISPR/cas system in the development of bacteriophage resistance’, *Advances in virus research*, 82, pp. 289–338. Available at: https://doi.org/10.1016/B978-0-12-394621-8.00011-X.

Szostak, J.W., Bartel, D.P. and Luisi, P.L. (2001) ‘Synthesizing life’, *Nature*, 409(6818), pp. 387–390. Available at: https://doi.org/10.1038/35053176.

Takeda, M. *et al.* (2006) ‘Generation of Measles Virus with a Segmented RNA Genome’, *Journal of Virology*, 80(9), p. 4242. Available at: https://doi.org/10.1128/JVI.80.9.4242-4248.2006.

Takeshita, D. and Tomita, K. (2010) ‘Assembly of Qβ viral RNA polymerase with host translational elongation factors EF-Tu and -Ts’, *Proceedings of the National Academy of Sciences of the United States of America*, 107(36), pp. 15733–15738. Available at: https://doi.org/10.1073/PNAS.1006559107.

Terrance Walker, G. *et al.* (1992) ‘Isothermal in vitro amplification of DNA by a restriction enzyme/DNA polymerase system’, *Proceedings of the National Academy of Sciences of the United States of America*, 89(1), pp. 392–396. Available at: https://doi.org/10.1073/PNAS.89.1.392.

Theobald, D.L. (2010) ‘A formal test of the theory of universal common ancestry’, *Nature 2010 465:7295*, 465(7295), pp. 219–222. Available at: https://doi.org/10.1038/nature09014.

Tjivikua, T., Ballester, P. and Rebek, J. (1990) ‘A Self-Replicating System’, *Journal of the American Chemical Society*, 112(3), pp. 1249–1250. Available at: https://doi.org/10.1021/JA00159A057.

Tomita, K. (2014a) ‘Structures and functions of Qβ replicase: Translation factors beyond protein synthesis’, *International Journal of Molecular Sciences*, 15(9), pp. 15552–15570. Available at: https://doi.org/10.3390/ijms150915552.

Tomita, K. (2014b) ‘Structures and functions of Qβ replicase: Translation factors beyond protein synthesis’, *International Journal of Molecular Sciences*. MDPI AG, pp. 15552–15570. Available at: https://doi.org/10.3390/ijms150915552.

Tomita, K., Ichihashi, N. and Yomo, T. (2015) ‘Replication of partial double-stranded RNAs by Qβ replicase’, *Biochemical and biophysical research communications*, 467(2), pp. 293–296. Available at: https://doi.org/10.1016/J.BBRC.2015.09.169.

Trachman, R.J. *et al.* (2018) ‘Crystal Structures of the Mango-II RNA Aptamer Reveal Heterogeneous Fluorophore Binding and Guide Engineering of Variants with Improved Selectivity and Brightness’, *Biochemistry*, 57(26), pp. 3544–3548. Available at:

https://doi.org/10.1021/ACS.BIOCHEM.8B00399/ASSET/IMAGES/LARGE/BI-2018-00399Q_0004.JPEG.

Twort, F.W. (1915) 'AN INVESTIGATION ON THE NATURE OF ULTRA-MICROSCOPIC VIRUSES.', *The Lancet*, 186(4814), pp. 1241–1243. Available at: https://doi.org/10.1016/S0140-6736(01)20383-3.

Ueda, K. *et al.* (2019) 'A Fusion Method to Develop an Expanded Artificial Genomic RNA Replicable by Qβ Replicase', *Chembiochem : a European journal of chemical biology*, 20(18), pp. 2331–2335. Available at: https://doi.org/10.1002/CBIC.201900120.

Ugarov, V.I. *et al.* (1994) 'Expression and stability of recombinant RQ-mRNAs in cell-free translation systems', *FEBS letters*, 341(1), pp. 131–134. Available at: https://doi.org/10.1016/0014-5793(94)80255-6.

Ugarov, V.I. and Chetverin, A.B. (2008a) 'Functional Circularity of Legitimate Qβ Replicase Templates', *Journal of Molecular Biology*, 379(3), pp. 414–427. Available at: https://doi.org/10.1016/J.JMB.2008.03.074.

Ugarov, V.I. and Chetverin, A.B. (2008b) 'Functional Circularity of Legitimate Qβ Replicase Templates', *Journal of Molecular Biology*, 379(3), p. 414. Available at: https://doi.org/10.1016/J.JMB.2008.03.074.

Ugarov, V.I., Demidenko, A.A. and Chetverin, A.B. (2003) 'Qβ Replicase Discriminates between Legitimate and Illegitimate Templates by Having Different Mechanisms of Initiation', *Journal of Biological Chemistry*, 278(45), pp. 44139–44146. Available at: https://doi.org/10.1074/JBC.M305992200.

Urabe, H. *et al.* (2010) 'Compartmentalization in a water-in-oil emulsion repressed the spontaneous amplification of RNA by Qβ replicase', *Biochemistry*, 49(9), pp. 1809–1813. Available at: https://doi.org/10.1021/BI901805U/SUPPL_FILE/BI901805U_SI_001.PDF.

Usui, K. *et al.* (2013) 'Kinetic model of double-stranded RNA formation during long RNA replication by Qβ replicase', *FEBS Letters*, 587(16), pp. 2565–2571. Available at: https://doi.org/10.1016/j.febslet.2013.06.033.

Usui, K., Ichihashi, N. and Yomo, T. (2015a) 'A design principle for a single-stranded RNA genome that replicates with less double-strand formation', *Nucleic acids research*, 43(16), pp. 8033–8043. Available at: https://doi.org/10.1093/NAR/GKV742.

Usui, K., Ichihashi, N. and Yomo, T. (2015b) ‘A design principle for a single-stranded RNA genome that replicates with less double-strand formation’, *Nucleic acids research*, 43(16), pp. 8033–8043. Available at: https://doi.org/10.1093/NAR/GKV742.

Vagt, T. *et al.* (2006) ‘Membrane binding and structure of de novo designed α-helical cationic coiled-coil-forming peptides’, *ChemPhysChem*, 7(6), pp. 1361–1371. Available at: https://doi.org/10.1002/cphc.200600010.

Vaidya, N. *et al.* (2012a) ‘Spontaneous network formation among cooperative RNA replicators’, *Nature*, 491(7422), pp. 72–77. Available at: https://doi.org/10.1038/NATURE11549.

Vaidya, N. *et al.* (2012b) ‘Spontaneous network formation among cooperative RNA replicators’, *Nature*, 491(7422), pp. 72–77. Available at: https://doi.org/10.1038/NATURE11549.

Varanda, C. *et al.* (2021) ‘An Overview of the Application of Viruses to Biotechnology’, *Viruses*, 13(10). Available at: https://doi.org/10.3390/V13102073.

Vasiliev, N.N. *et al.* (2010) ‘Isolation and crystallization of a chimeric Qβ replicase containing Thermus thermophilus EF-Ts’, *Biochemistry (Moscow)*, 75(8), pp. 989–994. Available at: https://doi.org/10.1134/S0006297910080067.

Vasilyev, N.N. *et al.* (2013) ‘Ribosomal protein S1 functions as a termination factor in RNA synthesis by Qβ phage replicase’, *Nature communications*, 4. Available at: https://doi.org/10.1038/NCOMMS2807.

Vincent, M., Xu, Y. and Kong, H. (2004) ‘Helicase-dependent isothermal DNA amplification’, *EMBO reports*, 5(8), pp. 795–800. Available at: https://doi.org/10.1038/SJ.EMBOR.7400200.

de Vries, C.R. *et al.* (2021) ‘Phages in vaccine design and immunity; mechanisms and mysteries’, *Current Opinion in Biotechnology*, 68, pp. 160–165. Available at: https://doi.org/10.1016/J.COPBIO.2020.11.002.

Waga, S., Bauer, G. and Stillman, B. (1994) ‘Reconstitution of complete SV40 DNA replication with purified replication factors.’, *Journal of Biological Chemistry*, 269(14), pp. 10923–10934. Available at: https://doi.org/10.1016/S0021-9258(17)34146-7.

Wagner, A., Weise, L.I. and Mutschler, H. (2022) ‘In vitro characterisation of the MS2 RNA polymerase complex reveals host factors that modulate emesviral replicase activity’, *Communications biology*, 5(1). Available at: https://doi.org/10.1038/S42003-022-03178-2.

Walker, G.T. *et al.* (1992) 'Strand displacement amplification--an isothermal, in vitro DNA amplification technique', *Nucleic acids research*, 20(7), pp. 1691–1696. Available at: https://doi.org/10.1093/NAR/20.7.1691.

Weber, H. and Weissmann, C. (1970) 'The 3'-termini of bacteriophage Q-beta plus and minus strands', *Journal of molecular biology*, 51(2), pp. 215–224. Available at: https://doi.org/10.1016/0022-2836(70)90138-5.

Weise, Laura I. *et al.* (2019) 'Cell-free expression of RNA encoded genes using MS2 replicase', *Nucleic Acids Research*, 47(20), pp. 10956–10967. Available at: https://doi.org/10.1093/NAR/GKZ817.

Weise, Laura I *et al.* (2019) 'Cell-free expression of RNA encoded genes using MS2 replicase', *Nucleic Acids Research*, pp. 1–12. Available at: https://doi.org/10.1093/nar/gkz817.

Weissmann, C. *et al.* (1973) 'Structure and function of phage RNA', *Annual review of biochemistry*, 42, pp. 303–328. Available at: https://doi.org/10.1146/ANNUREV.BI.42.070173.001511.

Whitman, W.B., Coleman, D.C. and Wiebe, W.J. (1998) 'Prokaryotes: The unseen majority', *Proceedings of the National Academy of Sciences*, 95(12), pp. 6578–6583. Available at: https://doi.org/10.1073/PNAS.95.12.6578.

Witzany, G. (2016) 'Crucial steps to life: From chemical reactions to code using agents', *Bio Systems*, 140, pp. 49–57. Available at: https://doi.org/10.1016/J.BIOSYSTEMS.2015.12.007.

Wommack, K.E. and Colwell, R.R. (2000) 'Virioplankton: Viruses in Aquatic Ecosystems', *Microbiology and Molecular Biology Reviews*, 64(1), pp. 69–114. Available at: https://doi.org/10.1128/MMBR.64.1.69-114.2000/ASSET/70DA7E32-478F-4F61-8A54-5220F57170E4/ASSETS/GRAPHIC/MR0100009007.JPEG.

Yao, Y. *et al.* (2019) 'A Direct RNA-to-RNA Replication System for Enhanced Gene Expression in Bacteria', *ACS Synthetic Biology*, 8(5), pp. 1067–1078. Available at: https://doi.org/10.1021/acssynbio.8b00521.

Zhang, H. *et al.* (2013a) 'Crystal structure of 3WJ core revealing divalent ion-promoted thermostability and assembly of the Phi29 hexameric motor pRNA', *RNA*, 19(9), pp. 1226–1237. Available at: https://doi.org/10.1261/RNA.037077.112.

Zhang, H. *et al.* (2013b) 'Crystal structure of 3WJ core revealing divalent ion-promoted thermostability and assembly of the Phi29 hexameric motor pRNA', *Rna*, 19(9), pp. 1226–1237. Available at: https://doi.org/10.1261/rna.037077.112.

Zhang, W. and Wu, Q. (2020a) 'Applications of phage-derived RNA-based technologies in synthetic biology', *Synthetic and Systems Biotechnology*, 5(4), pp. 343–360. Available at: https://doi.org/10.1016/j.synbio.2020.09.003.

Zhang, W. and Wu, Q. (2020b) 'Applications of phage-derived RNA-based technologies in synthetic biology', *Synthetic and Systems Biotechnology*. KeAi Communications Co., pp. 343–360. Available at: https://doi.org/10.1016/j.synbio.2020.09.003.

Zhang, W. and Wu, Q. (2020c) 'Applications of phage-derived RNA-based technologies in synthetic biology', *Synthetic and Systems Biotechnology*, 5(4), pp. 343–360. Available at: https://doi.org/10.1016/J.SYNBIO.2020.09.003.

Zhuravlev, Y.N. and Avetisov, V.A. (2006) 'The definition of life in the context of its origin', *Biogeosciences*, 3(3), pp. 281–291. Available at: https://doi.org/10.5194/BG-3-281-2006.

Zielinski, W.S. and Orgel, L.E. (1987) 'Autocatalytic synthesis of a tetranucleotide analogue', *Nature*, 327(6120), pp. 346–347. Available at: https://doi.org/10.1038/327346A0.

Figures 1, 2, 4, 5, 6, 7, 9, 11, 12, 13, 18, 28, 29 were created using BioRender (https://biorender.com).

8. Appendix

8.1. Table of oligonucleotides

All the oligonucleotides were synthesized by IDT.

Primer name	Sequence 5'→3'	Additional information
Fragment_3'RQ135_ExXy'.REV	ATCTCTCAAATCCCTCGGATGGAAA GTAGCGTGCACTTTTGC	PCR of the pRNA for Gibson assembly
Fragment_RQ135_ExXy'.FOR	ATCCCCCGTGCGTCCCTTCGGGAATG GTACGGTACTTCCATTGT	PCR of the pRNA for Gibson assembly
Fragment_RQ135_ExXy'.REV	CTCTCAAATCCCTCGGATATGGAAA GTAGCGTGCACTTTTGC	PCR of the pRNA for Gibson assembly
Fragment_sfGFP_ExXy'.FOR	CATGGATGAGCTCTACAAATAGATG GAATGGTACGGTACTTCCATTGTCA	PCR of the pRNA for Gibson assembly
RQ_rev	GGGCTAACAGTGCGGTAACACGC	For (+) RQ135 scaffold PCR amplification
T7_RQ_fw	GAAATTAATACGACTCACTATAGGG GTTCCAACCGGAAGTTG	For (+) RQ135 scaffold PCR amplification
Vector_pgemt_rq135notiecorv_1.FOR	CGAAGGGACGCACGGG	PCR vector pgemt_rq135notiecorv _sfGFPwt
Vector_pgemt_rq135notiecorv_1.REV	ATATCCGAGGGATTTGAGAGATGCC	PCR vector pgemt_rq135notiecorv _sfGFPwt
11	CGCGTCGAAATTAATACGACTCACT ATAGGGAATGGTACGGTACTTCCATT GTCATGTGTATGTTGGGGATTAAGAC GTGCTGAT	pRNA fill-in
13	CGCGTCGAAATTAATACGACTCACT ATAGGGAATGGTACGGTACTTCCATT GTCATGTGTATGTTGGGGATTAAGGC TAGCTGAT	pRNA fill-in
14	CGCGTCGAAATTAATACGACTCACT ATAGGGAATGGTACGGTACTTCCATT GTCATGTGTATGTTGGGGATTAGCGT TCTCTGAT	pRNA fill-in
15	CGCGTCGAAATTAATACGACTCACT ATAGGGAATGGTACGGTACTTCCATT GTCATGTGTATGTTGGGGATTAAGTG GACCTGAT	pRNA fill-in
16	CGCGTCGAAATTAATACGACTCACT ATAGGGAATGGTACGGTACTTCCATT GTCATGTGTATGTTGGGGATTAAGTG GACCTGAT	pRNA fill-in
19	GGAAAGTAGCGTGCACTTTTGCCAT GATTGACAGGCTAGAATCAACAAAG TATGTGGGCTGAACTCAATCAGCAC GTCTTAATCCCCAA	pRNA fill-in
21	GGAAAGTAGCGTGCACTTTTGCCAT GATTGACGCGTTCTAATCAACAAAG TATGTGGGCTGAACTCAATCAGCTA GCCTTAATCCCCAA	pRNA fill-in
22	GGAAAGTAGCGTGCACTTTTGCCAT GATTGACACAGGCAAATCAACAAAG TATGTGGGCTGAACTCAATCAGAGA ACGCTAATCCCCAA	pRNA fill-in
23	GGAAAGTAGCGTGCACTTTTGCCAT GATTGACAGTGGACAATCAACAAAG TATGTGGGCTGAACTCAATCAGTGCC TGTTAATCCCCAA	pRNA fill-in

25	GGAAAGTAGCGTGCACTTTTGCCAT GATTGACAGACGTGAATCAACAAAG TATGTGGGCTGAACTCAATCAGGTCC ACTTAATCCCCAA	pRNA fill-in
26	GGAAAGTAGCGTGCACTTTTGCCAT GATTGACAGGCTAGAATCAACAAAG TATGTGGGCTGAACTCAATCAGGTCC ACTTAATCCCCAA	pRNA fill-in
27	GGAAAGTAGCGTGCACTTTTGCCAT GATTGACGCGTTCTAATCAACAAAG TATGTGGGCTGAACTCAATCAGGTCC ACTTAATCCCCAA	pRNA fill-in
28	GGAAAGTAGCGTGCACTTTTGCCAT GATTGACACAGGCAAATCAACAAAG TATGTGGGCTGAACTCAATCAGGTCC ACTTAATCCCCAA	pRNA fill-in
86	CTAATACGACTCACTATAGGGGACC	For (+) MDV-1 scaffold PCR amplification
87	GGGAACCCCCCTTCGGGGGGTCACC	For (+) MDV-1 scaffold PCR amplification
136	GGGACCCCCCCGGAAG	For (-) MDV-1 scaffold PCR amplification
141	CTAATACGACTCACTATAGGGGAAC CCCCCTTCGG	For (-) MDV-1 scaffold PCR amplification
164	ATGGCAAAAGTGCACGCTACTTTCC GGATCCCACGGGCTAG	
165	ACATGACAATGGAAGTACCGTACCA TTCCGCATGCGTCACGGTC	
178	GACAATGGAAGTACCGTACCATTCC CGAAGGGACGCACGG	PCR of the pRNA for Gibson assembly
179	AAAAGTGCACGCTACTTTCCCGAGG GATTTGAGAGATGCCTA	PCR of the pRNA for Gibson assembly
180	GGGGTTCCAACCGGAAGTTG	For (-) RQ135 scaffold PCR amplification
181	GAAATTAATACGACTCACTATAGGG CTAACAGTGCGGTAACACGC	For (-) RQ135 scaffold PCR amplification

8.2. Table of RNA replicons

RNA sequences of the replicons obtained by IVT.

RNA sequence name	Sequence 5'→3'
(+) RQ135_pRNA	GGGGUUCCAACCGGAAGUUGAGGGAUGCCUAGGCAUCCCCCGUGCG UCCCUUCGGGAAUGGUACGGUACUUCCAUUGUCAUGUGUAUGUUGG GGAUUAAGUGGACCUGAUUGAGUUCAGCCCACAUACUUUGUUGAUU UGCCUGUGUCAAUCAUGGCAAAAGUGCACGCUACUUUCCAUAUCCG AGGGAUUUGAGAGAUGCCUAGGCAUCUCCCGCGCGCCGGUUUCGGA CCUCCAGUGCGUGUUACCGCACUGUUAGCCC
(+) RQ135_pRNA_sfGFP	GGGGUUCCAACCGGAAGUUGAGGGAUGCCUAGGCAUCCCCCGUGCG UCCCUUCGGCGGCCGCGAUAAAUUGUUAAAGAGCAGUAAGGAGGUG AAUGAGCAAAGGAGAAGAACUUUUCACUGGAGUUGUCCCAAUUCUU GUUGAAUUAGAUGGUGAUGUUAAUGGGCACAAAUUUUCUGUCCGU GGAGAGGGUGAAGGUGAUGCUACAAACGGAAAACUCACCCUUAAAU UUAUUUGCACUACUGGAAAACUACCUGUUCCAUGGCCAACACUUGU CACUACUCUGACCUAUGGUGUUCAAUGCUUUUCCCGUUAUCCGGAU CACAUGAAACGGCAUGACUUUUUCAAGAGUGCCAUGCCCGAAGGUU AUGUACAGGAACGCACUAUAUCUUUCAAAGAUGACGGGACCUACAA GACGCGUGCUGAAGUCAAGUUUGAAGGUGAUACCCUUGUUAAUCGU AUCGAGUUAAAAGGUAUUGAUUUUAAAGAAGAUGGAAACAUUCUC GGACACAAACUCGAGUACAACUUUAACUCACACAAUGUAUACAUCA CGGCAGACAAACAAAAGAAUGGAAUCAAAGCUAACUUCAAAAUUCG CCACAACGUUGAAGAUGGUUCCGUUCAACUAGCAGACCAUUAUCAA CAAAAUACUCCAAUUGGCGAUGGCCCUGUCCUUUUACCAGACAACC AUUACCUGUCGACACAAUCUGUCCUUUCGAAAGAUCCCAACGAAAA GCGUGACCACAUGGUCCUUCUUGAGUUUGUAACUGCUGCUGGGAUU ACACAUGGCAUGGAUGAGCUCUACAAAUAGAUGGAAUGGUACGGU ACUUCCAUUGUCAUGUGUAUGUUGGGGAUUAAGUGGACCUGAUUG AGUUCAGCCCACAUACUUUGUUGAUUUGCCUGUGUCAAUCAUGGCA AAAGUGCACGCUACUUUCCAUCCGAGGGAUUUGAGAGAUGCCUAGG CAUCUCCCGCGCGCCGGUUUCGGACCUCCAGUGCGUGUUACCGCAC UGUUAGCCC
(+) MDV-1 _F30Bro	GGGAACCCCCCUUCGGGGGGUCACCUCGCGCAGCGGGCUGCGCGAA GGAGCCACGCUGCGAAGCAGCGUGGCGGUUCUCGUGCGUCACCGAA ACGCACGAAGGUCGCGCCUCUUCACGAGGCGUCACCUGGGAGAGCG CGAAAGCGCUAGCCCGUGGGAUCCUUGCCAUGAAUGAUCCCGAAGG AUCAUCAGAGUAUGUGGGAGCCCACACUCUACUCGACAGAUACGAA UAUCUGGACCCGACCGUCUCCCACAUACACAUGGCAAGCAUGCGUC ACGGUCGAACUCCCGUACGAGGUGCCCGCACCUCGUCCCCCCCUUCC GGGGGGGUCCCC
(+) MDV-1 _F30Bro_pRNA	GGGGACCCCCCCGGAAGGGGGGGACGAGGUGCGGGCACCUCGUACG GGAGUUCGACCGUGACGCAUGCGGAAAGUAGCGUGCACUUUUGCCA UGAUUGACACAGGCAAAUCAACAAAGUAUGUGGGCUGAACUCAAUC AGGUCCACUUAAUCCCCAACAUACACAUGACAAUGGAAGUACCGUA CCAUUCCUUGCCAUGAAUGAUCCCGAAGGAUCAUCAGAGUAUGUGG GAGCCCACACUCUACUCGACAGAUACGAAUAUCUGGACCCGACCGU CUCCCACAUACACAUGGCAAGGAUCCCACGGGCUAGCGCUUUCGCG CUCUCCCAGGUGACGCCUCGUGAAGAGGCGCGACCUUCGUGCGUUU CGGUGACGCACGAGAACCGCCACGCUGCUUCGCAGCGUGGCUCCUU CGCGCAGCCCGCUGCGCGAGGUGACCCCCCGAAGGGGGGUUCCC
(+) MDV-1 _F30Mango_pRNA	GGGGACCCCCCCGGAAGGGGGGGACGAGGUGCGGGCACCUCGUACG GGAGUUCGACCGUGACGCAUGCGGAAAGUAGCGUGCACUUUUGCCA UGAUUGACAGUGGACAAUCAACAAAGUAUGUGGGCUGAACUCAAUC AGUGCCUGUUAAUCCCCAACAUACACAUGACAAUGGAAGUACCGUA CCAUUCCUUGCCAUGAAUGAUCCCGAAGGAUCAUCAGAGUAUGUGG GGUACGAAUAUACCACAUACCAAACCUUCCUUCGUACCCCACAUAC ACAUGGCAAGGAUCCCACGGGCUAGCGCUUUCGCGCUCUCCCAGGU GACGCCUCGUGAAGAGGCGCGACCUUCGUGCGUUUCGGUGACGCAC GAGAACCGCCACGCUGCUUCGCAGCGUGGCUCCUUCGCGCAGCCCG CUGCGCGAGGUGACCCCCCGAAGGGGGGUUCCC
(+) MDV-1 _pRNA_ExAb	GGACCCCCCCGGAAGGGGGGGACGAGGUGCGGGCACCUCGUACGGG AGUUCGACCGUGACGCAUGC GGAAUGGUACGGUACUUCCAUUGUCAUGUGUAUGUUGGGGAUUAA GUGGACCUGAUUGAGUUCAGCCCACAUACUUUGUUGAUUUGCCUGU

	GUCAAUCAUGGCAAAAGUGCACGCUACUUUCCGGAUCCCACGGGCU AGCGCUUUCGCGCUCUCCCAGGUGACGCCUCGUGAAGAGGCGCGAC CUUCGUGCGUUUCGGUGACGCACGAGAACCGCCACGCUGCUUCGCA GCGUGGCUCCUUCGCGCAGCCCGCUGCGCGAGGUGACCCCCCGAAG GGGGGUUCCC
(+) MDV-1 _pRNA_ExBa	GGACCCCCCCGGAAGGGGGGGACGAGGUGCGGGCACCUCGUACGGG AGUUCGACCGUGACGCAUGC GGAAUGGUACGGUACUUCCAUUGUCAUGUGUAUGUUGGGGAUUAA CAGGCACUGAUUGAGUUCAGCCCACAUACUUUGUUGAUUGUCCACU GUCAAUCAUGGCAAAAGUGCACGCUACUUUCCGGAUCCCACGGGCU AGCGCUUUCGCGCUCUCCCAGGUGACGCCUCGUGAAGAGGCGCGAC CUUCGUGCGUUUCGGUGACGCACGAGAACCGCCACGCUGCUUCGCA GCGUGGCUCCUUCGCGCAGCCCGCUGCGCGAGGUGACCCCCCGAAG GGGGGUUCCC
(+) MDV-1 _pRNA_ExCb	GGACCCCCCCGGAAGGGGGGGACGAGGUGCGGGCACCUCGUACGGG AGUUCGACCGUGACGCAUGC GGAAUGGUACGGUACUUCCAUUGUCAUGUGUAUGUUGGGGAUUAG CGUUCUCUGAUUGAGUUCAGCCCACAUACUUUGUUGAUUUGCCUGU GUCAAUCAUGGCAAAAGUGCACGCUACUUUCCGGAUCCCACGGGCU AGCGCUUUCGCGCUCUCCCAGGUGACGCCUCGUGAAGAGGCGCGAC CUUCGUGCGUUUCGGUGACGCACGAGAACCGCCACGCUGCUUCGCA GCGUGGCUCCUUCGCGCAGCCCGCUGCGCGAGGUGACCCCCCGAAG GGGGGUUCCC
(+) MDV-1 _pRNA_ExAc	GGACCCCCCCGGAAGGGGGGGACGAGGUGCGGGCACCUCGUACGGG AGUUCGACCGUGACGCAUGCGGAAUGGUACGGUACUUCCAUUGUCA UGUGUAUGUUGGGGAUUAAGUGGACCUGAUUGAGUUCAGCCCACA UACUUUGUUGAUUAGAACGCGUCAAUCAUGGCAAAAGUGCACGCUA CUUUCC GGAUCCCACGGGCUAGCGCUUUCGCGCUCUCCCAGGUGACGCCUCG UGAAGAGGCGCGACCUUCGUGCGUUUCGGUGACGCACGAGAACCGC CACGCUGCUUCGCAGCGUGGCUCCUUCGCGCAGCCCGCUGCGCGAG GUGACCCCCCGAAGGGGGGUUCCC
(+) MDV-1 _pRNA_ExDc	GGACCCCCCCGGAAGGGGGGGACGAGGUGCGGGCACCUCGUACGGG AGUUCGACCGUGACGCAUGCGGAAUGGUACGGUACUUCCAUUGUCA UGUGUAUGUUGGGGAUUAAGGCUAGCUGAUUGAGUUCAGCCCACA UACUUUGUUGAUUAGAACGCGUCAAUCAUGGCAAAAGUGCACGCUA CUUUCCGGAUCCCACGGGCUAGCGCUUUCGCGCUCUCCCAGGUGAC GCCUCGUGAAGAGGCGCGACCUUCGUGCGUUUCGGUGACGCACGAG AACCGCCACGCUGCUUCGCAGCGUGGCUCCUUCGCGCAGCCCGCUGC GCGAGGUGACCCCCCGAAGGGGGGUUCCC
(+) MDV-1 _pRNA_ExAd	GGACCCCCCCGGAAGGGGGGGACGAGGUGCGGGCACCUCGUACGGG AGUUCGACCGUGACGCAUGCGGAAUGGUACGGUACUUCCAUUGUCA UGUGUAUGUUGGGGAUUAAGUGGACCUGAUUGAGUUCAGCCCACA UACUUUGUUGAUUCUAGCCUGUCAAUCAUGGCAAAAGUGCACGCUA CUUUCCGGAUCCCACGGGCUAGCGCUUUCGCGCUCUCCCAGGUGAC GCCUCGUGAAGAGGCGCGACCUUCGUGCGUUUCGGUGACGCACGAG AACCGCCACGCUGCUUCGCAGCGUGGCUCCUUCGCGCAGCCCGCUGC GCGAGGUGACCCCCCGAAGGGGGGUUCCC
(+) MDV-1 _pRNA_ExFd	GGACCCCCCCGGAAGGGGGGGACGAGGUGCGGGCACCUCGUACGGG AGUUCGACCGUGACGCAUGCGGAAUGGUACGGUACUUCCAUUGUCA UGUGUAUGUUGGGGAUUAAGACGUGCUGAUUGAGUUCAGCCCACA UACUUUGUUGAUUCUAGCCUGUCAAUCAUGGCAAAAGUGCACGCUA CUUUCCGGAUCCCACGGGCUAGCGCUUUCGCGCUCUCCCAGGUGAC GCCUCGUGAAGAGGCGCGACCUUCGUGCGUUUCGGUGACGCACGAG AACCGCCACGCUGCUUCGCAGCGUGGCUCCUUCGCGCAGCCCGCUGC GCGAGGUGACCCCCCGAAGGGGGGUUCCC
(+) MDV-1 _pRNA_ExAf	GGACCCCCCCGGAAGGGGGGGACGAGGUGCGGGCACCUCGUACGGG AGUUCGACCGUGACGCAUGCGGAAUGGUACGGUACUUCCAUUGUCA UGUGUAUGUUGGGGAUUAAGUGGACCUGAUUGAGUUCAGCCCACA UACUUUGUUGAUUCACGUCUGUCAAUCAUGGCAAAAGUGCACGCUA CUUUCCGGAUCCCACGGGCUAGCGCUUUCGCGCUCUCCCAGGUGAC GCCUCGUGAAGAGGCGCGACCUUCGUGCGUUUCGGUGACGCACGAG AACCGCCACGCUGCUUCGCAGCGUGGCUCCUUCGCGCAGCCCGCUGC GCGAGGUGACCCCCCGAAGGGGGGUUCCC
(+) MDV-1 _F30_pRNA_ExAb	GGGGACCCCCCCGGAAGGGGGGGACGAGGUGCGGGCACCUCGUACG GGAGUUCGACCGUGACGCAUGCUUGCCAUGUGUAUGUGGGGGAAUG

	GUACGGUACUUCCAUUGUCAUGUGUAUGUUGGGGAUUAAGUGGAC CUGAUUGAGUUCAGCCCACAUACUUUGUUGAUUUGCCUGUGUCAAU CAUGGCAAAAGUGCACGCUACUUUCCCCCACAUACUCUGAUGAUCC UUCGGGAUCAUUCAUGGCAAGGAUCCCACGGGCUAGCGCUUUCGCG CUCUCCCAGGUGACGCCUCGUGAAGAGGCGCGACCUUCGUGCGUUU CGGUGACGCACGAGAACCGCCACGCUGCUUCGCAGCGUGGCUCCUU CGCGCAGCCCGCUGCGCGAGGUGACCCCCCGAAGGGGGGUUCCC
(+) MDV-1 _F30_pRNA_ExBa	GGGGACCCCCCCGGAAGGGGGGGACGAGGUGCGGGCACCUCGUACG GGAGUUCGACCGUGACGCAUGCUUGCCAUGUGUAUGUGGGGGAAUG GUACGGUACUUCCAUUGUCAUGUGUAUGUUGGGGAUUAACAGGCAC UGAUUGAGUUCAGCCCACAUACUUUGUUGAUUGUCCACUGUCAAUC AUGGCAAAAGUGCACGCUACUUUCCCCCACAUACUCUGAUGAUCCU UCGGGAUCAUUCAUGGCAAGGAUCCCACGGGCUAGCGCUUUCGCGC UCUCCCAGGUGACGCCUCGUGAAGAGGCGCGACCUUCGUGCGUUUC GGUGACGCACGAGAACCGCCACGCUGCUUCGCAGCGUGGCUCCUUC GCGCAGCCCGCUGCGCGAGGUGACCCCCCGAAGGGGGGUUCCC
(+) MDV-1 _F30_pRNA_ExCb	GGGGACCCCCCCGGAAGGGGGGGACGAGGUGCGGGCACCUCGUACG GGAGUUCGACCGUGACGCAUGCUUGCCAUGUGUAUGUGGGGGAAUG GUACGGUACUUCCAUUGUCAUGUGUAUGUUGGGGAUUAGCGUUCUC UGAUUGAGUUCAGCCCACAUACUUUGUUGAUUUGCCUGUGUCAAUC AUGGCAAAAGUGCACGCUACUUUCCCCCACAUACUCUGAUGAUCCU UCGGGAUCAUUCAUGGCAAGGAUCCCACGGGCUAGCGCUUUCGCGC UCUCCCAGGUGACGCCUCGUGAAGAGGCGCGACCUUCGUGCGUUUC GGUGACGCACGAGAACCGCCACGCUGCUUCGCAGCGUGGCUCCUUC GCGCAGCCCGCUGCGCGAGGUGACCCCCCGAAGGGGGGUUCCC
(+) MDV-1 _F30_pRNA_ExAc	GGGGACCCCCCCGGAAGGGGGGGACGAGGUGCGGGCACCUCGUACG GGAGUUCGACCGUGACGCAUGCUUGCCAUGUGUAUGUGGGGGAAUG GUACGGUACUUCCAUUGUCAUGUGUAUGUUGGGGAUUAAGUGGAC CUGAUUGAGUUCAGCCCACAUACUUUGUUGAUUAGAACGCGUCAAU CAUGGCAAAAGUGCACGCUACUUUCCCCCACAUACUCUGAUGAUCC UUCGGGAUCAUUCAUGGCAAGGAUCCCACGGGCUAGCGCUUUCGCG CUCUCCCAGGUGACGCCUCGUGAAGAGGCGCGACCUUCGUGCGUUU CGGUGACGCACGAGAACCGCCACGCUGCUUCGCAGCGUGGCUCCUU CGCGCAGCCCGCUGCGCGAGGUGACCCCCCGAAGGGGGGUUCCC
(+) RQ135_pRNA_ExAb	GGGGUUCCAACCGGAAGUUGAGGGAUGCCUAGGCAUCCCCCGUGCG UCCCUUCGGGAAUGGUACGGUACUUCCAUUGUCAUGUGUAUGUUGG GGAUUAAGUGGACCUGAUUGAGUUCAGCCCACAUACUUUGUUGAUU UGCCUGUGUCAAUCAUGGCAAAAGUGCACGCUACUUUCCCGAGGGA UUUGAGAGAUGCCUAGGCAUCUCCCGCGCGCCGGUUUCGGACCUCC AGUGCGUGUUACCGCACUGUUAGCCC
(+) RQ135_pRNA_ExBa	GGGGTTCCAACCGGAAGTTGAGGGATGCCTAGGCATCCCCCGTGCGT CCCTTCGGGAAUGGUACGGUACUUCCAUUGUCAUGUGUAUGUUGGG GAUUAACAGGCACUGAUUGAGUUCAGCCCACAUACUUUGUUGAUUG UCCACUGUCAAUCAUGGCAAAAGUGCACGCUACUUUCCCGAGGGAT TTGAGAGATGCCTAGGCATCTCCCGCGCGCCGGTTTCGGACCTCCAGT GCGTGTTACCGCACTGTTAGCCC
(+) RQ135_pRNA_ExCb	GGGGTTCCAACCGGAAGTTGAGGGATGCCTAGGCATCCCCCGTGCGT CCCTTCGGGAAUGGUACGGUACUUCCAUUGUCAUGUGUAUGUUGGG GAUUAGCGUUCUCUGAUUGAGUUCAGCCCACAUACUUUGUUGAUUU GCCUGUGUCAAUCAUGGCAAAAGUGCACGCUACUUUCCCGAGGGAT TTGAGAGATGCCTAGGCATCTCCCGCGCGCCGGTTTCGGACCTCCAGT GCGTGTTACCGCACTGTTAGCCC
(+) RQ135_pRNA_ExAc	GGGGTTCCAACCGGAAGTTGAGGGATGCCTAGGCATCCCCCGTGCGT CCCTTCGGGAAUGGUACGGUACUUCCAUUGUCAUGUGUAUGUUGGG GAUUAAGUGGACCUGAUUGAGUUCAGCCCACAUACUUUGUUGAUUA GAACGCGUCAAUCAUGGCAAAAGUGCACGCUACUUUCCCGAGGGAT TTGAGAGATGCCTAGGCATCTCCCGCGCGCCGGTTTCGGACCTCCAGT GCGTGTTACCGCACTGTTAGCCC
(+) RQ135_pRNA_ExDc	GGGGTTCCAACCGGAAGTTGAGGGATGCCTAGGCATCCCCCGTGCGT CCCTTCGGGAAUGGUACGGUACUUCCAUUGUCAUGUGUAUGUUGGG GAUUAAGGCUAGCUGAUUGAGUUCAGCCCACAUACUUUGUUGAUUA GAACGCGUCAAUCAUGGCAAAAGUGCACGCUACUUUCCCGAGGGAT TTGAGAGATGCCTAGGCATCTCCCGCGCGCCGGTTTCGGACCTCCAGT GCGTGTTACCGCACTGTTAGCCC
(+) RQ135_pRNA_ExAd	GGGGTTCCAACCGGAAGTTGAGGGATGCCTAGGCATCCCCCGTGCGT CCCTTCGGGAAUGGUACGGUACUUCCAUUGUCAUGUGUAUGUUGGG

	GAUUAAGUGGACCUGAUUGAGUUCAGCCCACAUACUUUGUUGAUUC UAGCCUGUCAAUCAUGGCAAAAGUGCACGCUACUUUCCCGAGGGAT TTGAGAGATGCCTAGGCATCTCCCGCGCGCCGGTTTCGGACCTCCAGT GCGTGTTACCGCACTGTTAGCCC

8.3. Table of pRNA sequences

Pro-head RNA sequences used in this work. Underlined the sequences of the D-loop and the CE-loop.

Name	RNA sequence (5′→ 3′)
pRNA ExBa	GGAAUGGUACGGUACUUCCAUUGUCAUGUGUAUGUUGGGGAUUAACAGGCACUGAUUGAG UUCAGCCCACAUACUUUGUUGAUUGUCCACUGUCAAUCAUGGCAAAAGUGCACGCUACUU UCC
pRNA ExCb	GGAAUGGUACGGUACUUCCAUUGUCAUGUGUAUGUUGGGGAUUAGCGUUCUCUGAUUGAG UUCAGCCCACAUACUUUGUUGAUUUGCCUGUGUCAAUCAUGGCAAAAGUGCACGCUACUU UCC
pRNA ExDc	GGAAUGGUACGGUACUUCCAUUGUCAUGUGUAUGUUGGGGAUUAAGGCUAGCUGAUUGAG UUCAGCCCACAUACUUUGUUGAUUAGAACGCGUCAAUCAUGGCAAAAGUGCACGCUACUU UCC
pRNA ExEd	GGAAUGGUACGGUACUUCCAUUGUCAUGUGUAUGUUGGGGAUUAAGCACCACUGAUUGAG UUCAGCCCACAUACUUUGUUGAUUCUAGCCUGUCAAUCAUGGCAAAAGUGCACGCUACUU UCC
pRNA ExFe	GGAAUGGUACGGUACUUCCAUUGUCAUGUGUAUGUUGGGGAUUAAGACGUGCUGAUUGAG UUCAGCCCACAUACUUUGUUGAUUUGGUGCUGUCAAUCAUGGCAAAAGUGCACGCUACUU UCC
pRNA ExAf	GGAAUGGUACGGUACUUCCAUUGUCAUGUGUAUGUUGGGGAUUAAGUGGACCUGAUUGAG UUCAGCCCACAUACUUUGUUGAUUCACGUCUGUCAAUCAUGGCAAAAGUGCACGCUACUU UCC
pRNA ExAb	GGAAUGGUACGGUACUUCCAUUGUCAUGUGUAUGUUGGGGAUUAAGUGGACCUGAUUGAG UUCAGCCCACAUACUUUGUUGAUUUGCCUGUGUCAAUCAUGGCAAAAGUGCACGCUACUU UCC
pRNA ExAc	GGAAUGGUACGGUACUUCCAUUGUCAUGUGUAUGUUGGGGAUUAAGUGGACCUGAUUGAG UUCAGCCCACAUACUUUGUUGAUUAGAACGCGUCAAUCAUGGCAAAAGUGCACGCUACUU UCC
pRNA ExAd	GGAAUGGUACGGUACUUCCAUUGUCAUGUGUAUGUUGGGGAUUAAGUGGACCUGAUUGAG UUCAGCCCACAUACUUUGUUGAUUCUAGCCUGUCAAUCAUGGCAAAAGUGCACGCUACUU UCC
pRNA ExFd	GGAAUGGUACGGUACUUCCAUUGUCAUGUGUAUGUUGGGGAUUAAGACGUGCUGAUUGAG UUCAGCCCACAUACUUUGUUGAUUCUAGCCUGUCAAUCAUGGCAAAAGUGCACGCUACUU UCC
pRNA ExGf	GGAAUGGUACGGUACUUCCAUUGUCAUGUGUAUGUUGGGGAUUACACUAUCCUGAUUGAG UUCAGCCCACAUACUUUGUUGAUUCACGUCUGUCAAUCAUGGCAAAAGUGCACGCUACUU UCC
pRNA ExAg	GGAAUGGUACGGUACUUCCAUUGUCAUGUGUAUGUUGGGGAUUAAGUGGACCUGAUUGAG UUCAGCCCACAUACUUUGUUGAUUGAUAGUGGUCAAUCAUGGCAAAAGUGCACGCUACUU UCC

8.4. Table of plasmids

Strain and plasmid name	Information	Use	Production	Antibiotic Resistance	Primers used for PCR of the replicon before IVT
pBAD33tutsfusion	Qβ + EF-Ts + EF-Tu	Qβ expression and purfication	In-house	CmR	-
pGEMT_RQ135 (NotI + EcoRV)	Only RQ135 sequence	Used for Qβ replicase activity assay	In-house	AmpR	-
pGEMT_RQ135notiecorv_sfGFPwt	RQ135 + sfGFP	Used as template for construction of 1.3_Assembled pgemt_rq135notiecorv + pRNA	In-house	AmpR	For (+) strand: T7_RQ_fw + RQ_rev
1.3_Assembled_pgemt_rq135notiecorv+pRNA	RQ135 + pRNA	Used as template for PCR of the replicon RQ135_pRNA	Gibson assembled	AmpR	For (+) strand: T7_RQ_fw + RQ_rev
1.6_Assembled_pgemt_rq135notiecorv+pRNA+sfGFP	RQ135 + pRNA + sfGFP	Used as template for PCR of the replicon RQ135_pRNA_sfGFP	Gibson assembled	AmpR	For (+) strand: T7_RQ_fw + RQ_rev
pDR39	MDV-1 + F30Brocoli	Used as template for PCR of the replicon MDV-1 _F30Brocoli	Synthetic (IDT)	AmpR	For (+) strand: 86 + 87
pDR40	MDV-1 + F30Brocoli + pRNA	Used as template for PCR of the replicon MDV-1 _F30Brocoli_pRNA	Synthetic (IDT)	AmpR	For (+) strand: 86 + 87
pDR41	MDV-1 + F30Mango + pRNA	Used as template for PCR of the replicon MDV-1 _F30Mango_pRNA	Synthetic (IDT)	AmpR	For (+) strand: 86 + 87
pDR57	MDV-1 + pRNA ExAb	Used as template for PCR of the replicon MDV-1 _pRNA_ExAb	Gibson assembled	AmpR	For (+) strand: 86 + 87 For (-) strand: 136 + 141
pDR58	MDV-1 + pRNA ExBa	Used as template for PCR of the replicon MDV-1 _pRNA_ExBa	Gibson assembled	AmpR	For (+) strand: 86 + 87 For (-) strand: 136 + 141
pDR59	MDV-1 + pRNA ExCb	Used as template for PCR of the replicon MDV-1 _pRNA_ExCb	Gibson assembled	AmpR	For (+) strand: 86 + 87 For (-) strand: 136 + 141
pDR60	MDV-1 + pRNA ExAc	Used as template for PCR of the replicon MDV-1 _pRNA_ExAc	Gibson assembled	AmpR	For (+) strand: 86 + 87 For (-) strand: 136 + 141
pDR61	MDV-1 + pRNA ExDc	Used as template for PCR of the replicon MDV-1 _pRNA_ExDc	Gibson assembled	AmpR	For (+) strand: 86 + 87 For (-) strand: 136 + 141
pDR62	MDV-1 + pRNA ExAd	Used as template for PCR of the replicon MDV-1 _pRNA_ExAd	Gibson assembled	AmpR	For (+) strand: 86 + 87 For (-) strand: 136 + 141
pDR63	MDV-1 + pRNA ExFd	Used as template for PCR of the replicon MDV-1 _pRNA_ExFd	Gibson assembled	AmpR	For (+) strand: 86 + 87 For (-) strand: 136 + 141
pDR64	MDV-1 + pRNA ExAf	Used as template for PCR of the replicon MDV-1 _pRNA_ExAf	Gibson assembled	AmpR	For (+) strand: 86 + 87

					For (-) strand: 136 + 141
pDR75	MDV-1 + F30 + pRNA ExAb	Used as template for PCR of the replicon MDV-1 _pRNA_ExAb	Sytnthetic from IDT	AmpR	For (+) strand: 86 + 87 For (-) strand: 136 + 141
pDR76	MDV-1 + F30 + pRNA ExBa	Used as template for PCR of the replicon MDV-1 _F30_pRNA_ExBa	Sytnthetic from IDT	AmpR	For (+) strand: 86 + 87 For (-) strand: 136 + 141
pDR77	MDV-1 + F30 + pRNA ExCb	Used as template for PCR of the replicon MDV-1 _F30_pRNA_ExCb	Sytnthetic from IDT	AmpR	For (+) strand: 86 + 87 For (-) strand: 136 + 141
pDR78	MDV-1 + F30 + pRNA ExAc	Used as template for PCR of the replicon MDV-1 _F30_pRNA_ExAc	Sytnthetic from IDT	AmpR	For (+) strand: 86 + 87 For (-) strand: 136 + 141
pDR79	RQ135 + pRNA ExAb	Used as template for PCR of the replicon RQ135_pRNA_ExAb	Gibson assembled	AmpR	For (+) strand: T7_RQ_fw + RQ_rev For (-) strand: 180 + 181
pDR80	RQ135 + pRNA ExBa	Used as template for PCR of the replicon RQ135_pRNA_ExBa	Gibson assembled	AmpR	For (+) strand: T7_RQ_fw + RQ_rev For (-) strand: 180 + 181
pDR81	RQ135 + pRNA ExCb	Used as template for PCR of the replicon RQ135_pRNA_ExCb	Gibson assembled	AmpR	For (+) strand: T7_RQ_fw + RQ_rev For (-) strand: 180 + 181
pDR82	RQ135 + pRNA ExAc	Used as template for PCR of the replicon RQ135_pRNA_ExAc	Gibson assembled	AmpR	For (+) strand: T7_RQ_fw + RQ_rev For (-) strand: 180 + 181
pDR83	RQ135 + pRNA ExDc	Used as template for PCR of the replicon RQ135_pRNA_ExDc	Gibson assembled	AmpR	For (+) strand: T7_RQ_fw + RQ_rev For (-) strand: 180 + 181
pDR84	RQ135 + pRNA ExAd	Used as template for PCR of the replicon RQ135_pRNA_ExAd	Gibson assembled	AmpR	For (+) strand: T7_RQ_fw + RQ_rev For (-) strand: 180 + 181

8.5. Plasmids maps

Plasmids maps used in this work. Maps were created with SnapGene (Insightful Science).

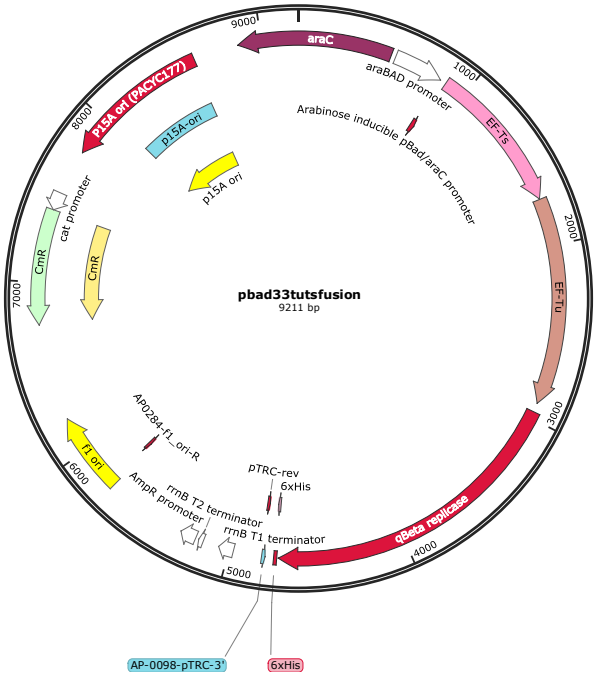

Plasmid pBAD33tutsfusion. *Plasmid containing the EF-Ts, EF-Tu and Qβ replicase gene under the control of the pBAD promoter. Used for the expression and purification of the Qβ replicase and its cofactors.*

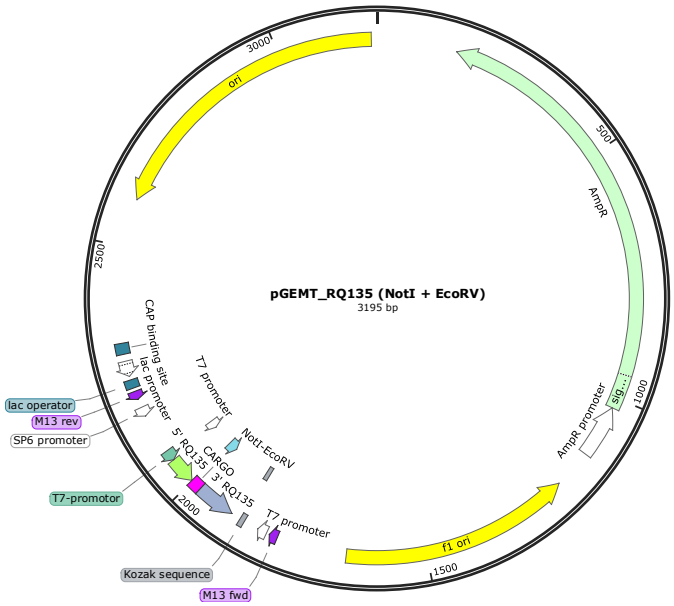

Plasmid pGEMT_RQ135 (NotI + EcoRV). *Plasmid containing the replicon RQ135 without any cargo. The NotI + EcoRV restrictions sites are positioned inside the replicons for a possible insertion of the cargo, in case the Gibson assembly method wound't be adopted.*

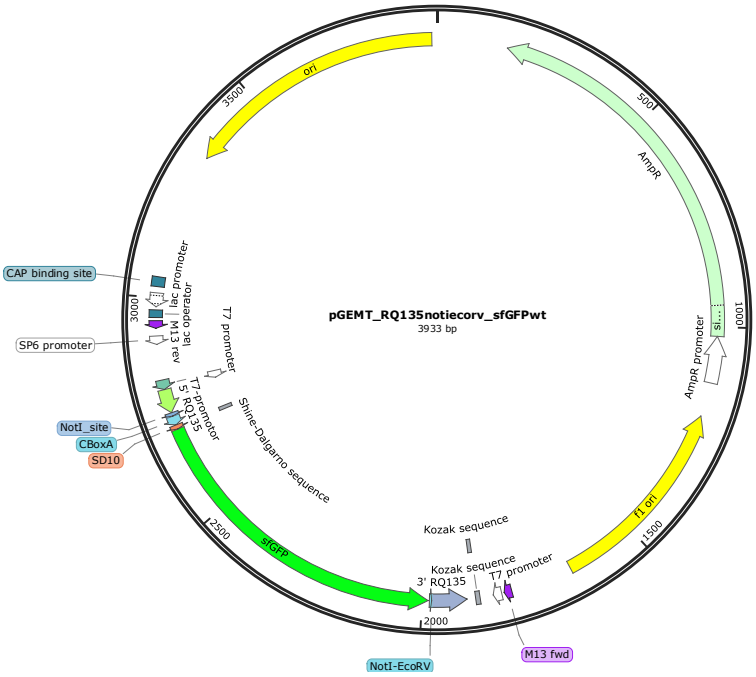

Plasmid pGEMT_RQ135notiecorv_sfGFPwt. *Plasmid containing the replicon RQ135 and, as cargo, the sfGFP protein sequence.*

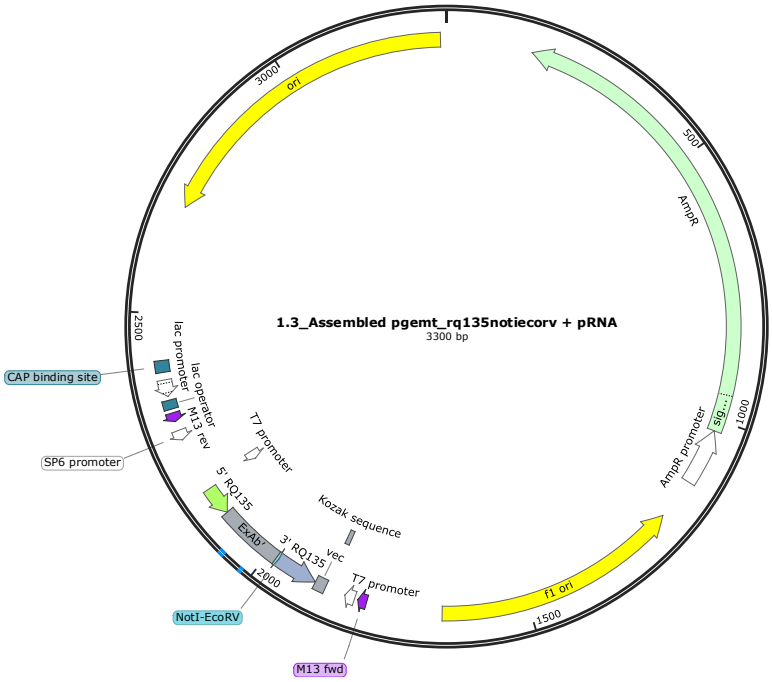

Plasmid 1.3_Assembled pgemt_rq135notiecorv + pRNA. *Plasmid containing the replicon RQ135 and, as cargo, the pRNA sequence ExAb.*

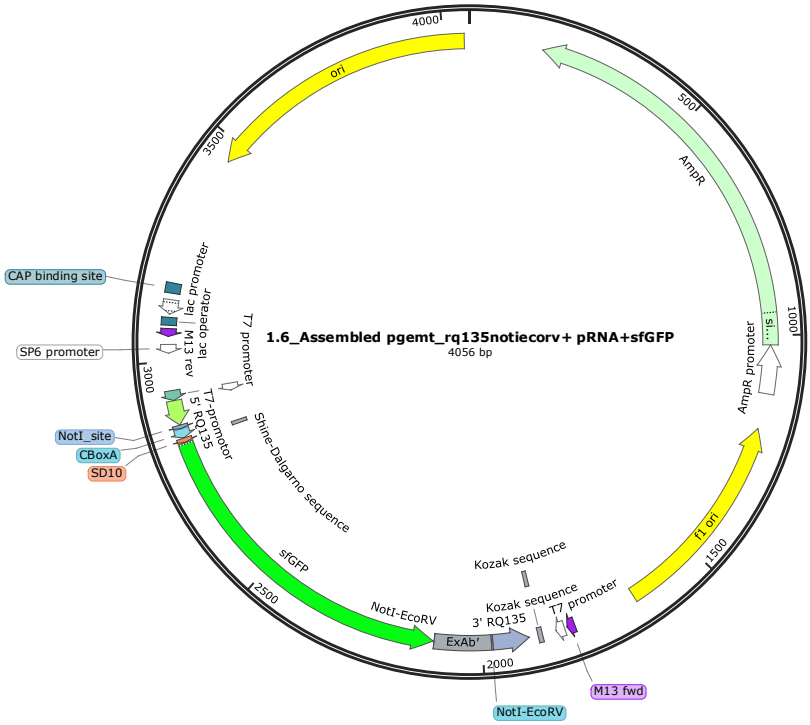

Plasmid 1.6_Assembled pgemt_rq135notiecorv+ pRNA+sfGFP. *Plasmid containing the replicon RQ135 and, as cargo, the sfGFP protein sequence and the pRNA sequence ExAb.*

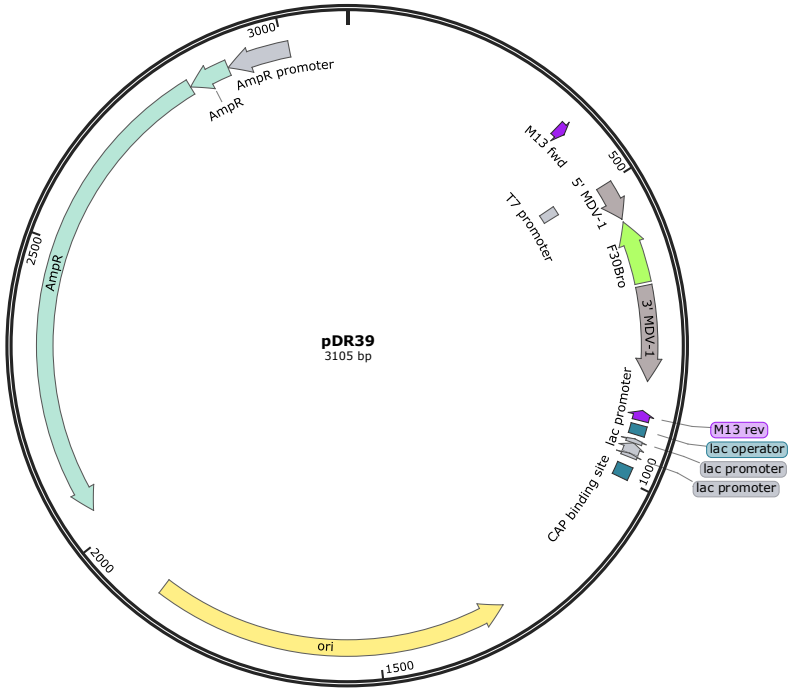

Plasmid pDR39. *Plasmid containing the replicon MDV-1 and, as cargo, the F30-Broccoli aptamer.*

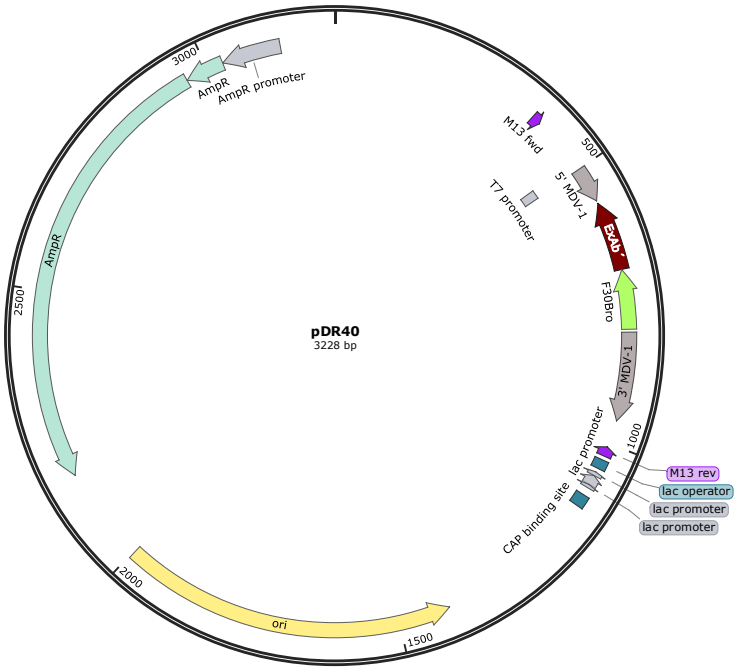

Plasmid pDR40. *Plasmid containing the replicon MDV-1 and, as cargo, the F30-Broccoli aptamer and the pRNA sequence ExAb.*

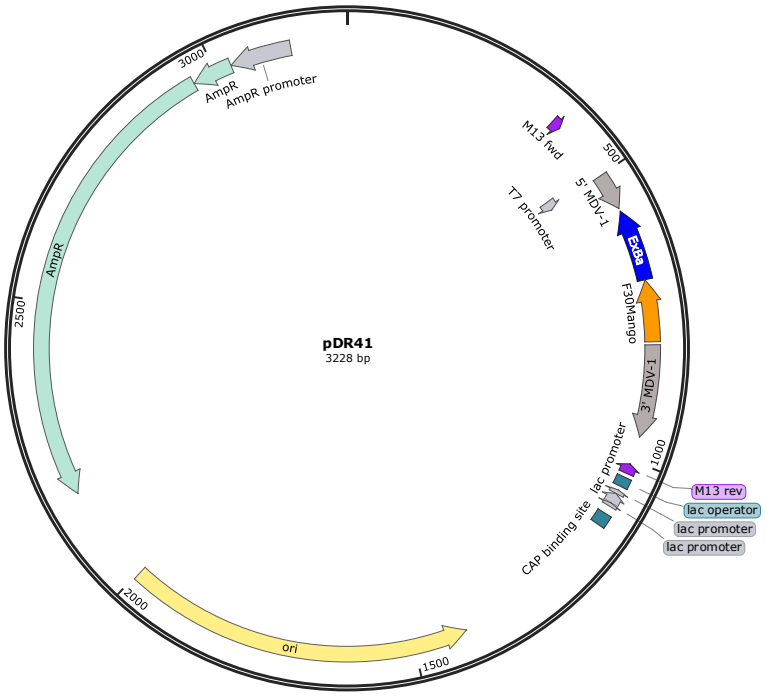

Plasmid pDR41. *Plasmid containing the replicon MDV-1 and, as cargo, the F30-Mango aptamer and the pRNA sequence ExBa.*

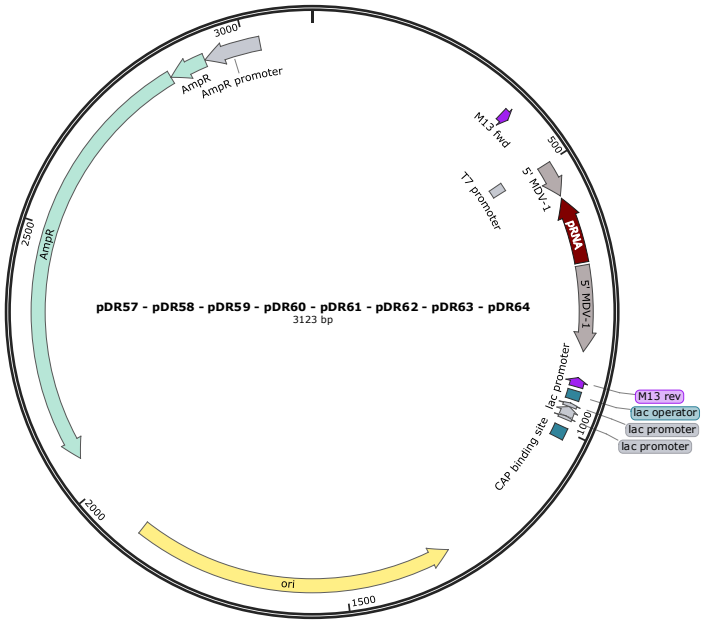

Plasmid series pDR57, pDR58, pDR59, pDR60, pDR61, pDR62, pDR63, pDR64. *These series of plasmids contain a replication sequence MDV-1, the F30 sequence and each of them a distinct pRNA. pDR57: ExAb, pDR58: ExBa, pDR59: ExCb, pDR60: ExAc, pDR61: ExDc, pDR62: ExAd, pDR63: ExFd, pDR64: ExAf.*

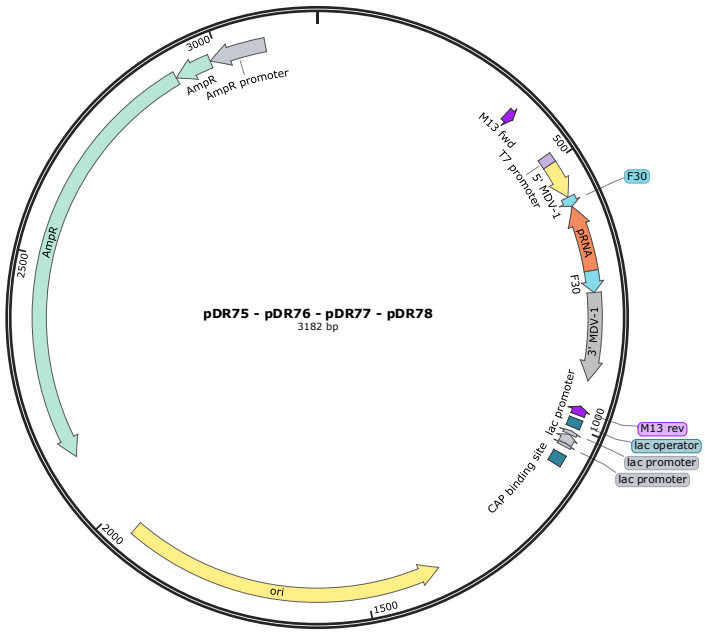

Plasmid series pDR75, pDR76, pDR77, pDR78. *These series of plasmids contain the replication sequence MDV-1, the F30 sequence and each of them a distinct pRNA. pDR75: ExAb, pDR76: ExBa, pDR77: ExCb, pDR78: ExAc.*

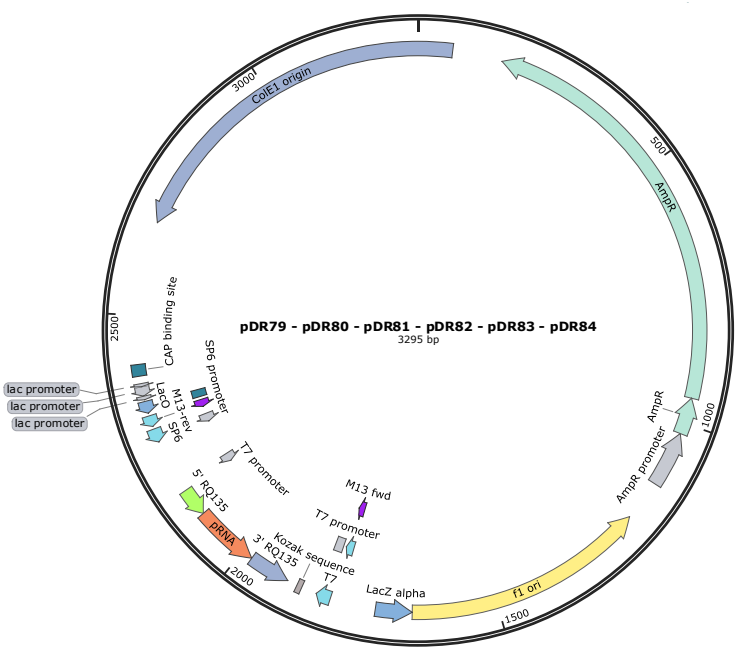

Plasmid series pDR79, pDR80, pDR81, pDR82, pDR83, pDR84. *These series of plasmids contains the a replication sequence RQ135 and each of them a distinct pRNA. pDR79: ExAb, pDR80: ExBa, pDR81: ExCb, pDR82: ExAc, pDR83: ExDc, pDR84: ExAd.*